Dissertation zur Erlangung des Doktorgrades
der Fakultät für Chemie und Pharmazie
der Ludwig-Maximilians-Universität München

Structural and Functional Characterization of Bacterial Cyclic-di-AMP Signaling Pathways

von

Martina Müller

aus

Landau in der Pfalz (Deutschland)

2015

Erklärung

Diese Dissertation wurde im Sinne von § 7 der Promotionsordung vom 28. November 2011 von Herrn Prof. Dr. Karl-Peter Hopfner betreut.

Eidesstattliche Versicherung

Diese Dissertation wurde eigenständig und ohne unerlaubte Hilfe erarbeitet.

München, 27. Juli 2015

.....

Martina Müller

Dissertation eingereicht am	28.07.2015
1. Gutachter	Prof. Dr. Karl-Peter Hopfner
2. Gutachter	PD Dr. Dietmar Martin
Mündliche Prüfung am	13.10.2015

This thesis has been prepared from September 2012 to July 2015 in the laboratory of Professor Dr. Karl-Peter Hopfner at the Gene Center of the Ludwig-Maximilians-University Munich.

This is a cumulative thesis based on following publications:

Müller, M., Hopfner, K.-P. and Witte, G. (2015) c-di-AMP recognition by Staphylococcus aureus PstA. FEBS letters. 589, 45-51

Müller, M., Deimling, T., Hopfner, K.-P. and Witte, G. (2015) Structural analysis of the di-adenylate cyclase reaction of DNA-integrity scanning protein A (DisA) and its inhibition by 3′-dATP. Biochemical Journal. 469 (3), 367-374

TABLE OF CONTENTS

1 SUMMARY

Second messengers exist in all domains of life to amplify and transduce external stimuli inside the cell. Recently, a new second messenger molecule was identified in bacteria: Cyclic di-AMP. C-di-AMP is synthesized in many bacterial species by different enzymes containing a DAC domain. These enzymes are regulated in response to DNA damage, sporulation and other, so far unidentified events. Subsequently, c-di-AMP is sensed by various receptors, such as ion channels, a transcription factor, a transcription factor regulator, a metabolic enzyme, a riboswitch and other, less well-characterized, proteins. The intracellular pool of c-di-AMP is adjusted not only by regulated synthesis, but also by degradation through different classes of phosphodiesterases. These enzymes are regulated by small molecules including Heme and the starvation signal (p)ppGpp. C-di-AMP was shown to influence a variety of important cellular processes: For example, sporulating bacteria depend on c-di-AMP signaling to produce viable spores upon DNA damage. Furthermore, potassium homeostasis, cell wall- and membrane metabolism are regulated by this second messenger. Most importantly, c-di-AMP was shown to be essential in almost all species studied so far and to influence the susceptibility or resistance to cell wall targeting antibiotics. Moreover, c-di-AMP is sensed by the mammalian innate immune system and triggers defense mechanisms against bacteria. As a consequence c-di-AMP pathways are not only interesting from the microbiological point of view, but also for the development of new antimicrobial drugs.

In order to gain insights into the synthesis of this new second messenger, the reaction mechanism of c-di-AMP synthesis by the DAC prototype DisA was studied. The protein was crystallized in the nucleotide-free state, in complex with different substrate analogs representing reaction intermediates, and in the product state. Additionally, manganese ions were added to identify the binding site of the metal ion essential for catalysis. With the resulting crystal structures as well as biochemical analysis, the coordination and activation of the substrate ATP necessary to perform the cyclase reaction were elucidated. The high conservation of the catalytically essential amino acids gives strong evidence that the reaction mechanism is universal for all DAC domain proteins. As c-di-AMP is essential and both increased as well as decreased levels of this second messenger lead to severe phenotypes, DAC enzymes are promising new targets for antimicrobial therapy. Interestingly, the commercially available non-reactive substrate analog 3′-dATP was found to act as a potent inhibitor of DisA. This ATP analog is certainly not a specific DisA inhibitor; however, it was shown to provide not only antimicrobial activity but is also being tested in therapy of cancer and inflammatory diseases.

Alongside the investigation of c-di-AMP synthesis, the receptor PstA was analyzed. PstA binds c-di-AMP selectively and with high affinity. Additional structural investigation revealed that the protein is distantly related to the widely spread class of

P_{II} signal transduction proteins. However, due to structural differences, ligand binding differs between PstA and canonical P_{II} proteins and the mode of action of PstA in signal transduction still remains elusive. Nevertheless, PstA occurs in numerous bacterial species and is likely to have an important function in c-di-AMP signaling.

The role of c-di-AMP signaling is still far from being understood, even though it has become an active field of research in recent years. Future work will reveal not only which cellular processes are regulated and why this second messenger is essential, but also how this knowledge can be applied in the development of new antimicrobial drugs.

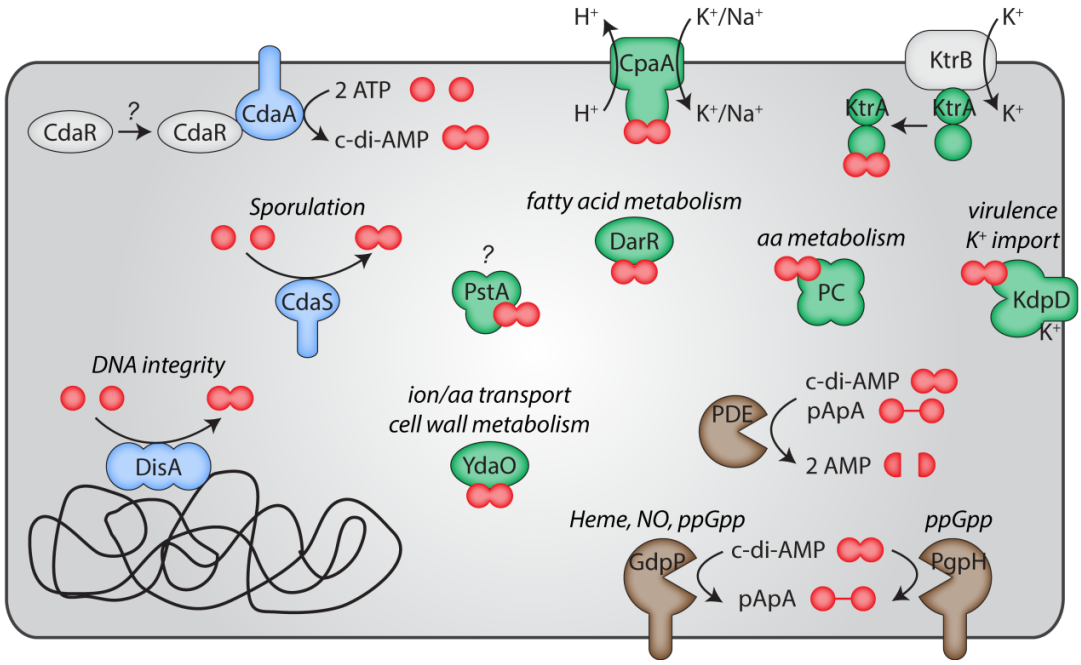

Figure 1: Overview on bacterial c-di-AMP pathways identified and characterized in different bacterial species. C-di-AMP synthases (blue), receptors (green) and phosphodiesterases (brown) are depicted. Explanation of acronyms: PC = pyruvate carboxylase; aa = amino acid; PDE = phosphodiesterase

2 INTRODUCTION

In order to react to their environment, living organisms need to sense external factors such as nutrients, light or temperature. The signals from these first messengers are then transduced and amplified inside the cell by production of second messenger molecules. Subsequently, the second messengers initiate a signal cascade, resulting finally in a specific output such as motility, metabolic changes or sporulation. In bacteria, there exist different types of second messengers: nucleotide-derived molecules and substances such as nitric oxide or calcium-ions. These diffuse rapidly through the cell and allow for a large variety of processes being specifically and expeditiously regulated [1].

2.1 BACTERIAL NUCLEOTIDE SECOND MESSENGERS

Aside from cyclic di-AMP, which will be described in detail later on, several other nucleotide-derived second messengers occur in bacteria, some of them well known for decades. Their diverse functions and associated signaling pathways are briefly described in the following chapters.

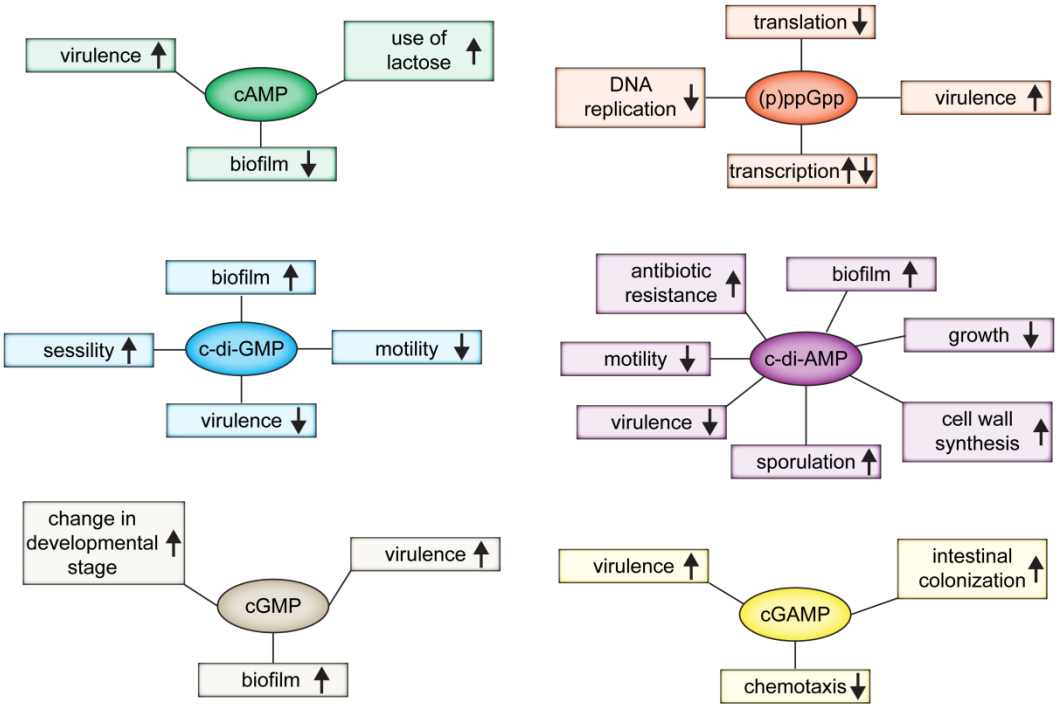

Figure 2: Overview on bacterial nucleotide second messengers and processes they regulate.

2.1.1 CYCLIC AMP

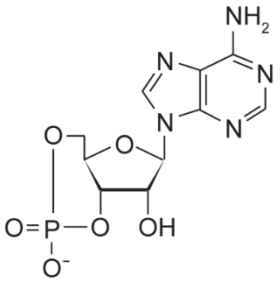

Figure 3: Cyclic AMP

Cyclic AMP (cAMP, Figure 3) was the first nucleotide second messenger to be described already in 1958 [2] and its diverse functions in eukaryotes as well as in bacteria have been studied in great detail since then. Most bacteria, but not all (e.g. *Bacillus subtilis*), produce cAMP. The second messenger is not essential; however, mutants lacking cAMP are impaired in growth or development. cAMP is synthesized by adenylyl cyclases organized in different classes: while class III comprises a large variety of enzymes and is found in all kingdoms of life, classes I, II and IV are exclusively present in bacteria and play important roles for example in catabolite repression, biofilm formation and virulence. As diverse as the pathways adenylyl cyclases are involved in, are their structures. The enzymes are either monomeric or dimeric with one or two active sites and sometimes additional ligand binding sites and regulatory domains. Moreover, the cyclases are either soluble, associated to the cell membrane or are even integral membrane proteins. The intracellular levels of cAMP are regulated by three different mechanisms. The adenylyl cyclase's activity itself is modulated on the transcriptional level, via covalent modifications or by interactions with other proteins or small molecules (e.g. Ca^{2+} or CO_2). Secondly, the degradation of cAMP by phosphodiesterases (PDE) is tightly regulated, and thirdly, cAMP is secreted to the medium to a large extend (reviewed in [3]).

Two prominent examples of bacterial cAMP pathways shall illustrate the diversity of mechanisms regulated by this second messenger. One of the most well-known pathways dependent on cAMP is carbon catabolite repression in *Escherichia coli*. When high levels of glucose are present in the cell, the ratio between phosphoenolpyruvate and pyruvate is low, leading to dephosphorylation of the glucose specific phosphotransferase system $EIIA^{Glc}$. Dephosphorylated $EIIA^{Glc}$ binds to and thereby inactivates metabolic enzymes and transporters of secondary carbon sources. However, when the intracellular glucose concentration decreases $EIIA^{Glc}$ gets phosphorylated and activates CyaA, a membrane bound class I adenylate cyclase. CyaA then produces cAMP which is sensed by the transcription activator CRP. The CRP-cAMP complex finally activates promoters of different catabolic genes and operons such as the *lac* operon required for secondary carbon source metabolism (reviewed in [4]).

Some pathogenic bacteria are able to interfere with their host's cAMP signaling pathways to suppress the immune response and facilitate their propagation. Bacteria either directly secrete cAMP into the host cells (e.g. *Mycobacterium tuberculosis*), export toxins, which activate adenylate cyclases of the host (e.g. *Vibrio cholerae*), or secrete adenylate cyclases of class II, which are active in the host's cells (e.g. *Bacillus anthracis*). *B. anthracis* produces the oedema factor toxin, which is a

calmodulin-dependent adenylate cyclase. With the help of an additional toxin, the oedema factor is first taken up endocytotically by the host cell and then released from the endosome into the cytosol, where it binds calmoduline and thereupon produces cAMP. The resulting increase in cAMP levels interferes with the host cell's bactericidal functions and is therefore an important virulence factor of *B. anthracis* (reviewed in [5] and [6]).

2.1.2 (p)ppGpp

GDP-3′-diphosphate and GTP-3′-diphosphate ((p)ppGpp, Figure 4) were initially identified 1969 in *E. coli* responding to amino acid starvation [7] and were subsequently found to signal the lack of other nutrients like phosphate, fatty acids, carbon and iron as well. (p)ppGpp influences numerous cellular processes such as transcription, translation, replication and the metabolism and thereby triggers the 'stringent response', allowing the cell to survive under and adapt to unfavorable conditions, for example by reduction of the growth rate. Nevertheless, knockouts of (p)ppGpp synthases are possible, therefore this second messenger is not essential, but the cells depend on it to correctly respond to different stresses.

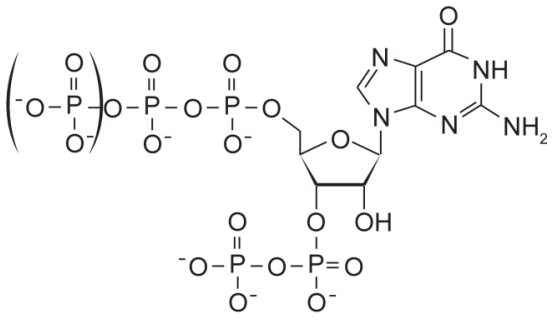

Figure 4: (p)ppGpp

Synthesis and degradation of (p)ppGpp are performed by three classes of proteins, which co-exist in many bacteria: RelA/SpoT homologous proteins (RSH) comprise two domains, one for synthesis of (p)ppGpp and one for its hydrolysis, while small alarmone synthases contain only the synthase domain and small alarmone hydrolases only degrade (p)ppGpp. These three protein classes are regulated in their activity by different mechanisms. *E. coli* RelA for example senses amino acid starvation directly by interacting with an uncharged tRNA bound to the A-site of the ribosome and thereupon synthesizes (p)ppGpp. (p)ppGpp then binds to the RNA polymerase and acts as an allosteric regulator, activating transcription of genes essential for amino acid synthesis, while inhibiting transcription of e.g. rRNA and tRNA. Besides the multiple metabolic processes regulated by (p)ppGpp, it also plays a role in antibiotic resistance. Expression of small alarmone synthase proteins e.g. from *B. subtilis* or *Staphylococcus aureus* is strongly induced by antibiotics targeting cell wall synthesis such as ampicillin and vancomycin, at the same time lack of (p)ppGpp renders bacteria more sensitive towards antibiotics (reviewed in [8] and [9]).

2.1.3 CYCLIC DI-GMP

Cyclic di-GMP (c-di-GMP, Figure 5) was discovered in 1987 as an activator of a bacterial cellulose synthase [10]; however, the main function of this second messenger was found to be the regulation of the transition from single motile cells to biofilms. This change is achieved by reduction of motility, while adhesion to surfaces and polysaccharide production to form the biofilm matrix are increased.

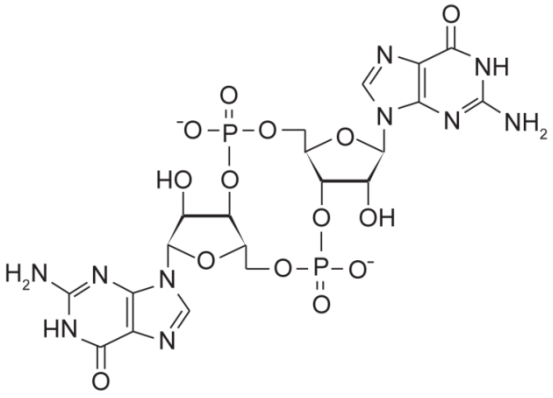

Figure 5: Cyclic di-GMP

Synthesis and degradation of c-di-GMP are regulated in response to external stimuli such as oxygen, nitric oxide, light and nutrients, which are sensed by regulatory domains connected to c-di-GMP synthases and hydrolases. Diguanylate cyclases (DGC) contain a catalytically active GGDEF or GGEEF domain with highly conserved active site residues. Regulation of DGC often occurs *via* product inhibition: the enzyme contains an additional inhibitory site c-di-GMP can bind to and thereby allosterically inhibits c-di-GMP synthesis. Furthermore, two classes of c-di-GMP phosphodiesterases were identified. While HD-GYP domain proteins hydrolyze c-di-GMP directly to two molecules of GMP, EAL domain enzymes generate the linear product pGpG. Moreover, hybrid proteins comprising GGDEF as well as EAL or HD-GYP domains occur. These proteins either have both synthase and hydrolase activity or only one function, whereby the second domain is inactive and may fulfill a regulatory role. Numerous c-di-GMP receptors initiate downstream signaling responses. PilZ domain proteins for example induce reduced motility, transcription factors, different enzymes and riboswitches regulate processes such as biofilm matrix synthesis, surface adhesion, and virulence. Biofilm formation is often connected to a less virulent but antibiotic tolerant phenotype characteristic for chronic infections. Therefore c-di-GMP pathways are also interesting targets for antimicrobial therapies (reviewed in [11] and [12]).

2.1.4 CYCLIC GMP

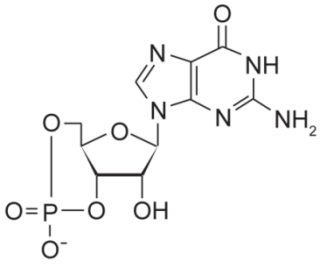

Figure 6: Cyclic GMP

For a long time cyclic GMP (cGMP, Figure 6) was thought to be only a by-product of cAMP synthesis and its potential function in bacteria was unknown. However, in 2000 the specific cGMP synthase Cya2, which is homologous to class III adenylate cyclases, was identified in the cyanobacterium *Synechocystis* [13]. Aside from cAMP phosphodiesterases, which are also active towards

cGMP, evidence for a specific cGMP phosphodiesterase was also found in *Synechocystis* [14]. Moreover, it was shown that cGMP is essential for *Rhodospirillum centenum* to change between different developmental states [15] and the plant pathogen *Xanthomonas campestris* depends on cGMP for virulence and biofilm formation [16]. Still, the function of cGMP in bacteria is poorly understood.

2.1.5 CYCLIC GMP-AMP

Cyclic 3′-5′GMP-AMP (cGAMP, Figure 7) was only recently identified in *Vibrio cholerae,* but homologs of the cGAMP synthase DncV were subsequently found in other pathogenic bacteria such as *E. coli* and *Acinetobacter baumannii*. Interestingly, DncV adapts a similar fold as eukaryotic nucleotidyl transferases, such as the 2′-5′cGAMP synthase cGAS. DncV is not essential; however, it is important for bacterial virulence: cGAMP stimulates intestinal colonization of *V. cholerae* and at the same time downregulates chemotaxis, resulting in a phenotype associated with hyperinfectivity [17]. It was shown that DncV is inhibited by folic acid, the biological role of this regulation is however not understood [18]. Finally, three cGAMP phosphodiesterases were identified in *V. cholerae* producing first pApG and in a second step ApG [19]. Nevertheless, the precise function of cGAMP in bacteria living in an abiotic environment as well as in their host remains to be investigated.

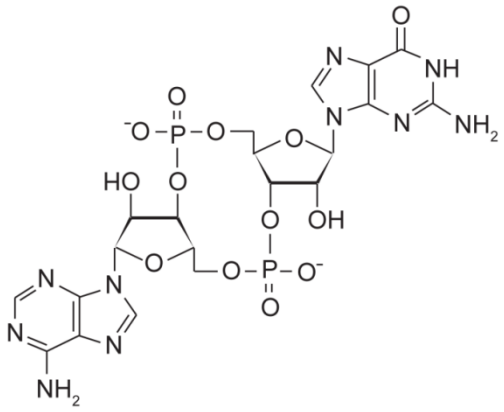

Figure 7: Cyclic GMP-AMP

2.2 THE DISCOVERY OF C-DI-AMP

In 2006, Bejerano-Sagie *et al.* characterized the *B. subtilis* protein YacK in the context of a study on proteins involved in sporulation. The authors found that a knockout of YacK had no effect on cell division, sporulation, competence or on the response to DNA damage. However, upon treatment with the DNA damaging agents nalidixic acid and mitomycin C a YacK knockout strain produced more spores in total, but less viable spores. Based on these findings the authors concluded that YacK participates in a DNA damage checkpoint prior to sporulation and delays checkpoint activation in case of DNA damage. Furthermore it was found that YacK forms a single focus in the cell, co-localized with DNA. This globular focus moves rapidly in the cell until it binds to the site of DNA damage, where it stalls. Accordingly, YacK was renamed DisA (DNA integrity scanning protein A) [20].

Two years later, Witte *et al.* analyzed the DisA protein in detail in a combined structural and biochemical approach. The crystal structure of DisA from *Thermotoga maritima* comprises an N-terminal globular α/β domain of unknown function connected to a helix-hairpin-helix (HhH) domain via a bundle of three α-helices. DisA from *B. subtilis* as well as from *T. maritima* was found to form a homo-octamer with two tetrameric rings assembled head-to-head, whereby the domains of unknown function face each other (Figure 8).

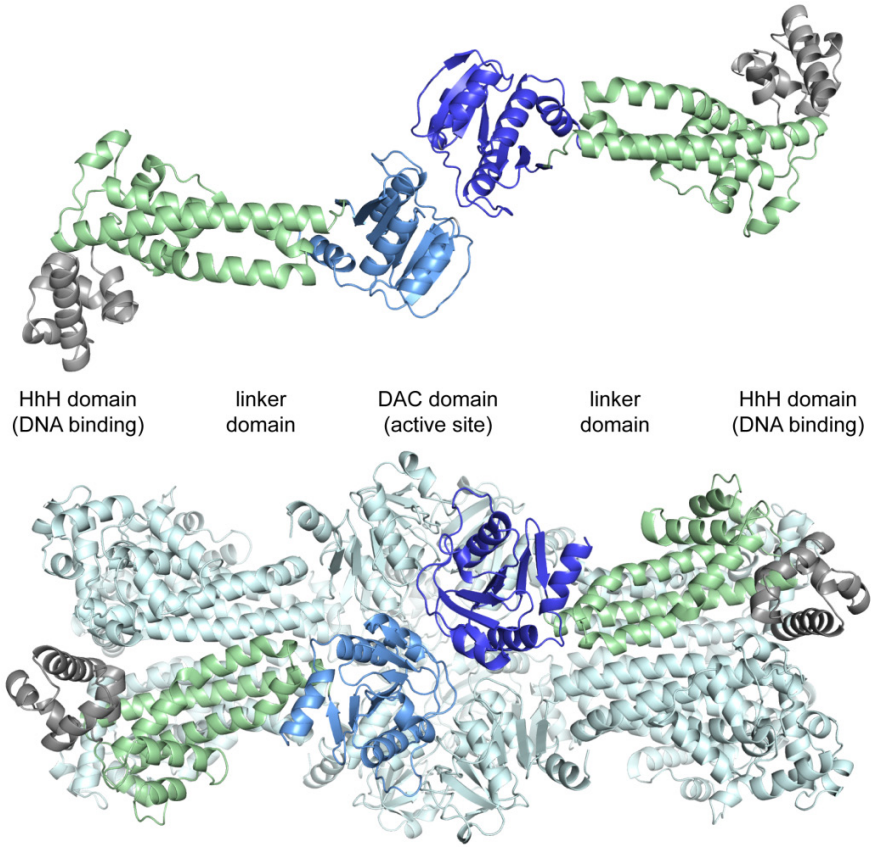

Figure 8: *T. maritima* DisA. **Top**: Two DisA monomers as present in the asymmetric unit of the crystal (coloring according to domains: HhH domain grey, helical linker green, DAC domain blue). **Bottom**: Octameric assembly of DisA (PDB 3c1y [21])

Surprisingly, in the interface between two domains of unknown function an additional electron density was found. Its shape, interacting amino acids and above all mass spectrometry analysis proved this density to belong to cyclic di-AMP (c-di-AMP, Figure 9). Since no nucleotide was added during purification or crystallization of DisA, c-di-AMP had to be co-purified from *E. coli* or synthesized by DisA. Activity assays proved that DisA specifically produces c-di-AMP from ATP and that the domain of unknown function has diadenylate cyclase (DAC) activity. This was the first description of c-di-AMP and the DAC domain is still the only identified domain specifically producing c-di-AMP.

Additionally, it was shown that DisA binds to branched DNA structures such as 3′ and 5′ single-strand flaps and above all three-way and four-way junctions, rather than single- and double-stranded DNA. Moreover, DisA not just binds to these DNA structures but is also inhibited in its DAC activity upon binding [21]. These findings indicate that DisA binds to recombination intermediates or stalled replication forks and signals this DNA damage by decreased c-di-AMP production. Consequently sporulation is delayed until the DNA is repaired and viable spores can be produced. However, the exact mechanism that leads to sporulation delay is still unknown.

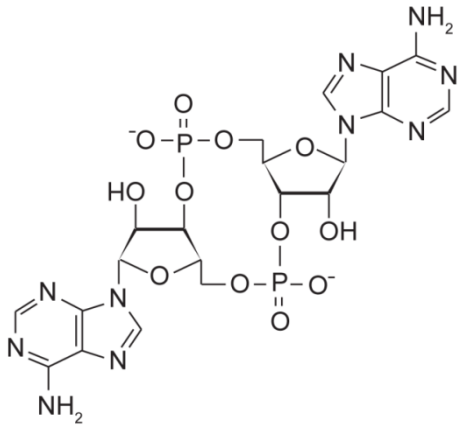

Figure 9: Cyclic di-AMP

2.3 DIADENYLATE CYCLASES

Different proteins comprising a DAC domain were identified bioinformatically in numerous bacteria since its discovery. DAC domain proteins are mainly found in Gram-positive bacteria of the phyla Firmicutes and Actinobacteria, but also in Gram-negative Bacteroidetes, Cyanobacteria, Chlamydiae, Fusobacteria and Deltaproteobacteria and even in archaea of the phylum Euryarchaeota [22]. To date different DAC domain proteins from several bacterial species have also been experimentally proven to produce c-di-AMP; many of these bacteria are well known pathogens (*Listeria monocytogenes* [23], *Staphylococcus aureus* [24], *Streptococcus pyogenes* [25], *Mycobacterium tuberculosis* [26], *Streptococcus pneumoniae* [27], *Bacillus thuringiensis* [28], *Mycobacterium smegmatis* [29] and *Borrelia burgdorferi* [30]).

Aside from DisA, two more major classes of DAC domain containing proteins occur. Homologs of *B. subtilis* YbbP (renamed DacA (diadenylyl cyclase A) [22] or CdaA (c-di-AMP synthase A) [31]) are the most abundant DAC domain proteins, representing 69% of all DACs. YojJ (renamed DacB (diadenylyl cyclase B) or CdaS (c-di-AMP synthase sporulation specific)) proteins represent 6% of all DAC proteins, while 24% are homologs of DisA [22]. The DAC domains from DacA and DacB are very similar (40% sequence identity), while the one from DisA shows larger sequence variability (19% sequence identity compared to DacA or DacB) [32]. Most bacteria have only a single DAC, whereas for example *B. subtilis* possesses three different ones (DisA, DacA and DacB).

DacA comprises three N-terminal transmembrane helices and a C-terminal DAC domain with relatively weak basal activity. However, YbbR from *B. subtilis*

(renamed CdaR, c-di-AMP synthase A regulator) was identified to be an interaction partner of DacA specifically activating its enzymatic activity more than 20-fold [31]. The regulation of CdaR and the mode of its interaction with DacA are however not understood. The expression level of DacA is higher during late exponential and stationary growth phase of *S. aureus* compared to early exponential phase, resulting in an increase of the intracellular c-di-AMP concentration from approximately 2.4 to 8.1 µM [33]. Still, the function of increased c-di-AMP levels in later growth-phases remains to be elucidated. It was suggested that DacA or its DAC activity is involved in the control of cell wall metabolism, but how precisely this regulation might work and how the cell distinguishes between c-di-AMP produced by DacA and the other DAC domain proteins is still unknown. After *T. maritima* DisA, DacA from *L. monocytogenes* is only the second biochemically characterized DAC which's crystal structure was solved [34]. The crystallized construct lacking the N-terminal transmembrane helices has the same fold as the DAC domain from *T. maritima* DisA and only the loop regions differ slightly (Figure 10 A), indicating a highly conserved structure and mechanism of DAC domains, which will be explained in detail in chapter 2.4.

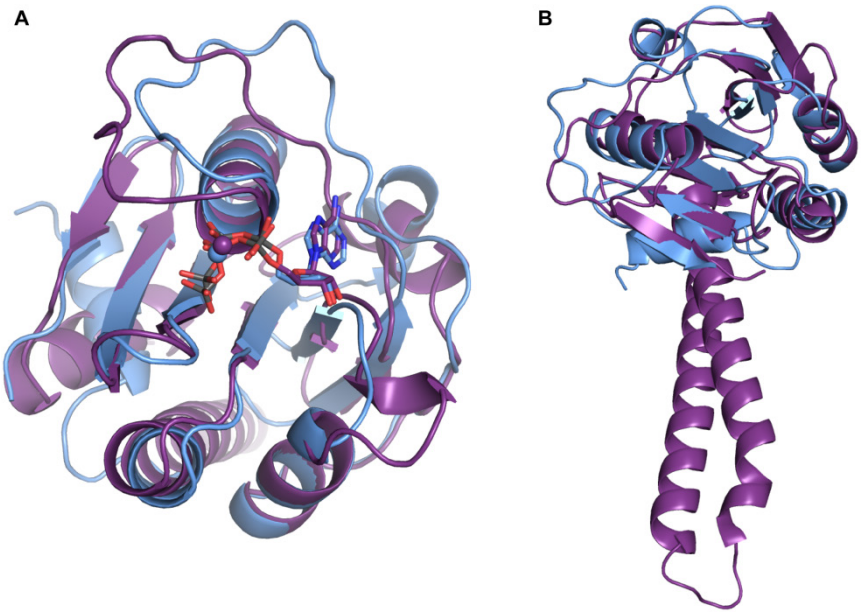

Figure 10: (**A**) DAC domain of *L. monocytogenes* DacA in complex with ATP and Mg^{2+} (purple, PDB 4rv7 [34]) in superposition with the DAC domain from *T. maritima* DisA in complex with 3′-dATP and Mn^{2+} (blue, PDB 4yvz [40]); rmsd 1.25 Å. (**B**) *B. cereus* BC_4920 (purple, PDB 2fb5 [37]) in superposition with the DAC domain of *T. maritima* DisA (blue); rmsd 1.81 Å.

DacB is found exclusively in bacteria of the order Bacillales [22] and is expressed only during sporulation [35]. Consistently, knockout of DacB in *B. subtilis* results in a decrease in germination efficiency [36], the affected pathways are however unknown. DacB comprises a YojJ domain formed by two α-helices N-terminal of the DAC domain. The DacB homolog from *Bacillus cereus* was crystallized, however,

the protein was not biochemically characterized [37]. Still, the typical DAC fold is also conserved in this protein (Figure 10 B). Point-mutations in the α-helical YojJ domain of *B. subtilis* DacB, as well as deletion of this domain, lead to strongly increased DAC activity, indicating a regulatory function. Due to the crystal packing of the *B. cereus* DacB homolog, it was suggested that the protein oligomerizes *via* its YojJ domain also in solution in a manner that prevents the DAC domains from forming functional dimers [31,36]. However, the biological role of this regulation and how the autoinhibitory effect of the YojJ domain is overcome *in vivo* remains to be shown.

DisA is the most active DAC of the three present in *B. subtilis* (DisA 79187 ng c-di-AMP/mg protein; DacA + CdaR 5256 ng c-di-AMP/mg protein; DacB 562 ng c-di-AMP/mg protein) [31], and is at the same time the most abundant DAC (DisA 179-465 proteins/cell; CdaA 60-239 proteins/cell; CdaS expressed only during sporulation) [38]. It was shown that the expression level of DisA is higher during sporulation. This allows screening for DNA damage not only prior to sporulation, but also before germination and outgrowth of the spores and to stall these processes in case of DNA damage [39]. Two different mechanisms of DisA regulation were identified so far. Firstly, the inactivation of DisA upon binding to branched DNA structures, as described in chapter 2.2; secondly, DisA is inactivated by interaction with RadA (radiation-sensitive gene A) [29]. The AAA+ ATPase RadA was found to interact with DisA in *M. smegmatis*, leading to inhibition of the DAC activity. Overexpression of DisA results in reduced motility and growth rate in *M. smegmatis*, which can be overcome by co-expression of RadA – indicating that the *in vitro* findings are of biological relevance [29]. Still, it is unknown how DisA and RadA interact in a manner inactivating DisA and upon which stimulus RadA binds to DisA.

2.4 Synthesis of c-di-AMP

C-di-AMP is synthesized from two ATP molecules, which are cyclized by two 3′-5′ linkages (Figure 9, page 17). Structural and biochemical studies revealed how the substrate ATP is coordinated in the active sites of DisA and DacA, respectively, and which conserved amino acids are essential for the reaction to take place. As shown in Figure 10 (page 18), the DAC domains from *T. maritima* DisA and *L. monocytogenes* DacA are very similar and also the bound nucleotides superimpose well, indicating a common structure and mechanism for all DAC domain proteins.

DAC domains need to dimerize face-to-face in order to form a functional active site, positioning two ATP molecules in the correct orientation for the cyclization to take place. DisA forms a stable octamer in solution, as well as in the crystal structure, with the DAC domains in the center forming four active sites per octamer (Figure 8, page 16) [21,40]. Figure 11 illustrates how two molecules 3′-deoxy ATP (3′-dATP) are bound in the active site of *T. maritima* DisA. The two nucleotides are in ideal orientation for the nucleophilic attack from the 3′ hydroxyl group to the α-phosphate

to take place, while pyrophosphate is released [40]. The DAC domain of *L. monocytogenes* DacA was crystallized with its native substrate ATP, since the crystal packing does not allow formation of functional DAC dimers [34]. Still, the overall structure and position of the nucleotide are very similar, as mentioned before.

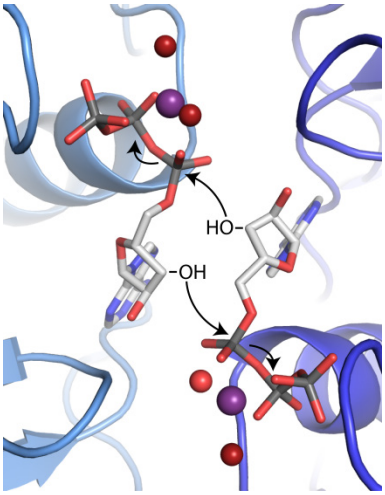

Figure 11: Close-up of one active site of *T. maritima* DisA (two monomers in light and dark blue) bound to 3′-dATP, Mn^{2+} (purple) and selected waters (red); PDB 4yvz [40]

Several highly conserved amino acids in the DAC domain, such as the DGA- and RHR-motifs, are essential for the reaction to take place. These residues were shown to interact with the nucleotides and/or the catalytically essential divalent metal ion [21,34,40,41]. The ion is octahedrally coordinated by Asp 75 belonging to the DGA-motif of the neighboring monomer, the nucleotide's three phosphate groups, which are wrapped around it, and two water molecules (Figure 11) [40]. DisA from *B. subtilis, T. maritima* and *B. thuringiensis* was shown to be active in presence of Mg^{2+} [21,28], while *M. tuberculosis* DisA prefers Mn^{2+} over Mg^{2+} [26]. In contrast, *L. monocytogenes* CdaA is inactive in presence of Mg^{2+} and prefers Co^{2+} over Mn^{2+} [34]. It is still unknown why these very similar DAC domains favor different metal ions.

Two studies with *M. tuberculosis* DisA indicate that the nucleophilic attacks from the 3′ hydroxyl groups to the α-phosphates do not take place simultaneously but rather in a sequential manner and that side-products of the reaction might occur. Analysis of an *in vitro* DAC reaction mixture by liquid chromatography revealed additional compounds next to ATP and c-di-AMP, which might be AMP, ADP and pApA [26] or pppApA [42]. Nevertheless, the dominant reaction taking place is still the formation of c-di-AMP from ATP.

After its synthesis, c-di-AMP is tightly bound in the active site of DisA, as shown already in the first crystal structure where c-di-AMP was present, even though no nucleotide was added during purification or crystallization [21]. This strong binding of c-di-AMP results from the high number of coordinating residues and from the difficult exit through the narrow tunnel connecting the active sites in the center of DisA to the surface of the protein. It seems like the accessibility of the active site, rather than the reaction itself, is the rate limiting step in c-di-AMP synthesis of DisA [40]. So far DisA is the only DAC protein crystallized in an active conformation, therefore the mechanistic details and the way c-di-AMP is released from other DACs might differ.

The di-nucleotidyl cyclase reactions catalyzed by DAC domain proteins, diguanylate cyclases, DncV and also eukaryotic cGAS produce very similar molecules. Still, the DAC domain shares neither its sequence nor fold or reaction mechanisms with the other enzymes. Similar to DACs, DGCs dimerize, whereby the active site is formed at the interface of both monomers. C-di-GMP is then synthesized in a two-step reaction *via* the reaction intermediate pppGpG, whereby the conserved GGDEF motif is involved in binding of GTP as well as Mg^{2+} or Mn^{2+} ions essential for the reaction to take place. Like DisA, also DGCs are rather static during the reaction cycle (reviewed in [12]). Nevertheless, no homology in sequence or structure can be observed between these enzymatic classes.

Even though DncV and cGAS share only low sequence homology, both adapt a very similar nucleotidyl transferase fold. In contrast to DAC and DGC enzymes, both DncV and cGAS are active as monomers and bind ATP and GTP simultaneously in their active sites, performing the cyclase reaction by a two-step mechanism. However, DncV selectively generates 3′-5′-linked cGAMP through the reaction intermediate pppApG [43], while activated cGAS synthesizes a hybrid 2′-5′,3′-5′-linked molecule *via* the intermediate pppG(2′-5′)pA [44,45]. This linear reaction intermediate presumably exits the active site and rebinds in reversed orientation for the second 3′-5′-linkage to be formed [46]. Obviously, the reaction mechanisms as well as the fold of the proteins differ strongly between DACs and DncV/cGAS.

2.5 C-DI-AMP SIGNALING PATHWAYS

Next to its role in DNA damage signaling and sporulation, c-di-AMP was identified to also play a role in various other signaling pathways. Several receptors for c-di-AMP sensing and downstream signal transduction were found in different bacterial species and will be described in the following chapters.

2.5.1 TRANSCRIPTION FACTOR DARR

The first c-di-AMP receptor was identified in *M. smegmatis* in an assay testing predicted transcription regulators for their ability to bind radioactively labeled c-di-AMP [47]. The protein DarR (c-di-AMP receptor regulator) comprises an N-terminal DNA-binding HTH domain and a C-terminal QacR-like receptor domain. DarR was found to specifically bind c-di-AMP with a moderate affinity of K_d = 2.3 µM. Moreover, binding of c-di-AMP increases the affinity of DarR towards its target DNA – a palindromic motif formed by two inverted repeats. Additional DNA binding experiments and analysis of the genome of *M. smegmatis* proved that DarR binds not only to its own promotor, but regulates also the expression of a predicted cold-shock protein, an uncharacterized major facilitator family transporter and a medium chain fatty acyl-CoA ligase. However, DarR is not essential; its knockout only results in an

increased cell length, consistent with c-di-AMP influencing cell wall and membrane metabolism. In contrast, strong overexpression of DarR is toxic for *M. smegmatis*. Comparison of the expression levels of DarR target genes in knockout and mildly overexpressed strains revealed that DarR is a negative regulator of its targets. These results indicate that c-di-AMP signaling is involved in the response to environmental stress, fatty acid metabolism and therefore cell membrane homeostasis, and transport. So far only DarR from *M. smegmatis* was analyzed and shown to act c-di-AMP dependently, however, several conserved homologs of this protein exist in other bacterial species (mycobacteria, *Corynebacterium variabile* and *Rhodococcus erythropolis*). Therefore DarR might not be specific to *M. smegmatis*, but seems not to be a universal c-di-AMP receptor as well [47].

2.5.2 POTASSIUM HOMEOSTASIS

Potassium (K^+) is not only an essential, but also the most abundant cation in cells and its import is crucial due to limited availability. K^+ is important for the activity of different enzymes, osmoregulation, cell volume control and pH homeostasis (reviewed e.g. in [48]). Several proteins involved in K^+ import were found to be c-di-AMP receptors. Corrigan *et al.* performed pull-downs with c-di-AMP coupled beads from *S. aureus* cell lysate and thereby identified three proteins associated to ion transport: KtrA, the cytosolic regulatory part of the KtrAB K^+ transporter, KdpD, a sensor histidine kinase controlling the expression of K^+ uptake systems and virulence factors, and CpaA, a cation/proton antiporter [49].

KtrB is a K^+ channel belonging to the superfamily of K^+ transporters present in bacteria, archaea, fungi and plants. It forms a stable dimer in the cell membrane, whereby each monomer comprises one K^+ channel in its center. KtrA is a cytosolic protein able to bind to KtrB and thereby modulates its activity. It comprises an N-terminal ATP/ADP/NADH binding domain with a Rossman fold and a less conserved C-terminal domain (reviewed e.g. in [50]). KtrA forms an octamer, whereby four dimers are assembled in a ring, interacting with KtrB *via* the N-terminal domains (Figure 12 A). While KtrB alone has weak ion transport activity, it is strongly increased when KtrA binds to the channel and even more, when KtrA is in complex with ATP instead of ADP. It was shown that the *B. subtilis* KtrA octamer adopts a square conformation when bound to ATP and a more oval 'diamond' conformation in complex with ADP due to rotation of the KtrA molecules relative to each other (Figure 12 B). This change is then transduced by a not fully understood mechanism to one of the ion-gate regions of KtrB to activate or inactivate the channel [51]. Interestingly, c-di-AMP does not bind to the N-terminal nucleotide binding domain of KtrA, but specifically to the C-terminal RCK_C domains of *S. aureus* and *B. subtilis* KtrA. Moreover, binding of c-di-AMP leads to inactivation of the channel [49]. Studies with KtrA from *S. pneumoniae* (also called CabP, c-di-AMP binding protein) revealed that KtrA in complex with c-di-AMP is not able to interact with KtrB and thereby leads to

closing of the channel, resulting in measurably reduced K^+ import into the cell [52]. The crystal structure of the RCK_C domain of *S. aureus* KtrA with c-di-AMP bound in a pocket in the dimer interface was solved recently (Figure 12 C) [53]. However, since the structure lacks the N-terminal domain necessary for interaction with KtrB it is not possible to speculate on structural changes leading to dissociation of KtrA from KtrB. In summary, there exist different mechanisms of KtrAB regulation: activation of the channel by binding of ATP-KtrA, mild inactivation in the ADP-KtrA state and strong inactivation upon dissociation of c-di-AMP-KtrA. However, it is unknown if ATP/ADP and c-di-AMP bind to KtrA simultaneously or even in a cooperative manner and what the effect on the KtrB activity state is. Nevertheless, KtrA is clearly important for bacteria to regulate K^+ uptake, as knockout strains are severely inhibited in growth and are more sensitive to hyperosmotic conditions and antibiotics [54].

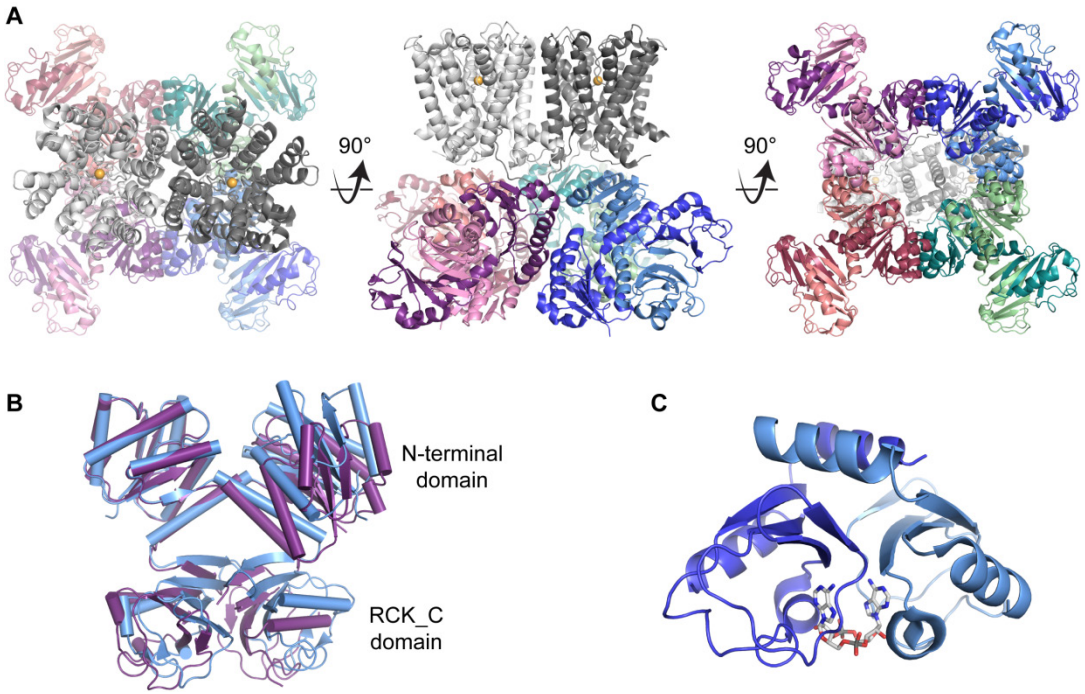

Figure 12: (**A**) KtrAB from *B. subtilis*. The channel KtrB (light and dark grey) with K^+ inside depicted as orange sphere, the KtrA octamer is coloured in green, blue, purple and red (PDB 4j7c [51]). (**B**) *B. subtilis* KtrA dimer in ATP (blue) and ADP (purple) bound state (PDB 4j90 and 4j91, respectively [51]). (**C**) RCK_C domain dimer of *S. aureus* KtrA (light and dark blue) in complex with c-di-AMP (PDB 4xtt [53]).

Aside from KtrA, an additional protein containing an RCK_C domain was identified in *S. aureus*. CpaA (cation/proton antiporter) comprises an N-terminal transmembrane region and a C-terminal RCK_C domain shown to bind to c-di-AMP [49]. CpaA was found to act as an H^+/Na^+ and H^+/K^+ antiporter without any preference for Na^+ or K^+ being imported into the cell. In contrast to KtrAB, binding of c-di-AMP to

the RCK_C domain of CpaA activates the transporter and results in increased ion transport. The crystal structure of CpaA lacking the transmembrane region was solved in complex with c-di-AMP. The overall fold of the crystallized construct is very similar to KtrA and also c-di-AMP is bound in a similar way. Still, the interaction of RCK_C with the transmembrane region remains obscure and it is therefore unknown how c-di-AMP facilitates activation of the transporter [55].

The third ion-homeostasis related c-di-AMP receptor identified in *S. aureus* is the membrane bound sensor histidine kinase KdpD [49]. The KdpD/KdpE system is widely spread among many different bacterial species, also those deficient of c-di-AMP. When bacteria lack K^+ or live in high osmolarity conditions, KdpD autophosphorylates and thereupon phosphorylates KdpE, which in turn activates transcription of the K^+ uptake system KpdFABC (reviewed e.g. in [56]). However, it was shown that the KdpD system has an additional function in *S. aureus*: next to K^+ transporters, KdpD/KdpE also controls the expression of virulence factors in dependence on the K^+ concentration [57]. The specific c-di-AMP binding activity was assigned to a conserved motif in the N-terminal USP domain of KdpD. Furthermore, c-di-AMP binding negatively regulates the expression of the K^+ transport protein KdpA [58]. To date, there is no structural information available on how c-di-AMP binding affects KdpD and how exactly KdpA expression is inhibited. Moreover, the biological function of three different K^+ importers being regulated oppositely, KtrAB and KdpD being inactivated by c-di-AMP and CpaA being inactivated, remains to be investigated.

2.5.3 PstA

PstA (P_{II}-like signal transduction protein A) was identified to bind c-di-AMP in *S. aureus* [49]. P_{II} proteins are a class of proteins omnipresent in bacteria, archaea and plants and are often involved in the regulation of nitrogen metabolism. They are able to sense ligands such as 2-oxoglutarate and/or adenosine nucleotides and initiate subsequent downstream signaling by interaction with transcription factors, transporters and different enzymes. P_{II} proteins share a compact trimeric head domain with a conserved ferredoxin-like fold and large protruding loops for interaction with their target proteins (reviewed e.g. in [59]). PstA from *S. aureus*, *L. monocytogenes* and *B. subtilis* (also called DarA, c-di-AMP receptor A) was analyzed in detail concerning its structural features and c-di-AMP binding characteristics [60–63]. PstA is also trimeric with the typical ferredoxin-like fold (Figure 13 A), but differs from canonical P_{II} proteins regarding the protruding loops, which are swapped in length: the T-loop, which usually comprises approximately 20 amino acids and interacts with target proteins, has only 8 residues, whereas the B-loop has a length of 33 amino acids in PstA compared to approximately 8 residues in P_{II} proteins. PstA selectively binds c-di-AMP with very high affinity (K_D = 109 – 370 nM; $k_a = 6.4 \cdot 10^5$ $M^{-1}s^{-1}$; k_d = 0.07 – 0.08 s^{-1}; numbers from [60] and [61] respectively) and binds only weakly to 3′5′-cGAMP [62]. The crystal structure shows that c-di-AMP is bound in a

positively charged pocket between two subunits (Figure 13 B). The short T-loop, which is flexible in the nucleotide free structure, bends towards the outer adenine moiety, while the inner is deeply buried and specifically recognized by a backbone interaction with N^6 (Figure 13 C). However, the large B-loop is flexible and therefore unresolved in the crystal structure. Still, there is some evidence, that the loop might become more structured upon binding of c-di-AMP. It is unknown whether the movement of the T-loop towards c-di-AMP observable in the crystal structure serves as the downstream signal, or if the large B-loop indeed undergoes structural changes initiating a response. Unfortunately, no interaction partners of PstA were identified so far, and therefore speculation on structural changes of PstA facilitating interaction with target proteins is not possible. It was shown that PstA is not essential in *B. subtilis* [62] and that knockouts show no phenotype in *L. monocytogenes* [63]. However, many bacteria producing c-di-AMP possess PstA [61], therefore this receptor is not universal, but probably still important. The signaling pathway modulated by PstA still needs to be discovered to understand the structural findings in its context.

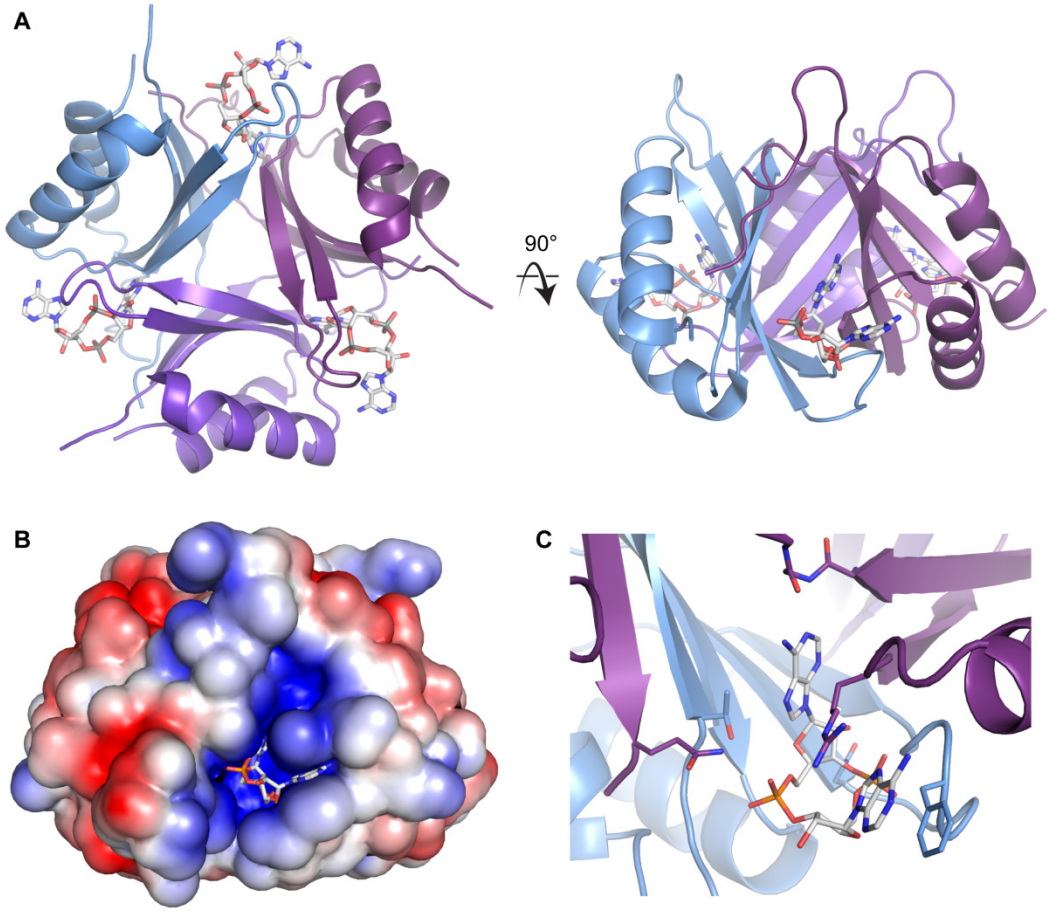

Figure 13: (**A**) Trimeric assembly of *S. aureus* PstA in complex with c-di-AMP. (**B**) Electrostatic surface representation (red: negative charge, blue: positive); c-di-AMP is buried in a positively charged pocket between two subunits. (**C**) Close up of c-di-AMP in its binding pocket (PDB 4wk1 [60]).

2.5.4 YDAO RIBOSWITCH

In addition to the protein receptors described before, the Ydao riboswitch class was identified to specifically recognize c-di-AMP and to regulate gene expression dependent on the second messenger's binding. The YdaO riboswitch class is one of the most common and is present in numerous bacterial species. It is associated with genes involved for example in cell wall metabolism, osmotic stress and sporulation. Moreover, it was shown that the riboswitch specifically binds c-di-AMP with very high affinity ($K_D \leq 0.7$ nM) and acts as a negative regulator of gene expression [64]. The c-di-AMP sensing domains of the YdaO riboswitches from *Thermoanaerobacter tengcongensis*, *Thermoanaerobacter pseudethanolicus* and *Thermovirga lienii* were crystallized in complex with c-di-AMP, elucidating the details of ligand binding [65,66]. YdaO forms a square-shaped pseudosymmetrical structure comprising five helices, a pseudoknot and long range tertiary pairs (Figure 14). Unexpectedly, the riboswitch showed to bind two molecules of c-di-AMP in pseudo two-fold symmetric manner in binding pockets in opposite corners of the square shaped RNA. Upon formation of the structure characteristic for the c-di-AMP bound state, the 3′ expression platform of the riboswitch is able to form a transcription terminator and thereby switches off transcription. In contrast, when YdaO is in its ligand-free state the stem P1 (green in Figure 14) is not formed leading to alternate base pairing, which disrupts the terminator structure [65,66]. Numerous genes are regulated *via* this mechanism and the YdaO riboswitch class is clearly an important and widely spread c-di-AMP receptor.

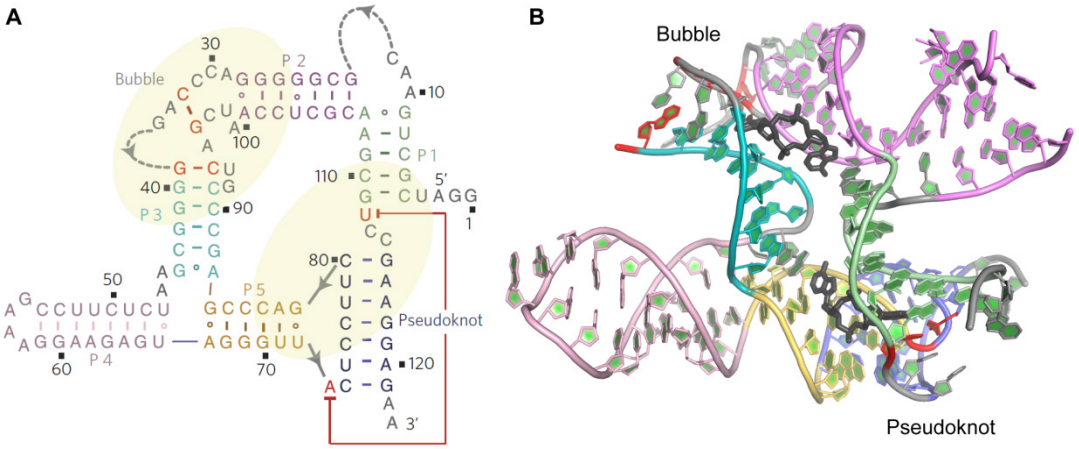

Figure 14: (**A**) Secondary structure of the *T. tengcongensis* YdaO riboswitch as observed in the crystal structure (c-di-AMP binding regions highlighted in yellow). (**B**) Crystal-structure of the riboswitch in complex with c-di-AMP (color code as in A, c-di-AMP grey) (PDB 4qln [65]). Figure adapted from [65].

2.5.5 PYRUVATE CARBOXYLASE

The most recently identified c-di-AMP receptor is the PC (pyruvate carboxylase), shown to bind c-di-AMP in *L. monocytogenes* [67]. The PC is a central metabolic enzyme synthesizing oxaloacetate, a precursor e.g. for amino acid biosynthesis, from pyruvate. Due to its central function, the PC is essential for growth of *L. monocytogenes* intra-, as well as extracellularly [68]. The PC forms a homo-tetramer and comprises four domains per polypeptide chain: the N-terminal biotin carboxylase (BC) domain, the carboxyltransferase (CT) domain, an allosteric or tetramerization (PT) domain and the C-terminal biotin carboxyl carrier protein (BCCP) domain. During the reaction cycle, covalently bound biotin is first carboxylated in the BC active site by ATP and bicarbonate; then the carboxy group is transferred from biotin to pyruvate in the active site of the CT domain to generate oxaloacetate. To facilitate this two-step reaction, the BCCP domain transfers biotin between the two distinct active sites of the BC and CT domains. It was shown that the PC of different species is allosterically activated by acetyl-CoA. Acetyl-CoA binds to the PT domain and activates the PC by decreasing the distance between neighboring active sites [69]. In contrast, c-di-AMP was found to inhibit the *L. monocytogenes* PC allosterically (K_i = 3 μM) [67]. The crystal structure of PC in complex with c-di-AMP revealed that c-di-AMP is bound at the dimer interface of two CT domains, 25 Å away from the CT active sites (Figure 15 A). Comparison with the *apo* form of the enzyme shows major rearrangements of the domains upon ligand binding. In general, the four monomers in *apo* PC have larger variability in respect of their domain orientation and, more specifically, the position of the BC domains relative to the CT domains change upon binding of c-di-AMP (Figure 15 B). The PC needs to undergo large movements during the reaction cycle in order to carry biotin first to the active site of the BC and then to the CT domains, consistent with the less static *apo* structure. Presumably c-di-AMP locks the PC in a conformation incompatible with catalysis [67].

C-di-AMP was shown to reduce the rate of PC dependent amino acid biosynthesis in *L. monocytogenes* resulting in metabolic imbalance; the biological function of this regulatory mechanism is however not understood. Similarly, it is not clear how widely spread the c-di-AMP sensory function of the PC is. The c-di-AMP binding site is poorly conserved; still, it was shown that c-di-AMP inhibits not only the PC from *L. monocytogenes*, but also the one from *Enterococcus faecalis*; the PC from *S. aureus* however, is not responsive to c-di-AMP [67].

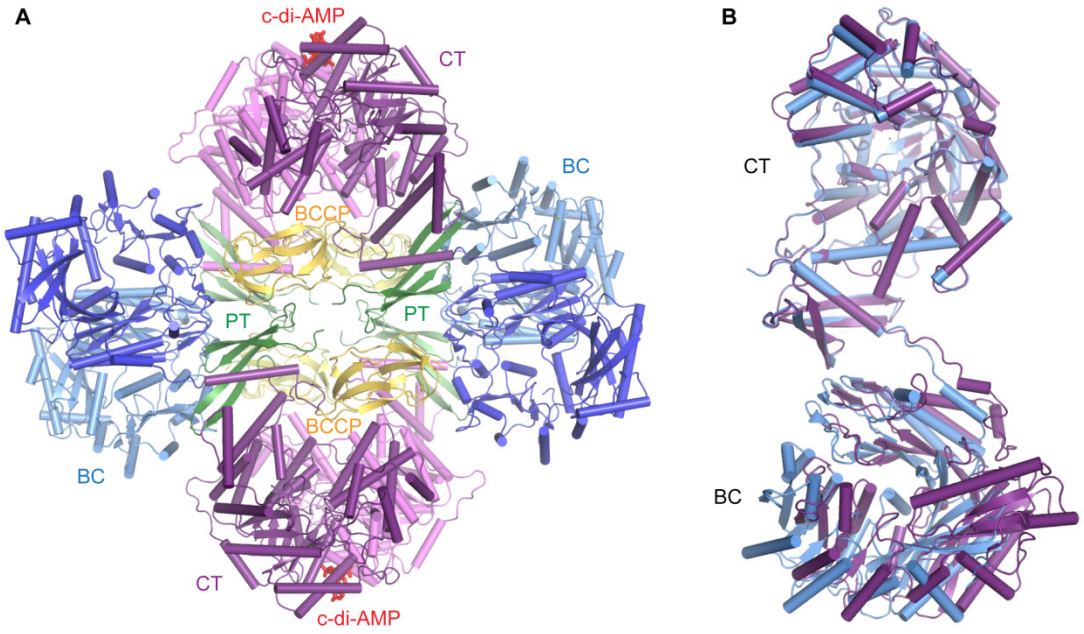

Figure 15: (**A**) *L. monocytogenes* pyruvate carboxylase bound to c-di-AMP (red) in tetrameric assembly (biotin carboxylase domains blue, carboxyltransferase domains purple, tetramerization domains green, biotin carboxyl carrier protein domains yellow; PDB 4qsh). (**B**) Superposition of a PC monomer (CT, PT and BC domains shown) in c-di-AMP bound (blue) and *apo* form (purple) (PDBs 4qsh and 4qsl, respectively [67]).

2.5.6 Crosstalk between c-di-AMP and (p)ppGpp pathways

A link between c-di-AMP pathways and the stringent response second messenger (p)ppGpp was identified, when the *B. subtilis* c-di-AMP phosphodiesterase GdpP was found to be inhibited by (p)ppGpp, resulting in increased intracellular c-di-AMP concentrations (described in detail in chapter 2.6) [70]. More recently, c-di-AMP was found to interact also with (p)ppGpp pathways in *S. aureus* [33]. A GdpP knockout strain with strongly elevated c-di-AMP concentrations was analyzed. Interestingly, this strain exhibits a similar expression pattern as observed during stringent response, with genes e.g. for amino acid synthesis and transport being activated. Moreover, the intracellular concentration of (p)ppGpp is increased in a methicillin resistant strain and even more strongly elevated in methicillin sensitive *S. aureus*. This increase in (p)ppGpp was assigned to the bi-functional (p)ppGpp synthase and hydrolase RSH (also known as RelA). However, the transcription of RSH is not elevated in the GdpP knockout strain and no direct interaction of RSH with c-di-AMP was observed [33]. Therefore the mechanism of c-di-AMP dependent RSH activation is still unknown. In summary, c-di-AMP indirectly activates RSH, which produces more (p)ppGpp. (p)ppGpp in turn inhibits GdpP, leading to increased c-di-AMP levels, activating the RSH even more. However, it is unknown so far how this positive

feedback regulation is stopped and its biological function is also not understood in detail.

Another study describes a very different interplay between c-di-AMP and (p)ppGpp. *L. monocytogenes* expresses only a single DAC protein, DacA, which is essential. However, ΔDacA *L. monocytogenes* strains could be obtained after suppressor mutations were introduced in bacteria grown in macrophages [71]. 94% of these mutations occurred in the oppABCDF operon encoding the oligopeptide permease Opp that lost its function due to the mutations. 2% were loss of function point-mutations in the synthase domain of the bi-functional (p)ppGpp synthase/hydrolase RelA. RelA synthesizes (p)ppGpp in response to starvation and is at the same time the only (p)ppGpp hydrolase present in *L. monocytogenes*, while two additional synthases (RelP and RelQ) with low basal activity exist. Despite a weak growth defect, knockout of RelA as well as of all three (p)ppGpp synthases (ΔRelAPQ) made DacA dispensable. In contrast, a conditional depletion of DacA in wild type *L. monocytogenes* resulted in strongly increased (p)ppGpp levels also under non-starvation conditions and a severe growth defect. This led to the conclusion that DacA is essential due to toxic accumulation of (p)ppGpp in its absence. Interestingly, the ΔRelAPQ strain not dependent on DacA exhibited reduced virulence. The link between virulence and (p)ppGpp levels was searched *via* suppressor mutations. The mutant strain most similar to wild type bacteria harbored a loss of function mutation in the negative transcription regulator CodY [71]. It was shown already before that when *L. monocytogenes* comprises high intracellular levels of (p)ppGpp, GTP synthesis is strongly inhibited. However, GTP is a cofactor of CodY, which becomes inactive when it is not bound to this nucleotide. Consequently, inactive CodY does not repress transcription of its target genes anymore. Among the numerous genes usually repressed by CodY are for example those needed for adaptation to lack of nutrients, but in *B. subtilis* also the oppABCDF operon (reviewed in [72]). Consistently, knockout of CodY leads to constitutive expression of the genes usually repressed. Surprisingly, in the ΔRelAPQΔCodY mutant strain DacA was found to be essential, implying that genes expressed in absence of CodY are toxic in the absence of c-di-AMP [71]. To summarize, in *L. monocytogenes* c-di-AMP reduces (p)ppGpp levels via an unknown mechanisms. These low (p)ppGpp concentrations lead to indirect activation of the negative transcription regulator CodY, which represses transcription of genes which are toxic in absence of c-di-AMP. It is however not known which gene products might be toxic in cells lacking c-di-AMP.

In contradiction to the finding that c-di-AMP reduces the concentration of (p)ppGpp described by [71], another study showed that *L. monocytogenes* lacking its c-di-AMP PDE PgpH has increased levels of (p)ppGpp due to accumulation of c-di-AMP [73]. This is consistent with the findings in *S. aureus* that c-di-AMP and (p)ppGpp regulate each other positively [33]. The interplay between c-di-AMP and (p)ppGpp clearly needs to be studied in more detail to properly evaluate the previously described findings.

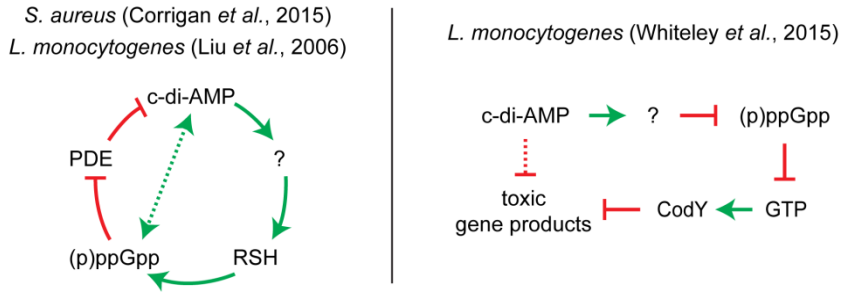

Figure 16: Overview on the crosstalk between c-di-AMP and (p)ppGpp

2.6 C-DI-AMP DEGRADATION

Controlled degradation of c-di-AMP is as important as the regulation of its synthesis. Three different types of c-di-AMP specific phosphodiesterases (PDE) have been identified in several bacterial species: Homologs of *B. subtilis* GdpP (GGDEF domain protein containing phosphodiesterase, formerly YybT; PdeI in *S. pneumoniae*, PdeA in *L. monocytogenes*) comprise N-terminal trans-membrane helices, a regulatory PAS domain, a degenerated GGDEF domain and C-terminal DHH/DHHA1 domains for c-di-AMP hydrolysis [24,27,70,74,75]. In addition, a shorter version of this protein lacking the N-terminal domains is present in several bacterial species [27,30,76,77]. The third type of c-di-AMP PDE identified in *L. monocytogenes* comprises an extracellular 7TMR-HDED domain, a transmembrane region and the intracellular c-di-AMP hydrolyzing HD domain [78] (Figure 17).

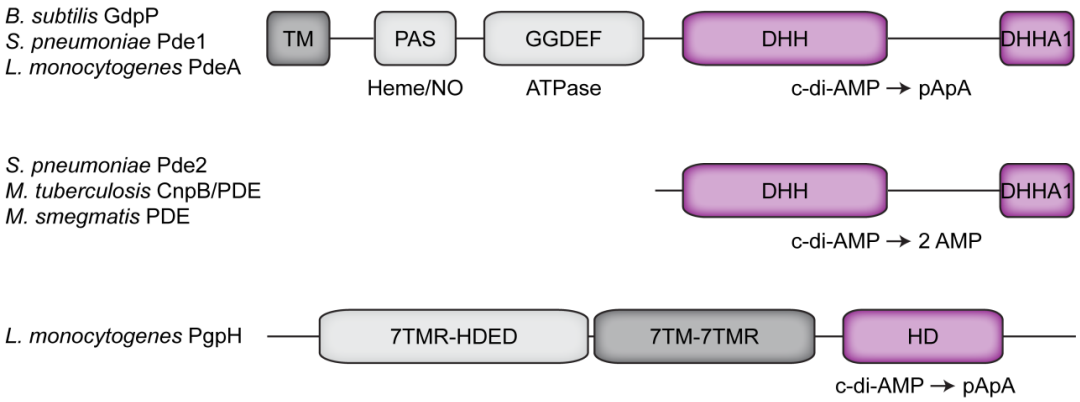

Figure 17: Domain organization of different c-di-AMP phosphodiesterases (TM = transmembrane helices).

B. subtilis GdpP was the first c-di-AMP PDE identified [70]. The c-di-AMP degrading activity was assigned to the C-terminal DHH/DHHA1 domains that hydrolyze c-di-AMP, and less efficiently also c-di-GMP, exclusively to the linear product 5′-pApA. The enzymatic activity is dependent on Mn^{2+} and several conserved amino acids presumably involved in its coordination [24,70]. The N-terminal transmembrane helices anchor the protein to the cell-membrane. The correct localization of GdpP seems to be important for its function, as was shown in *S. pyogenes* [75]. The GGDEF domain C-terminal to the DHH/DHHA1 domains is usually associated with c-di-GMP synthesis. However, in GdpP this domain is highly modified compared to canonical GGDEF proteins and lacks the characteristic amino acid motif. It was shown that the GGDEF domain of *B. subtilis* GdpP has weak ATPase activity; it is however unknown what the biological significance of this activity might be [70].

The small N-terminal PAS (Per-ARNT-Sim) domain was shown to regulate c-di-AMP hydrolysis. PAS domains in general are known to be redox, oxygen or carbon monoxide (CO) sensors in different proteins. The PAS domains from *Geobacillus thermodenitrificans* and *B. subtilis* GdpP were analyzed in detail regarding their ligand binding characteristics [79]. The purified protein was found to contain low amounts of type B heme and could be reconstituted to bind heme in a 1:1 stoichiometry. Heme bound GdpP was found to be less active than *apo* GdpP, indicating a regulatory function of heme. Moreover, GdpP in complex with Fe(II) heme is able to bind NO (nitric oxide), CO and CN^- (cyanide), while oxidized Fe(III) heme only binds to CN^-. NO, as well as CN^-, weakly activate heme-GdpP in both, oxidized and reduced state. NO, being a reactive nitrogen species synthesized by the mammalian immune system in order to kill bacteria, likely represents the physiological ligand of heme-GdpP. Therefore the PAS domain of GdpP seems to function as a sensor for heme or NO, which might act as markers for the mammalian host environment [79]. The NMR structure of the PAS domain from *G. thermodenitrificans* GdpP was elucidated and revealed a hydrophobic pocket for heme binding (Figure 18) [80]. Heme was shown to be bound in a hexacoordinated state in the PAS domain, while Fe(II)-NO heme is pentacoordinated, implying that an amino acid dissociates from heme upon NO binding [70]. However, a suitable ligand, such as histidine or cysteine, was not identified so far and the exact mechanism of inactivation or activation of GdpP upon binding of Heme(-NO) is not understood. While *B. subtilis* GdpP lacking the PAS domain was shown to be less active than the full-length protein (full-length *B. subtilis apo*

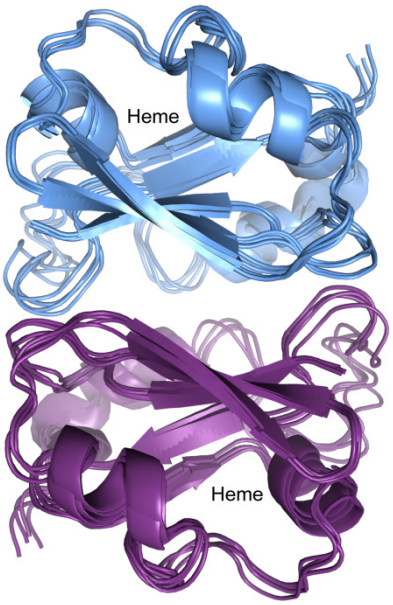

Figure 18: NMR structure of dimeric PAS domain of *G. thermodenitrificans* GdpP (PDB 2m1c [80])

GdpP: k_{cat} = 0.55 s^{-1}, K_m = 1.3 µM; holo-GdpP k_{cat} = 0.024 s^{-1}, K_m = 16 µM; ΔPAS *B. subtilis* GdpP: k_{cat} = 0.074 s^{-1}, K_m = 3 µM) [70,79], a study with the homologous *S. pneumoniae* Pde1 showed that a truncated version of the protein lacking the PAS domain has the same activity as the full-length enzyme [27]. Clearly, the PAS domain needs to be studied in context of the whole protein to fully understand the mechanism of PDE activity regulation.

There is evidence, that the expression levels of *B. subtilis* GdpP are higher during sporulation and that GdpP expression depends on the presence of DisA [20]. However, another study shows that GdpP is constitutively expressed during the whole growth cycle of *S. aureus* [33]. There might be species specific differences in the expression pattern of GdpP, which need to be further analyzed to understand the biological function of its regulation. Surprisingly, the stringent response second messenger ppGpp was found to act as a competitive inhibitor of GdpP (*B. subtilis*: apparent IC_{50} = 234 µM, K_I = 36 µM; *S. aureus* K_I = 130 µM; intracellular ppGpp concentration > 1 mM). ppGpp is known to signal starvation in bacteria and presumably also leads to an increase in the c-di-AMP concentration by inhibition of its degradation [33,70]. Further details on the crosstalk between c-di-AMP and (p)ppGpp pathways were given already in chapter 2.5.6, page 28.

After the DHH/DHHA1 domains were identified to hydrolyze c-di-AMP, proteins comprising only these domains and lacking the transmembrane helices and the GGDEF and PAS domains were found in different bacterial species. In contrast to GdpP, *S. pneumoniae* Pde2, *M. tuberculosis* CnpB or PDE and *M. smegmatis* PDE, which are all homologous despite their different names, specifically hydrolyze c-di-AMP and pApA to AMP. PDEs from this class are dimeric and, like GdpP, depend on Mn^{2+} [27,42,76,77]. Little is known about the mechanism of c-di-AMP or pApA hydrolysis. The conserved DHH and DxD motifs presumably coordinate Mn^{2+} and are therefore essential for catalysis. *S. pneumoniae* Pde2 was shown to prefer pApA over c-di-AMP (pApA V_{max} = 334 nmol $mg^{-1}min^{-1}$; c-di-AMP V_{max} = 49 nmol $mg^{-1}min^{-1}$). Nevertheless, knockouts of the GdpP homolog Pde1 and also Pde2 result in comparably decreased intracellular c-di-AMP levels in *S. pneumoniae*, therefore Pde2 also possesses c-di-AMP hydrolyzing activity *in vivo* [27]. *Borrelia burgdorferi* DhhP, the only characterized PDE from a Gram negative bacterium, comprises the same DHH/DHHA1 domain organization as the enzymes described previously. However, it was shown to produce pApA rather than AMP from c-di-AMP. Moreover, DhhP is essential *in vivo* as well as *in vitro*, unlike other PDEs investigated so far [30].

The third class of c-di-AMP PDEs contains only one characterized enzyme so far. *L. monocytogenes* PgpH comprises an extracellular 7TMR-HDED domain, seven transmembrane helices and an intracellular HD domain. The HD domain belongs to a superfamily containing also c-di-GMP PDEs; the HD domain from PgpH however was shown to strongly prefer c-di-AMP over c-di-GMP to synthesize the linear product pApA. Like the DHH/DHHA1 domain PDEs also PgpH depends on Mn^{2+}, which is

coordinated by the characteristic His-Asp motif (Figure 19). Interestingly, ppGpp was found to inhibit PgpH allosterically (IC_{50} = 200-400 µM), in contrast to GdpP, which is inhibited competitively [78]. However, the binding site of ppGpp and the way it inhibits the enzyme was not identified so far. *L. monocytogenes* possesses two c-di-AMP PDEs: next to PgpH it has a GdpP homolog named PdeA providing a PAS-GGDEF-DHH/DDHA1 domain architecture as described previously [74]. However, PgpH seems to be the major PDE, since a knockout of PgpH has a larger effect on the amount of c-di-AMP secreted by *L. monocytogenes* than a knockout of PdeA has [78]. Even though only one member of HD domain c-di-AMP PDEs was characterized so far, this class of PDEs seems to play an important role in c-di-AMP hydrolysis. Homologs of *L. monocytogenes* PgpH were identified in 36% of all DAC containing bacteria, among them also species shown to comprise also a DHH/DHHA1 PDE, for example *B. subtilis* [78].

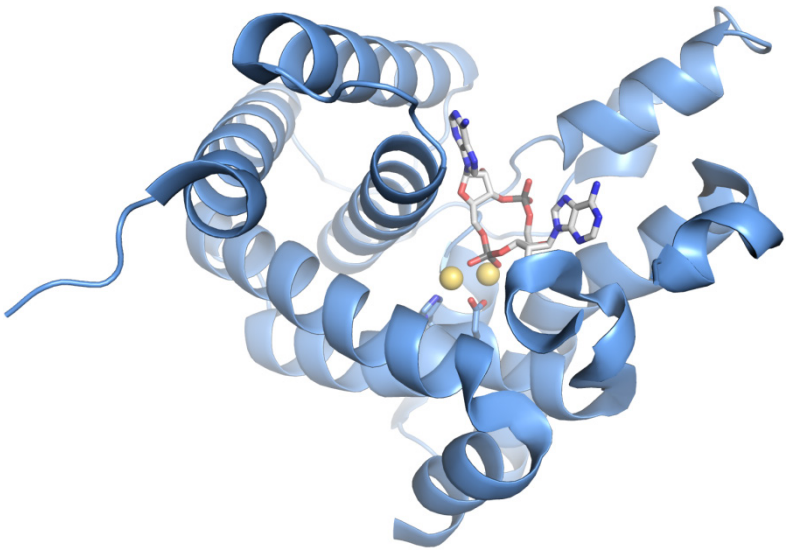

Figure 19: HD domain of *L. monocytogenes* PgpH in complex with c-di-AMP and two Fe(II) ions shown as yellow spheres, HD motif as sticks (PDB 4s1b [78])

2.7 THE IMPORTANCE OF C-DI-AMP IN BACTERIA

Overexpression and knockouts of DACs and PDEs lead to increased or reduced cellular c-di-AMP levels with characteristic and severe phenotypes. Many of them are not understood in detail and cannot be assigned to specific pathways yet. Moreover, in all but one c-di-AMP synthesizing species, which were analysed so far, c-di-AMP was found to be essential. In *B. subtilis* double knockouts of DisA and DacA are not possible [31,81] and knockouts of the single DAC domain proteins in *L. monocytogenes* [23,71,74], *S. pyogenes* [25], *S. pneumoniae* [27] and *S. aureus* [33] showed to be lethal

as well. Therefore the effects of decreased c-di-AMP levels were investigated either by conditional depletion of DACs or by overexpression of PDEs, both resulting in similar phenotypes. As described already in chapter 2.2 (page 15), knockout of *B. subtilis* DisA results in production of non-viable spores upon introduction of DNA damage [20] and renders the cells more sensitive to DNA damaging agents [82]. These effects most likely represent DisA specific phenotypes and not a general result of the lack of c-di-AMP. Concerning the overall cell characteristics, low c-di-AMP levels lead to slower bacterial growth in *L. monocytogenes* and *S. aureus* [33,74], while faster growth was observed in methicillin resistant *S. aureus* (MRSA), a phenotype usually associated with decreased antibiotic resistance in this species [83]. Similarly, less intracellular growth of *L. monocytogenes* was observed also in host cells [74]. Furthermore, decreased levels of c-di-AMP seem to have a destabilizing effect on the bacterial cell wall, as more cell lysis occurred in *B. subtilis* and *L. monocytogenes* [74,81], while S. aureus was shown to form incomplete septa [33] and M. smegmatis produces less fatty acids [77]. Consequently, bacteria lacking c-di-AMP are more susceptible towards cell wall targeting antibiotics such as β-lactams. This has been shown for *B. subtilis*, *L. monocytogenes* and MRSA [74,81,83,84]. *M. tuberculosis* is the only species identified so far, where c-di-AMP was found to be not essential. A knockout of its only DAC could be generated and the bacteria subsequently had a growth defect and a more virulent phenotype [76,85].

An increase in c-di-AMP levels by DAC over-expression or PDE knockout also leads to severe phenotypes. In *B. subtilis* an elevated c-di-AMP concentration results in rapid entry into sporulation [41] and more spores are produced after generation of DNA damage [70]. Additionally, several phenotypes regarding growth and morphology were described for different species after increasing the c-di-AMP concentration. *B. subtilis* [31], *M. smegmatis* [29], *S. pneumoniae* [27], *S. aureus* [33] and *L. monocytogenes* [78] have a slower growth rate upon increase in c-di-AMP concentrations and similarly *M. tuberculosis* [85] and *L. monocytogenes* [78] were shown to grow more slowly or not at all in host cells. Reduced cell size was observed in *S. aureus* [24], *S. pneumoniae* [27] and *M. tuberculosis* [76], while *M. smegmatis* [29,77] and *B. burgdorferi* [30] show elongated cells due to defective cell division. In addition, *B. subtilis* forms curled cell filaments [31] and *M. smegmatis* cells aggregate and are less motile [29,77]. Consistently, *S. aureus* produces more biofilms upon an increase in c-di-AMP levels [24]. The effect of high c-di-AMP concentration on the bacterial cell wall is complementary to the phenotypes observed in c-di-AMP depleted cells. High c-di-AMP levels lead to more cross-linked peptidoglycane in *S. aureus* and compensate for lipoteichoic acid depletion [24]. Furthermore, *L. monocytogenes* comprises a thicker cell wall [84] and increased acid resistance [74], which is also true for *B. subtilis* [70]. As a result of the more robust cell wall bacteria with high c-di-AMP levels are more resistant to cell wall antibiotics, as was shown for *S. aureus* [24,86], *B. subtilis* [81], *S. pyogenes* [75] and *L. monocytogenes* [74,84]. Nevertheless, an increase in c-di-AMP concentration leads to a less virulent phenotype in *S. pyogenes* [75], *S.*

pneumoniae [27], *M. tuberculosis* [76,85], *B. burgdorferi* [30] and *L. monocytogenes* [78]. There exists one exception to the phenotypes described before: *B. burgdorferi*, the only Gram negative species producing c-di-AMP characterized in detail so far, does not show increased resistance to antibiotics upon an increase in c-di-AMP levels and is the only species for which was shown that the PDE is essential [30].

The phenotypes observed after increase or decrease of c-di-AMP levels concern sporulation, cell growth and morphology, virulence and above all the cell wall and antibiotic resistance. Even though neither the cellular pathways modulated by c-di-AMP to result in these phenotypes, nor the key mechanism making c-di-AMP essential are understood in detail, it is obvious that the intracellular concentration of c-di-AMP needs to be precisely regulated. This is why DAC inhibitors have been suggested as new antimicrobial drugs. Two compounds inhibiting DisA were investigated so far (Figure 20). Bromophenol thiohydantoin (bromophenol TH) was identified as a DisA inhibitor during the screening of a whole library of small molecules. The inhibitor presumably acts allosterically with an IC_{50} of approximatey 100 µM [87]. The second inhibitor identified, 3′-dATP, is a competitive inhibitor of *T. maritima* DisA and likely also other DACs, since it is a non-reactive substrate analog binding in the active site of DisA (Figure 10 and Figure 11, pages 18-20). 3′-dATP inhibits DisA with an IC_{50} of 3 µM [40] and has previously been shown to inhibit growth of Clostridium species [88]. Since 3′-dATP is an ATP analog it probably affects many different enzymes, but DACs are certainly among them. Moreover, the pro-drug 3′-deoxy adenosine, which is phosphorylated to 3′-dATP in the cell, is also tested in cancer therapy in clinical trials.

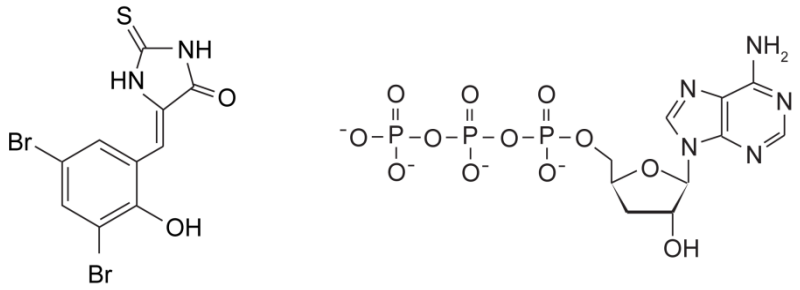

Figure 20: The two DisA inhibitors identified so far, Bromophenol-TH [87] and 3′-dATP [40]

2.8 C-DI-AMP IN EUKARYOTES

2.8.1 INTRACELLULAR BACTERIA

L. monocytogenes and *M. tuberculosis* are intracellular pathogens able to replicate also in eukaryotic host cells. *L. monocytogenes* possesses multidrug efflux pumps (MDR) for export of small molecules, often prerequisite for antibiotic resistance. It was however shown that the bacterium also secretes c-di-AMP with the help of its MDRs into the cytosol of its host cell [23,89]. A clear correlation between the amount of produced and subsequently secreted c-di-AMP and the intensity of the host cell's immune response, measured *via* the interferone-β (IFN-β) concentration, was observed. In particular, knockdown of DACs and therefore reduced c-di-AMP levels lead to less IFN-β production, while DAC overexpression or PDE knockout results in elevated IFN-β levels, compared to infections with wild type bacteria. It was shown that *L. monocytogenes* secrets c-di-AMP via its MDRs; it is however unknown how *M. tuberculosis* exports the nucleotide. Still, both species initiate enhanced IFN-β synthesis in response to increased levels of c-di-AMP. High induction of IFN-β expression is associated to a less virulent bacterial infection [74,76,78,85]. Similarly, less c-di-AMP leads to reduced IFN-β production and a more virulent phenotype of *M. tuberculosis* [76,85]; however, the opposite was shown for *L. monocytogenes*. In this species low c-di-AMP levels destabilize the bacterial cell wall and therefore promote cell lysis. Consequently, bacterial DNA and other molecules are released into the host cytosol and lead to a strong immune response [74]. This shows that c-di-AMP acts as a PAMP (pathogen-associated molecular pattern) triggering the host immune response. However, the effects of c-di-AMP up- or down-regulation on the bacteria, as well as on the host, differ in a species specific manner.

2.8.2 SENSING OF C-DI-AMP BY EUKARYOTES

In order to react to the PAMP c-di-AMP, the immune system needs a suitable pattern recognition receptor (PRR) to initiate an immune reaction. STING (stimulator of interferon genes) as well as the DEAD box helicase DDX41 were identified to sense c-di-AMP. STING comprises an N-terminal transmembrane domain anchoring the protein in the membrane of the endoplasmic reticulum, and a C-terminal ligand binding domain. After binding of an activating ligand, STING relocates to punctuate perinuclear vesicular compartments where it recruits and activates the kinase TBK1. TBK1 in turn phosphorylates IRF3, which activates transcription of type I interferons (reviewed e.g. in [90,91]). It was shown that STING is essential for interferon expression in response to infection with *L. monocytogenes*, *Chlamydia trachomatis* and *M. tuberculosis*, all of these pathogens producing c-di-AMP [85,92,93]. Indeed, cyclic dinucleotides, such as c-di-AMP, c-di-GMP and cGAMP were identified to bind to the C-terminal domain of STING and activate the protein [94,95]. Upon binding of the

nucleotides, the two C-terminal domains of dimeric STING move closer together and form a lid closing the binding pocket (Figure 21) [96]. Still, the exact mechanism of STING activation is not understood. Interestingly, STING recognizes not only bacterial cyclic dinucleotides, but is also activated by an endogenous signal. The cytosolic DNA sensor cGAS synthesizes non-canonical 2′-5′cGAMP, which serves as an activator of STING, in response to binding to double stranded DNA derived from pathogens or cellular damage [97]. Therefore STING acts as a direct sensor of cyclic dinucleotides produced by pathogenic bacteria, as well as a link between cytosolic DNA sensing and the subsequent immune response. Like this, STING integrates two different ways of pathogen recognition making it a key protein in innate immune response.

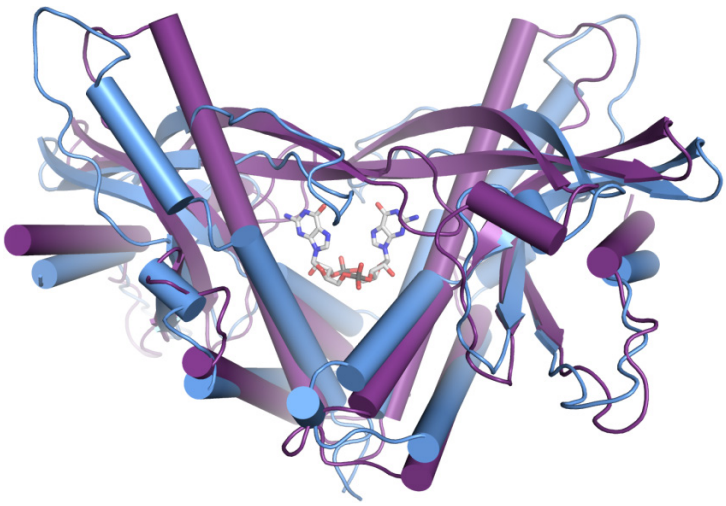

Figure 21: Dimeric C-terminal domain of human STING in *apo* (blue) and c-di-GMP bound (purple) state, c-di-GMP is shown as sticks (PDBs 4f5e and 4f5d [96])

In addition to STING, a second PRR for c-di-AMP was identified – the DEAD box helicase DDX41. This protein senses not only c-di-AMP and c-di-GMP, but also DNA, with its DEAD box domain [98,99]. Similar to STING, knockdown of DDX41 results in reduced interferon expression in response to c-di-AMP, c-di-GMP and DNA, as well as pathogenic bacteria such as *L. monocytogenes* and *M. tuberculosis* [85,98,99]. Moreover, DDX41 was shown to co-localize and interact with the transmembrane domain of STING *via* its DEAD box domain after activation with DNA or cyclic dinucleotides [98,99]. DDX41 and cGAS/STING seem to have a similar function and it is not entirely understood how the interplay between both pathways works. DDX41 binds c-di-GMP with higher affinity than STING and might therefore have a function upstream of STING [99]. Clearly the DDX41 pathways and its interaction with STING need to be studied further to understand how c-di-AMP sensing by the immune system works in detail. Interestingly, c-di-AMP was shown to act as an adjuvant when co-administered with an antigen, suggesting another medically relevant function of this molecule [100].

3 PUBLICATIONS

3.1 REACTION MECHANISM AND INHIBITION OF DISA

Müller, M., Deimling, T., Hopfner, K.-P. and Witte, G. (2015) Structural analysis of the di-adenylate cyclase reaction of DNA-integrity scanning protein A (DisA) and its inhibition by 3′-dATP. Biochemical Journal. 469 (3), 367-374

DOI: 10.1042/BJ20150373

http://www.biochemj.org/content/469/3/367

The accepted manuscript of the publication is included in this thesis.

In this publication, the reaction mechanism of *T. maritima* DisA and an inhibitor of this enzyme are described. The active site of DisA shows to be highly conserved when compared to different DAC domain proteins, and several amino acids essential for the reaction to take place were identified. The crystal structures of DisA in complex with non-reactive substrate analogs as well as the reaction product c-di-AMP show the coordination of the nucleotides and the catalytically essential metal ion. The comparison of the different reaction states reveals that DisA does not undergo movements during the reaction cycle; therefore DisA catalyzes the reaction by positioning of the two ATP molecules in the correct orientation. Presumably, the c-di-AMP synthesis rate is limited by the narrow tunnels connecting the active sites to the surface of the protein, making it difficult for c-di-AMP to exit the active site. *In vitro* activity assays support these structural findings. Additionally, the non-reactive substrate analog 3′-dATP was found to act as a potent competitive inhibitor of DisA. Since c-di-AMP is essential in DAC domain containing bacteria, c-di-AMP pathways might be promising targets for antimicrobial therapy.

Author contribution

I purified DisA, crystallized it in complex with 3′-dATP/Mn^{2+} and c-di-AMP and solved and interpreted the structures. Furthermore, I analyzed the oligomeric state of DisA by size-exclusion chromatography, static light scattering and SAXS. Additionally, I investigated the activity of different mutant proteins I generated and tested the inhibitory effect of 3′-dATP on DisA. I wrote the manuscript together with G. Witte. Experimental design and data analysis was supported by G. Witte.

Structural analysis of the di-adenylate cyclase reaction of DNA-integrity scanning protein A (DisA) and its inhibition by 3′-dATP

Martina Müller*, Tobias Deimling*, Karl-Peter Hopfner*† and Gregor Witte*‡

* Gene Center and Department of Biochemistry, Ludwig-Maximilians-Universität, 81377 Munich, Germany
† Center for Integrated Protein Sciences, Munich, Germany

‡ To whom correspondence should be addressed:
Gregor Witte
Gene Center (LMU)
Feodor-Lynen-Str. 25
D-81377 Munich, Germany
Tel.:+49 (0) 89 2180 76988
e-mail: witte@genzentrum.lmu.de
web: http://www.grk1721.genzentrum.lmu.de/gregor-witte/

Running title: Structural analysis of the DisA reaction mechanism

Keywords: c-di-AMP, crystal structure, DAC domain, reaction-mechanism, inhibition

Summary statement:
Structures of *T. maritima* DisA protein in different reaction states describe the di-adenylate-cyclase reaction and the possibility of its inhibition. We conclude that the mechanisms of cyclic-di-AMP synthesis and its inhibition are conserved among different DAC enzymes and bacterial species.

ABSTRACT
The identification of the essential bacterial second messenger cyclic-di-AMP synthesized by the DNA-integrity scanning protein DisA opened up a new and emerging field in bacterial signaling. To further analyze the di-adenylate cyclase reaction catalyzed by the DAC domains of DisA, we crystallized *Thermotoga maritima* DisA in presence of different ATP analogs and metal ions to identify the metal binding site and trap the enzyme in pre- and post-reaction states. Through structural and biochemical assays we identified important residues essential for the reaction in the active site of the DAC domains. Our structures resolve the metal binding site and thus explain the activation of ATP for the DAC reaction. Moreover, we were able to identify a potent inhibitor of the DAC domain. Based on the available structures and homology to annotated DAC domains we propose a common mechanism for c-di-AMP synthesis by DAC domains in c-di-AMP producing species and a possible approach for its effective inhibition.

INTRODUCTION

Nucleotide second messengers are widely spread throughout all domains of life. Bacteria in particular are known to use cyclic AMP, cyclic GMP, cyclic-di-GMP and (p)ppGpp in order to regulate the most different signaling pathways. In 2008, however, an additional secondary messenger was found: cyclic-di-AMP (c-di-AMP). C-di-AMP was initially identified in the crystal structure of the *Thermotoga maritima* sporulation checkpoint protein DNA integrity scanning protein A (DisA) [1], and was subsequently shown to be produced by a variety of enzymes containing a diadenylate-cyclase (DAC) domain. DAC domain proteins are mainly found in Gram-positive bacteria belonging to the phyla Firmicutes and Actinobacteria, including pathogenic bacteria such as *Listeria monocytogenes* or *Staphylococcus aureus*. The DAC prototype protein DisA forms a homooctameric complex, composed of two head-to-head tetrameric rings. The catalytic active sites are located at the interface between the two tetramers, whereby two opposing monomers form one reaction center. These DAC domains are connected to the C-terminal DNA-binding HhH motifs by a long spine consisting of three antiparallel α-helices.

So far little is known about the mode, function and regulation of bacterial c-di-AMP signaling. DisA was found to bind to branched DNA, such as replication intermediates or stalled replication forks, and its enzymatic activity is thereupon inhibited, suggesting a role in DNA-damage signaling [1, 2]. In agreement with these findings, it was shown that reduced c-di-AMP levels cause a delay in sporulation in *Bacillus subtilis*, whereas an elevated c-di-AMP concentration promotes sporulation [3]. Additionally, in *B. subtilis* CdaS was identified as a DAC domain protein expressed only during sporulation. The third DAC protein in *B. subtilis*, CdaA, is activated through interaction with CdaR and is presumably involved in control of cell wall biosynthesis [4]. Additional studies showed that c-di-AMP is involved in the regulation of cell-wall characteristics and cell size in *S. aureus* and *B. subtilis* [5, 6]. Although the DAC domain is widespread, the pathways regulated by c-di-AMP are so far not well understood. A genome-wide screen identified several proteins in *S. aureus* (KtrA, CpaA, KdpD and PstA) that act as c-di-AMP receptors, thereby linking c-di-AMP to potassium transport [7, 8]. Very recently, the mode of c-di-AMP recognition by PstA/DarA, which is structurally related to the class of P_{II}-like proteins, was elucidated [9-12] suggesting that additional cellular processes are regulated by c-di-AMP. Moreover, it was shown that c-di-AMP is a high affinity ligand for the ydaO riboswitch, explaining why c-di-AMP affects such a wide range of processes and linking c-di-AMP to the regulation of gene expression involved in peptidoglycan synthesis, germination and osmotic shock response in bacteria [13, 14]. Although the details of c-di-AMP signaling are poorly understood, it is nevertheless obvious that the cellular levels of c-di-AMP need to be tightly regulated. Total knockouts of DAC domain proteins in *B. subtilis, L. monocytogenes* and *S. pneumoniae* are lethal [6, 15, 16]. Similarly, an increase or decrease in c-di-AMP concentrations by overexpression or knockouts of DAC domain proteins or c-di-AMP degrading phosphodiesterases, respectively, severely impairs bacterial growth and affects the virulence of pathogenic bacteria [4, 15, 16]. More specifically, it was shown that a decrease of the cellular c-di-AMP concentration renders bacteria more sensitive towards β-lactam antibiotics [6]. Based on this, DAC domain proteins might prove to be promising targets for antibiotic therapies.

In this study we have structurally analyzed the reaction mechanism of *T. maritima* DisA for the synthesis of c-di-AMP. We crystallized DisA in presence of different substrate analogs and metal ions, and are thus able to show the pre- and post-catalytic states of the reaction cycle. We were able to pinpoint the essential divalent cation binding site and identified catalytically important residues. Using *in vitro* activity assays we analyzed the impact of mutations in the active site. We were additionally able to identify a potent, commercially-available DAC inhibitor. A structural- and sequence-based comparison of the active sites of known DAC domains suggests that our findings can probably be directly transferred to other c-di-AMP producing enzymes and help to understand their activity and regulation.

EXPERIMENTAL PROCEDURES

Cloning, expression and protein purification

His-tagged *T. maritima* DisA was cloned and recombinantly expressed as reported previously [1]. Primers used for protein mutant generation are included in the supplementary data (supplementary table S1). For protein purification cells were lysed by sonication in buffer A (50 mM Tris-HCl, 300 mM NaCl, 10 mM imidazole, pH 8.0). After centrifugation, the supernatant was applied to a Ni-NTA column (Qiagen) and extensively washed with buffer A and buffer W (50 mM Tris-HCl, 1 M NaCl, 20 mM imidazole, pH 8.0). Protein was eluted using buffer B (50 mM Tris-HCl, 300 mM NaCl, 250 mM imidazole, pH 8.0) and DisA-containing fractions were pooled and dialyzed against SEC buffer (20 mM Tris, 200 mM NaCl, pH 8.0). The protein was applied to a Superdex 200 preparative-grade size-exclusion column (GE Healthcare) and the fractions were analyzed by SDS-PAGE. Fractions containing only DisA were pooled and concentrated. The protein was flash-frozen in liquid nitrogen and stored at -80°C until usage.

Crystallization

1 µL of DisA (8 mg mL^{-1}) in SEC buffer with 2 mM of nucleotide and 20 mM $MgCl_2$ was mixed with 1 µL of reservoir solution (30 - 32.5 % (v/v) MPD, 200 mM ammonium acetate and 100 mM Tris-HCl pH 8.0 - 8.3). Crystals were grown within 7 days at 15°C through hanging-drop vapor diffusion. Reservoir solution containing 35 % (v/v) MPD was used as cryo-protectant prior to flash-cooling crystals in liquid nitrogen. For crystals containing manganese, 0.2 M $MnCl_2$ was added to the cryo-solution and crystals were soaked for a few seconds.

Crystallographic data collection, processing and refinement

Diffraction data were collected at the beamlines SLS X06SA (Paul-Scherrer Institute, Villigen, Switzerland) and PETRA-3 P14 (EMBL c/o DESY Hamburg, Germany) at 100K. Diffraction data were processed using XDS and XSCALE [17]. Molecular replacement was performed using the apo DisA structure (PDB code 3c1z) as a search model in PHASER [18] within the CCP4 suite [19]. Structure refinement comprised automatic refinement steps using PHENIX [20] and manual building in COOT [21]. All structures show typical statistics for the resolution (Table 1). The coordinates and structure factors have been deposited in the PDB with the accession codes 4yvz, 4yxj and 4yxm. Figures of crystal structures were generated using PyMOL [22], the tunnels shown in figure 3A were computed and displayed with CAVER Analyst [23].

Small-angle X-ray scattering (SAXS)

SAXS data were collected at EMBL/DESY Hamburg beamline X33. Protein samples after size exclusion chromatography and centrifugation were measured at different concentrations between 1 and 5 mg mL^{-1}. Before and after each sample the corresponding buffer was measured and used for buffer correction. No sample showed signs of aggregation or radiation damage and scattering data were processed and analyzed using programs of the ATSAS package [24] as described e.g. in [25]. Theoretical scattering curves of crystal structures were calculated using CRYSOL [26].

Size-exclusion coupled static light scattering (SEC-RALS)

Size-exclusion coupled static light scattering was performed using an ÄKTAmicro system (GE Healthcare Life Sciences) equipped with a RI-device and right-angle laser light scattering detector (RALS, Viscotek/Malvern Instruments) with a Superdex S200 10/300 size-exclusion column (GE Healthcare). BSA (66 kDa) was used as standard protein for calibration. Analysis of data was performed using the Viscotek Software OmniSEC.

DAC activity assays

Photometric di-adenylate-cyclase assays were performed similar to [27] in an optimized reaction buffer (50 mM glycin/NaOH pH 9.5, 50 mM NaCl, 10 mM $MgCl_2$, 0.3 mM ATP, 0.1 mU yeast pyrophosphatase (Thermo Scientific)) in a total volume of 50 µL. The ATP concentration was optimized in order to perform all assays under substrate saturating conditions. The inhibitor 3′-dATP (Jena Biosciences) was used in the concentrations indicated (0-150 µM). The reactions were started by addition of 24 nM *T. maritima* DisA (monomer concentration) and incubated at 60°C for 30 min. Reactions were stopped by addition of 100 µL BIOMOL Green reagent (Enzo) and absorbance at 620 nm was measured after 15 min in a platereader (Tecan M1000 Pro). The absorbance of a control without DisA was subtracted in order to calculate normalized activities. At least three independent experiments of all activity assays were performed to calculate standard deviations. The IC50 was determined using Prism (GraphPad Software).

RESULTS AND DISCUSSION

The DAC domain

The DAC domain is so far the only fold that has been show to specifically catalyze the reaction of two ATP molecules to c-di-AMP and both, its active site residues and fold, are highly conserved. Figure 1A shows a sequence comparison of the prototype *T. maritima* DisA N-terminus and the three encoded DACs of *B. subtilis* (DisA, CdaA and CdaS), in addition to DAC domains from various other species previously described in the literature. In good agreement with data from [1, 28], highly conserved residues of two opposing subunits, such as the DGA (residues 75-77, numbering referring to *T. maritima* DisA) and RHR motifs (residues 108-110), form the reaction center.

Previous *in vivo* experiments by Oppenheimer-Shaanan et al. showed that GFP-labeled DisA D75N, demonstrated to be inactive in DAC assays, abolished foci formation in *B. subtilis* as observed for the wildtype before [2]. This suggests that DisA D75N might not form the octamers essential for its activity [3]. We crystallized the TmaDisA mutant D75N and both the overall structure of DisA D75N and crystal packing are virtually identical to the wild-type DisA protein. To analyze the oligomeric state of DisA D75N in solution we performed size-exclusion chromatography coupled light scattering (SEC-RALS, Fig. 1B) and small-angle X-ray scattering (SAXS) experiments (Fig. 1C). DisA D75N elutes in a single peak with a molecular weight determined by SEC-RALS of $M_w^{SECRALS}$ D75N = 339 kDa, showing that the mutant protein still forms an octamer under the conditions used ($M_w^{theoretical\ octamer}$ = 336 kDa). The molecular parameters determined by SAXS (M_w^{SAXS} = 360 kDa, R_g = 5.5 ± 0.1 nm) and the shape of the scattering curve are only compatible with a homogenous octameric species ($Rg^{theoretical,\ unhydrated}$ = 5.34 nm). Thus, DisA D75N is still octameric in solution and the inactivity is instead due to changes in the active site.

Pre-reaction states

We solved the structure of DisA in complex with a non-reactive ATP analog (3′-dATP, cordycepin triphosphate) and $MnCl_2$ in order to trap the enzyme in the pre-reaction state and to identify the metal binding site. Manganese was chosen as a substitute for magnesium to allow us to identify the metal ion and distinguish it from well-coordinated water molecules by its anomalous signal. The ion is octahedrally coordinated with all six coordination positions occupied by oxygen ligands (Fig. 2A). The three phosphate groups from 3′-dATP together with Asp75 from the adjacent subunit and two water molecules are all located between 2.0 and 2.5 Å from the manganese, in good agreement with its ideal coordination distance. The 3′-dATP phosphate groups are bent around the metal ion, with the β- and γ-phosphate being additionally held in place via hydrogen bonds with Arg108

and His109 from the highly conserved RHR motif and Arg130. Thr107 interacts with the α-phosphate and additionally contacts ^{7}N of the adenine (also contacted by Leu94), and Thr111 forms a hydrogen bond with ^{6}N. The ribose is contacted at O4′ by Arg108 and at 2′-OH by backbone interactions with Gly76. The γ-phosphate is mainly polarized by Ser127, Arg128 and Arg130 facilitating the nucleophilic attack on the α-phosphate (see also supplementary table S2 and figure S1).
In summary, the pre-reaction state shows a highly coordinated arrangement of the two ATP (-analogs) in almost optimal distance for the nucleophilic attack of the 3′-OH on the α-phosphate of the neighboring ATP. The α-phosphate is well coordinated and additionally stabilized by the positive dipole of helix α5. In good agreement with these observations, point mutations of selected active site residues (Asp75, RHR motif 108-110, Arg130, Thr107, Thr111) lead to significantly decreased DAC activity of DisA *in vitro* (Fig. 2B and S2), proving the biological relevance of the structural features observed.
As 3′-dATP lacks the attacking hydroxyl group we crystallized DisA in the presence of the non-hydrolyzable ATP analog ApCpp (adenosine-5′-[(α,β)-methyleno]triphosphate). The structure of the DisA-ApCpp complex is highly similar to the structure with 3′-dATP (overall rmsd 1.2 Å) and only the phosphate groups adopt a slightly different orientation (Fig. 2C), presumably because the ApCpp complex structure lacks the metal ion coordinated by the phosphates. The distance between the 3′-hydroxyl group and the α-phosphate of 4.6-4.9 Å is consequently relatively large. The α-phosphate, however, probably moves closer towards the 3′-OH when interacting with a metal ion (as observed in the 3′-dATP structure), facilitating the nucleophilic attack, as implied by the structure with 3′-dATP and $MnCl_2$.
Interestingly, our attempts to crystallize DisA D75N, shown to be fully inactive in DAC-assays, with the native substrate ATP/Mg^{2+} unexpectedly produced crystals with unambiguous density for c-di-AMP bound in the active site (Fig. 2D). Obviously, the much longer time-scale of crystallization (compared to *in vitro* assays) allows the reaction to occur to a significant extent. Probably the correct orientation of the ATP nucleotides still takes place due to the high number of stabilizing interactions within the DAC site, even though the main interaction partner for ion-coordination (carboxyl-group of Asp75) is missing. Apparently, even imperfect binding of the nucleotides and their respective orientation is sufficient for the reaction to take place on the long time-scale of crystallization.

Post-reaction state

The first structural report of DisA described the product state in which c-di-AMP is bound, even though no nucleotide was added to the crystallization condition [1]. This indicates that the reaction product is tightly bound in the active site with very slow off-rate kinetics, even though c-di-AMP is less well coordinated than ATP, since most interactions in the reaction center occur with the three phosphate groups rather than the adenine or sugar moieties (Fig. 2D and supplementary table S3). In comparison, the product state only shows coordination of c-di-AMP by the DGA motif (residues 75-77), Thr107 and Thr111. We analyzed the accessible surface and cavities of DisA in order to identify the possible substrate and product release paths (Fig. 3A). A likely reason for the slow release of c-di-AMP from the active site is the size of the tunnel that leads from the reaction center to the surface. This has a bottleneck diameter of approximately 7.8 Å (supplementary figure S3), which is just large enough to allow c-di-AMP to pass through. To exit the DisA molecule, c-di-AMP has to first move to the center of DisA and then to the side, passing the loop connecting β5 and β6 (Arg128-130) of the DAC domain and finally to the surface, covering a total distance of approximately 40 Å. In figure 3A one of the possible paths c-di-AMP needs to follow is indicated. Since DisA is a symmetric octamer, c-di-AMP from any active site can of course exit by any of the eight tunnels. Due to the fact that we only observe snapshots in our

crystal structures, we cannot exclude a certain degree of "breathing" of the octameric assembly that might lead to other exit pathways. To test for flexibility of DisA we calculated a simulation of protein structure fluctuation [29] of one monomer and found only small predicted movements in loops on the surface, showing that DisA is very rigid and thereby indicating that the tunnels observed in the static crystal structure are probably similar in solution (supplementary figure S4). However, upon mutating the three arginine residues 128-130 in the loop that c-di-AMP needs to pass to exit the molecule to less bulky amino acids (R128-130A), the activity of DisA increases approximately 2-fold, even though Arg130 is a major factor in coordination of the γ-phosphate of ATP and the single mutation (R130A) is almost completely inactive (Fig. 2B). This indicates that the rate-limiting step of c-di-AMP synthesis by DisA is not defined by the reaction itself, but rather by the accessibility of the active site.

Structural comparison of the DAC reaction states and DAC domains

A comparison of apo-, pre- and post-reaction states in a superposition shows no major structural changes of DisA (Fig. 3B). Based on the structures, no small-scale movements of domains or loops can be observed, supporting the idea that binding and coordination of ATP/Mg^{2+} seems to be sufficient for the DAC reaction to take place. To test our hypothesis that DAC domains share this reaction site we superimposed the DAC domains of DisA (3′-dATP complex) and the recently reported structure of *L. monocytogenes* CdaA in complex with ATP [28] (Fig 3C). Both DAC domains show virtually identical arrangement of motifs and also the nucleotides superimpose very well (rmsd 1.25 Å) as previously observed for a DAC domain from *B. cereus* [1]. The CdaA construct used in [28] obviously does not form active dimers in DAC-to-DAC orientation and thus crystallized in presence of the native substrate ATP/Mg^{2+}, thereby supporting our pre-reaction state structure containing 3′-dATP (see above).

Inhibition of DisA

C-di-AMP synthesis is essential for bacteria, as shown through numerous failed attempts to knock out all DAC domain proteins in different species. Similarly, a decrease of the cellular c-di-AMP concentration renders bacteria more sensitive towards β-lactam antibiotics [6]. These findings suggest that DAC domain proteins may be promising targets for antibiotic therapy. Cordycepin (3′-deoxy-adenosine) is a natural adenosine analog produced by the fungus Cordyceps, which has been identified to offer a large variety of medically beneficial effects, such as anti-tumor, anti-inflammatory and anti-bacterial effects (e.g. reviewed in [30]). Inside the cell, cordycepin is phosphorylated to 5′-mono-, di- or tri-phosphate and subsequently interferes with different essential pathways (e.g. reviewed in [31]). Since cordycepin triphosphate (3′-dATP) is a non-reactive substrate analog for DisA that traps the enzyme in the pre-reaction state (see above), we investigated its effect on the *in vitro* DAC activity. We found commercially available 3′-dATP to be an effective inhibitor of DisA with an inhibitory constant (IC50) of 3 μM when 26 nM DisA and 300 μM ATP were used (Fig. 4A). Interestingly, it has already been shown that cordycepin isolated from Cordyceps fungi is able to inhibit growth of Clostridium species with similar efficiency as conventional antibiotics such as tetracycline and chloramphenicol [32]. This antibacterial effect is likely due to cordycepin affecting various essential cellular pathways as a nucleoside analog, probably also including those that require DAC activity. 3′-dATP is the second DisA inhibitor to be identified following bromphenol thiohydantoin (TH) [33]. In the bromphenol-TH activity assays significantly different concentrations of DisA and ATP were used for determination of the inhibitory constant, thus the inhibitory effectiveness of 3′-dATP versus bromphenol-TH cannot be directly compared between our study and [33]. The two inhibitors are furthermore likely to have different modes of action. The crystal structure shows that while 3′-dATP is a competitive inhibitor that binds in the same

position as ATP (Fig. 2A), bromphenol-TH seems to be an allosteric inhibitor that binds close to a tryptophan residue. The exact binding site for bromphenol-TH remains unknown and while it might be specific for DisA, the DAC domains from different proteins are highly conserved in their active site residues and we thus postulate that 3′-dATP has the potential to inhibit not only DisA but also other DAC domain proteins.

Hypothesis on the regulation of DisA

DisA recognizes recombination intermediate DNA structures via its HhH motifs and upon binding these DNAs displays strongly reduced or abolished DAC activity. The current model for the down-regulation of DisA is based on the fact that the HhH domains at the DisA C-terminus need to rearrange in order to be able to bind to DNA. This rearrangement and rotation of the DNA-binding motif is probably translated by the helical spine domain leading to changes in the orientations of the DACs and thus to their inactivation. So far we were not able to crystallize a DisA-DNA complex or identify these DisA/Holliday-junction complexes in electron microscopy, making it hard to predict which molecular rearrangements might lead to signaling or loss of DAC activity. In order to obtain a smaller version of DisA we created a F57R mutant of TmaDisA that was supposed to form tetramers, as the F57R mutation disturbs the DAC dimer-interfaces. However, depending on the salt concentration this mutant also forms lower oligomeric species, as observed in SEC experiments (Fig. 4B). This finding is in good agreement with the interactions between the helical spine domains being mainly ionic and suggests that once the DAC domains are disrupted by HhH-induced structural changes upon DNA binding, DisA might become unstable and dissociate. Dissociation and/or degradation of DisA as a result of the DNA complex formation would be a reasonable explanation of the measurable decrease in c-di-AMP levels in the cells upon DisA sensing DNA-damages [3] as it would affect more than one DisA. It would probably be impossible for the cell to sense the presence of recombination intermediates by just a single DisA being down regulated, while 25-50 other DisA-octamers [34, 35] and also CdaA and CdaS remain active in the cell. Of course, we might lack effector proteins that specifically recognize the DisA-DNA complex and amplify the signal, e.g. by RadA interaction [36, 37] or up-regulation of a c-di-AMP phosphodiesterase. However, the exact mechanism of regulation remains to be shown, as there is currently no structural information about the DisA-DNA or proposed DisA-RadA complexes.

In summary, our structural and biochemical analysis provides a model for the reaction mechanism of DNA-integrity scanning protein A that can probably be transferred to any other bacterial DAC domain protein because of structural and sequence similarity. Moreover, we were able to show that a commercially-available nucleotide analog that has also been shown to affect various other essential processes in the cell is also a potent inhibitor of c-di-AMP synthesis. The fact that c-di-AMP levels have been reported to influence e.g. MRSA antibiotic resistance renders the c-di-AMP pathway an interesting new target for antimicrobial therapy.

ACKNOWLEDGEMENTS

We thank the staffs of SLS X06SA and EMBL Hamburg X33/P14 for on-site help and discussions, Robert Byrne for comments on the manuscript and the Hopfner group for discussions.

AUTHOR CONTRIBUTIONS

Martina Müller and Tobias Deimling performed and evaluated experiments, Karl-Peter Hopfner supported experimental design and evaluation, Gregor Witte evaluated data, directed the work and prepared the manuscript with the help of Martina Müller.

FUNDING

This work was funded by grants from the Deutsche Forschungsgemeinschaft (DFG) to Gregor Witte (WI3717/2-1) and GRK1721 to Gregor Witte and Karl-Peter Hopfner; Martina Müller and Tobias Deimling are supported by GRK1721.

REFERENCES

1 Witte, G., Hartung, S., Büttner, K. and Hopfner, K. P. (2008) Structural biochemistry of a bacterial checkpoint protein reveals diadenylate cyclase activity regulated by DNA recombination intermediates. Molecular cell. 30, 167-178

2 Bejerano-Sagie, M., Oppenheimer-Shaanan, Y., Berlatzky, I., Rouvinski, A., Meyerovich, M. and Ben-Yehuda, S. (2006) A checkpoint protein that scans the chromosome for damage at the start of sporulation in Bacillus subtilis. Cell. 125, 679-690

3 Oppenheimer-Shaanan, Y., Wexselblatt, E., Katzhendler, J., Yavin, E. and Ben-Yehuda, S. (2011) c-di-AMP reports DNA integrity during sporulation in Bacillus subtilis. EMBO reports. 12, 594-601

4 Mehne, F. M., Gunka, K., Eilers, H., Herzberg, C., Kaever, V. and Stülke, J. (2013) Cyclic di-AMP homeostasis in bacillus subtilis: both lack and high level accumulation of the nucleotide are detrimental for cell growth. The Journal of biological chemistry. 288, 2004-2017

5 Corrigan, R. M., Abbott, J. C., Burhenne, H., Kaever, V. and Gründling, A. (2011) c-di-AMP is a new second messenger in Staphylococcus aureus with a role in controlling cell size and envelope stress. PLoS pathogens. 7, e1002217

6 Luo, Y. and Helmann, J. D. (2012) Analysis of the role of Bacillus subtilis sigma(M) in beta-lactam resistance reveals an essential role for c-di-AMP in peptidoglycan homeostasis. Molecular microbiology. 83, 623-639

7 Bai, Y., Yang, J., Zarrella, T. M., Zhang, Y., Metzger, D. W. and Bai, G. (2014) Cyclic di-AMP impairs potassium uptake mediated by a cyclic di-AMP binding protein in Streptococcus pneumoniae. Journal of bacteriology. 196, 614-623

8 Corrigan, R. M., Campeotto, I., Jeganathan, T., Roelofs, K. G., Lee, V. T. and Gründling, A. (2013) Systematic identification of conserved bacterial c-di-AMP receptor proteins. Proceedings of the National Academy of Sciences of the United States of America. 110, 9084-9089

9 Campeotto, I., Zhang, Y., Mladenov, M. G., Freemont, P. S. and Gründling, A. (2014) Complex Structure and Biochemical Characterization of the Staphylococcus aureus cyclic di-AMP binding Protein PstA, the Founding Member of a New Signal Transduction Protein Family. The Journal of biological chemistry

10 Choi, P. H., Sureka, K., Woodward, J. J. and Tong, L. (2015) Molecular basis for the recognition of cyclic-di-AMP by PstA, a PII-like signal transduction protein. MicrobiologyOpen

11 Gundlach, J., Dickmanns, A., Schroder-Tittmann, K., Neumann, P., Kaesler, J., Kampf, J., Herzberg, C., Hammer, E., Schwede, F., Kaever, V., Tittmann, K., Stülke, J. and Ficner, R. (2014) Identification, characterization and structure analysis of the c-di-AMP binding PII-like signal transduction protein DarA. The Journal of biological chemistry

12 Müller, M., Hopfner, K. P. and Witte, G. (2015) c-di-AMP recognition by Staphylococcus aureus PstA. FEBS letters. 589, 45-51
13 Gao, A. and Serganov, A. (2014) Structural insights into recognition of c-di-AMP by the ydaO riboswitch. Nature chemical biology. 10, 787-792
14 Ren, A. and Patel, D. J. (2014) c-di-AMP binds the ydaO riboswitch in two pseudo-symmetry-related pockets. Nature chemical biology. 10, 780-786
15 Bai, Y., Yang, J., Eisele, L. E., Underwood, A. J., Koestler, B. J., Waters, C. M., Metzger, D. W. and Bai, G. (2013) Two DHH subfamily 1 proteins in Streptococcus pneumoniae possess cyclic di-AMP phosphodiesterase activity and affect bacterial growth and virulence. Journal of bacteriology. 195, 5123-5132
16 Witte, C. E., Whiteley, A. T., Burke, T. P., Sauer, J. D., Portnoy, D. A. and Woodward, J. J. (2013) Cyclic di-AMP is critical for Listeria monocytogenes growth, cell wall homeostasis, and establishment of infection. mBio. 4, e00282-00213
17 Kabsch, W. (2010) Xds. Acta crystallographica. Section D, Biological crystallography. 66, 125-132
18 McCoy, A. J., Grosse-Kunstleve, R. W., Adams, P. D., Winn, M. D., Storoni, L. C. and Read, R. J. (2007) Phaser crystallographic software. Journal of applied crystallography. 40, 658-674
19 Winn, M. D., Ballard, C. C., Cowtan, K. D., Dodson, E. J., Emsley, P., Evans, P. R., Keegan, R. M., Krissinel, E. B., Leslie, A. G., McCoy, A., McNicholas, S. J., Murshudov, G. N., Pannu, N. S., Potterton, E. A., Powell, H. R., Read, R. J., Vagin, A. and Wilson, K. S. (2011) Overview of the CCP4 suite and current developments. Acta crystallographica. Section D, Biological crystallography. 67, 235-242
20 Afonine, P. V., Grosse-Kunstleve, R. W., Echols, N., Headd, J. J., Moriarty, N. W., Mustyakimov, M., Terwilliger, T. C., Urzhumtsev, A., Zwart, P. H. and Adams, P. D. (2012) Towards automated crystallographic structure refinement with phenix.refine. Acta crystallographica. Section D, Biological crystallography. 68, 352-367
21 Emsley, P. and Cowtan, K. (2004) Coot: model-building tools for molecular graphics. Acta crystallographica. Section D, Biological crystallography. 60, 2126-2132
22 Schrödinger, LLC. (2010) The PyMOL Molecular Graphics System, Version 1.3r1
23 Chovancova, E., Pavelka, A., Benes, P., Strnad, O., Brezovsky, J., Kozlikova, B., Gora, A., Sustr, V., Klvana, M., Medek, P., Biedermannova, L., Sochor, J. and Damborsky, J. (2012) CAVER 3.0: A Tool for the Analysis of Transport Pathways in Dynamic Protein Structures. PLoS Comput Biol. 8, e1002708
24 Petoukhov, M. V., Franke, D., Shkumatov, A. V., Tria, G., Kikhney, A. G., Gajda, M., Gorba, C., Mertens, H. D., Konarev, P. V. and Svergun, D. I. (2012) New developments in the program package for small-angle scattering data analysis. Journal of applied crystallography. 45, 342-350
25 Putnam, C. D., Hammel, M., Hura, G. L. and Tainer, J. A. (2007) X-ray solution scattering (SAXS) combined with crystallography and computation: defining accurate macromolecular structures, conformations and assemblies in solution. Quarterly reviews of biophysics. 40, 191-285
26 Svergun, D., Barberato, C. and Koch, M. H. J. (1995) CRYSOL - a Program to Evaluate X-ray Solution Scattering of Biological Macromolecules from Atomic Coordinates. Journal of applied crystallography. 28, 768-773
27 Chan, C., Paul, R., Samoray, D., Amiot, N. C., Giese, B., Jenal, U. and Schirmer, T. (2004) Structural basis of activity and allosteric control of diguanylate cyclase. Proceedings of the National Academy of Sciences of the United States of America. 101, 17084-17089

28 Rosenberg, J., Dickmanns, A., Neumann, P., Gunka, K., Arens, J., Kaever, V., Stülke, J., Ficner, R. and Commichau, F. M. (2015) Structural and Biochemical Analysis of the Essential Diadenylate Cyclase CdaA from Listeria monocytogenes. The Journal of biological chemistry. 290, 6596-6606
29 Jamroz, M., Kolinski, A. and Kmiecik, S. (2013) CABS-flex: Server for fast simulation of protein structure fluctuations. Nucleic Acids Res. 41, W427-431
30 Yue, K., Ye, M., Zhou, Z., Sun, W. and Lin, X. (2013) The genus Cordyceps: a chemical and pharmacological review. The Journal of pharmacy and pharmacology. 65, 474-493
31 Tuli, H. S., Sharma, A. K., Sandhu, S. S. and Kashyap, D. (2013) Cordycepin: a bioactive metabolite with therapeutic potential. Life sciences. 93, 863-869
32 Ahn, Y. J., Park, S. J., Lee, S. G., Shin, S. C. and Choi, D. H. (2000) Cordycepin: selective growth inhibitor derived from liquid culture of Cordyceps militaris against Clostridium spp. Journal of agricultural and food chemistry. 48, 2744-2748
33 Zheng, Y., Zhou, J., Sayre, D. A. and Sintim, H. O. (2014) Identification of bromophenol thiohydantoin as an inhibitor of DisA, a c-di-AMP synthase, from a 1000 compound library, using the coralyne assay. Chemical communications. 50, 11234-11237
34 Maass, S., Sievers, S., Zuhlke, D., Kuzinski, J., Sappa, P. K., Muntel, J., Hessling, B., Bernhardt, J., Sietmann, R., Volker, U., Hecker, M. and Becher, D. (2011) Efficient, global-scale quantification of absolute protein amounts by integration of targeted mass spectrometry and two-dimensional gel-based proteomics. Analytical chemistry. 83, 2677-2684
35 Muntel, J., Fromion, V., Goelzer, A., Maabeta, S., Mader, U., Büttner, K., Hecker, M. and Becher, D. (2014) Comprehensive absolute quantification of the cytosolic proteome of Bacillus subtilis by data independent, parallel fragmentation in liquid chromatography/mass spectrometry (LC/MS(E)). Molecular & cellular proteomics : MCP. 13, 1008-1019
36 Gándara, C. and Alonso, J. C. (2015) DisA and c-di-AMP act at the intersection between DNA-damage response and stress homeostasis in exponentially growing Bacillus subtilis cells. DNA repair. 27, 1-8
37 Zhang, L. and He, Z. G. (2013) Radiation-sensitive gene A (RadA) targets DisA, DNA integrity scanning protein A, to negatively affect cyclic Di-AMP synthesis activity in Mycobacterium smegmatis. The Journal of biological chemistry. 288, 22426-22436

Table 1: Crystal parameters, data collection and refinement statistics

Crystal data	TmaDisA 3′-dATP/Mn^{2+}	TmaDisA ApCpp	TmaDisA D75N c-di-AMP
Space group	$P42_12$	$P42_12$	$P42_12$
Molecules per ASU	2	2	2
Unit cell parameters			
a,b,c (Å)	107.49, 107.49, 168.79	108.25, 108.25, 166.40	108.55, 108.55, 165.92
α,β,γ (°)	90, 90, 90	90, 90, 90	90, 90, 90
Data collection statistics			
Diffraction source	PETRA3-P14	SLS X06SA	SLS X06SA
Wavelength (Å)	1.23953	1.00149	1.00000
Data processing statistics			
Resolution range (Å) No. of observed reflections	168.8-2.50 (2.56-2.50) 497086 (33161)	50-2.55 (2.61-2.55) 186053 (6649)	50 -2.25 (2.31-2.25) 625199 (45367)
No. of unique reflections	65492 (4613)	32830 (2248)	47778 (3483)
Completeness (%)	99.6 (94.5)	99.2 (93.9)	100 (100)
Multiplicity	7.6 (7.2)	5.7 (3.0)	13.1 (13.0)
Mean I/σI	15.9 (2.8)	15.5 (2.1)	18.3 (1.6)
R_{meas} (%)	11.6 (113.3)	14.7 (73.7)	11.9 (217.2)
Refinement			
Resolution (Å) No. of used reflections	168.8-2.50 65492	48.41-2.55 32808	49.28-2.25 47724
R_{work} (%) / R_{free}[a] (%)	16.42 / 21.89	18.99 / 24.33	18.86 / 23.73
No. of non H-atoms (total)	5775	5840	5797
Protein	5600	5592	5602
Ligand	60 (3′-dATP) / 4 (Mn^{2+})	62	44 (c-di-AMP) / 8 (MPD)
Water	111	186	143
Average B factors (Å^2)			
Wilson B factor	53.7	46.0	54.8
overall	51.5	47.3	60.3
Protein	52.8	46.2	55.9
Ligands / Water	3′-dATP 34.9 Mn^{2+} (active site) 44.1 Mn^{2+} (surface) 97.6 waters 46.3	ApCpp 50.0 waters 46.7	c-di-AMP 48.7 MPD 85.9 waters 55.2
R.m.s. deviations			
Bond lengths (Å) / angles (°)	0.008 / 1.103	0.009 / 1.125	0.007 / 1.046
Ramachandran plot analysis			
Favoured (%)	97.8	97.0	98.0
Allowed (%)	2.2	3.0	2.0
Disallowed (%)	0	0	0
PDB identifier	4yvz	4yxj	4yxm

Values in parentheses are for the highest resolution shell
[a]for the R_{free} calculations 5% of the total number of reflections was used.

FIGURE LEGENDS

Figure 1: DAC domain conservation and overall characteristics of DisA
A) Sequence alignment of DAC domains of selected DAC proteins from various organisms. Residues in TmaDisA that interact with substrate/product are marked by asterisks.
B) TmaDisA D75N is an octamer in solution as determined by SEC-RALS ($M_w^{SECRALS}$ D75N = 339 kDa)
C) Small-angle X-ray scattering of TmaDisA D75N (blue dots show the measured scattering data, black curve represents the theoretical scattering curve of an octameric DisA calculated with CRYSOL [26]).

Figure 2: DisA active site
A) Pre-reaction state of the cyclase reaction with 3′-dATP and a manganese-ion in the active site. The Mn^{2+} ion is shown with its anomalous difference density at 4σ, the two facing DAC domains are shown in light and dark blue. Some residues have been omitted for clarity.
B) *In vitro* di-adenylate cyclase assays with normalized activities of selected active site mutations. Error bars represent standard deviations of n = 3 independent experiments. Mutations of amino acids interacting with the substrate or the metal ion lead to a strong decrease in activity, while easier accessibility of the active site results in higher activity (R128-130A).
C) Superposition of the DisA/3′-dATP (blue, 3′-dATP shown as lines) and the DisA/ApCpp-structure (grey, ApCpp shown as sticks). The Mn^{2+} ion has been omitted for clarity. Note that the ApCpp structure does not contain a divalent metal ion and thus the triphosphates are in elongated conformation.
D) Close-up of the active site of the TmaDisA D75N mutant crystallized in presence of ATP/Mg^{2+}. Even though the D75N mutant is inactive in *in vitro* assays, c-di-AMP is present in the active site (c-di-AMP with annealed composite omit map at 1σ)

Figure 3: Reaction states of DisA
A) DAC domains in the octameric assembly with tunnels shown in blue (calculated with CAVER [23]), the RRR loop (residues 128-130) shown in black and c-di-AMP in red. Orange arrows show one possible path c-di-AMP has to follow in order to exit the active site.
B) Superposition of apo- (black), pre- (3′-dATP blue, ApCpp grey) and post-reaction state (green) of TmaDisA monomers (left panel) and their per-residue rmsd compared to the apo-structure (right panel). Whereas almost all residues have very low rmsds with respect to the apo-structure, a short loop region on the surface (indicated by an asterisk) has slightly higher deviations, probably because of flexibility.
C) Superposition of *L. monocytogenes* CdaA (green) and TmaDisA (blue) DAC domains bound to ATP/Mg^{2+} and 3′-dATP/Mn^{2+}, respectively (rmsd 1.25 Å)

Figure 4: DisA inhibition and regulation
A) Inhibition of c-di-AMP synthesis by the non-reactive nucleotide 3′-dATP under substrate saturating conditions (300 μM ATP, 26 nM DisA) shows an IC50 of 3 μM (R^2 = 0.997). Error bars represent standard deviations of n = 4 experiments.
B) TmaDisA F57R mutant shows salt dependent dissociation. The mutant (blue no salt buffer, green 10 mM NaCl buffer) elutes at higher volumes from a Superose 6 PC 3.2/30

column compared to wild-type TmaDisA (black curve) and thus is destabilized by salt, suggesting a dissociation from e.g. tetramers to monomers.

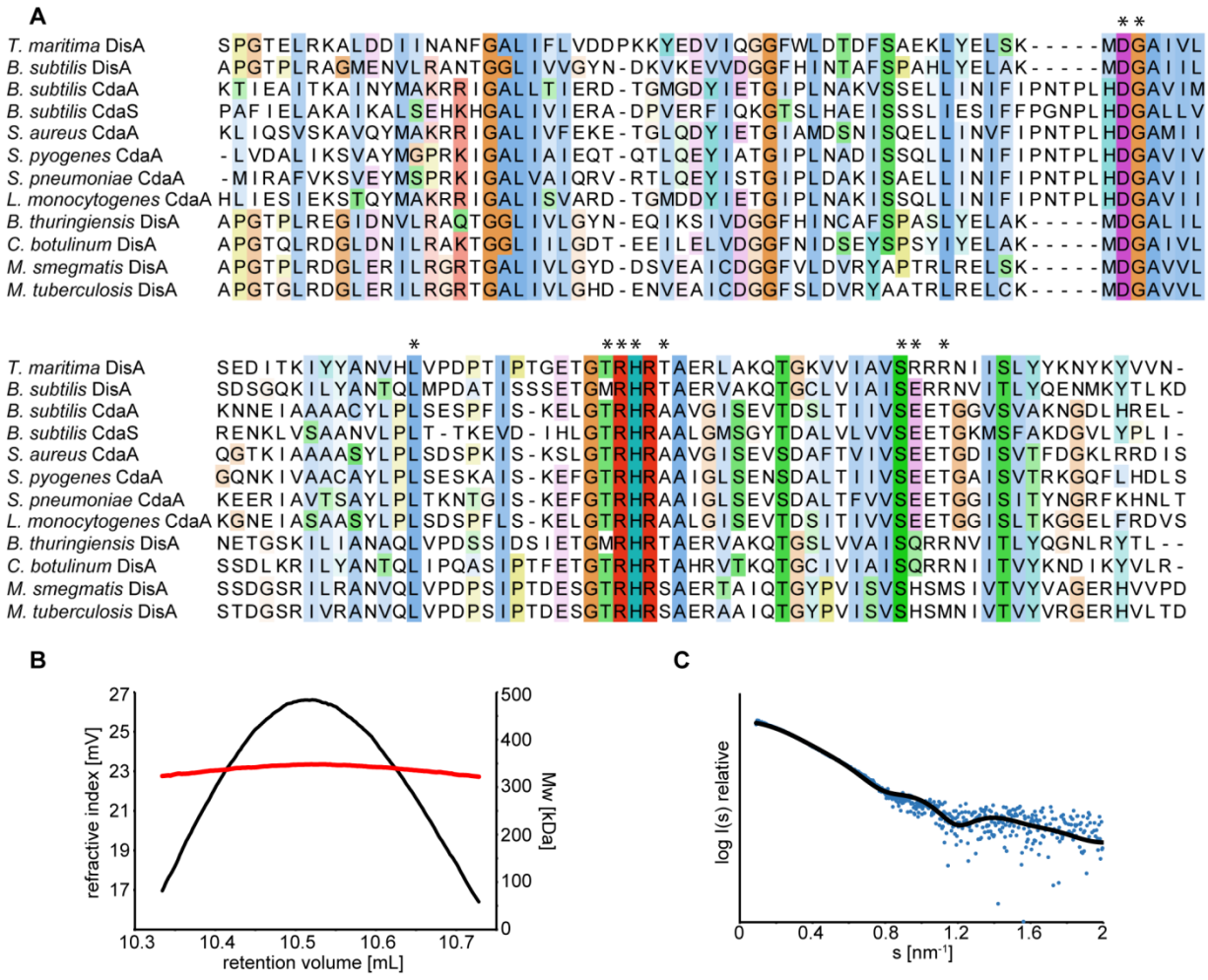

Figure 1: DAC domain conservation and overall characteristics of DisA

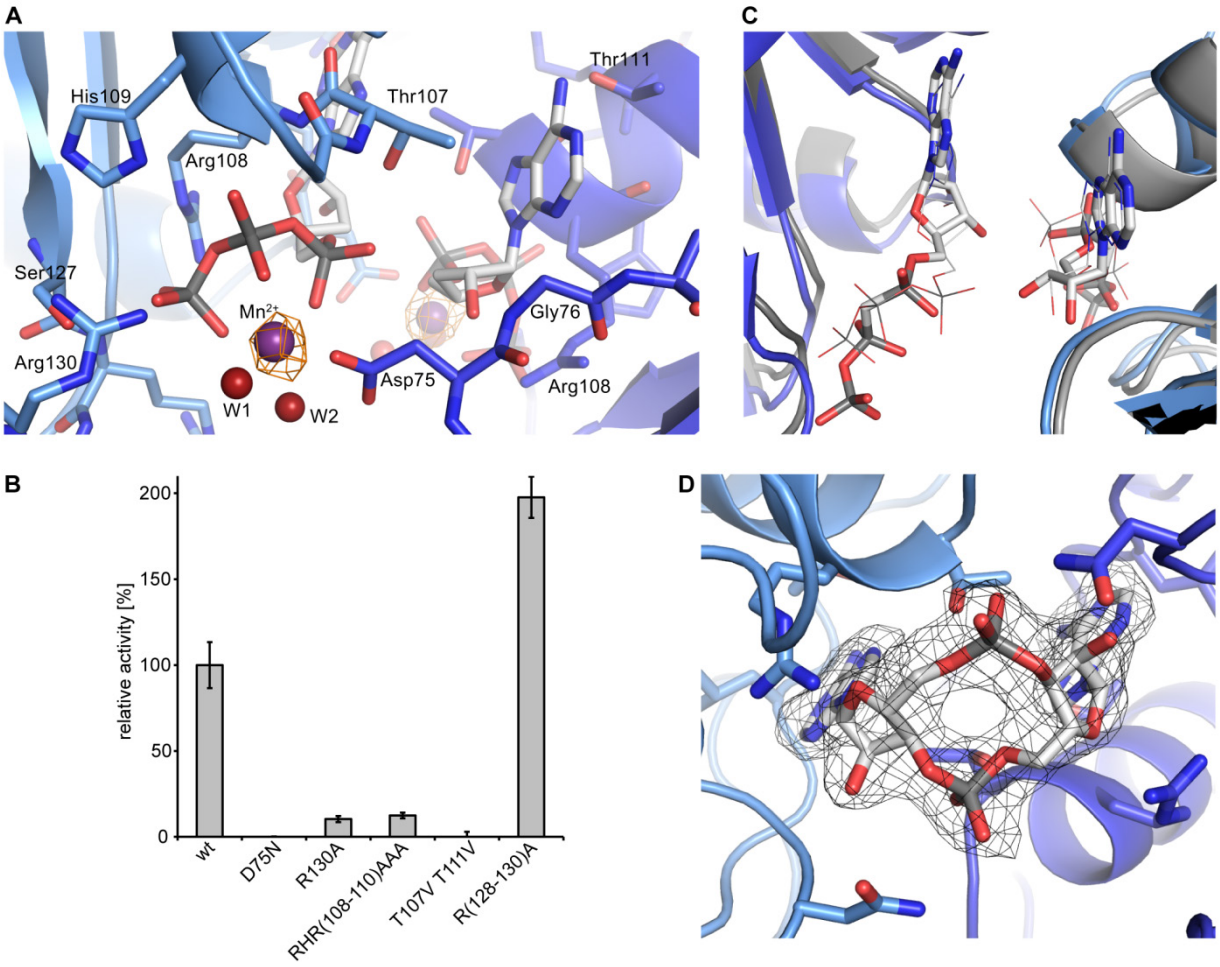

Figure 2: DisA active site

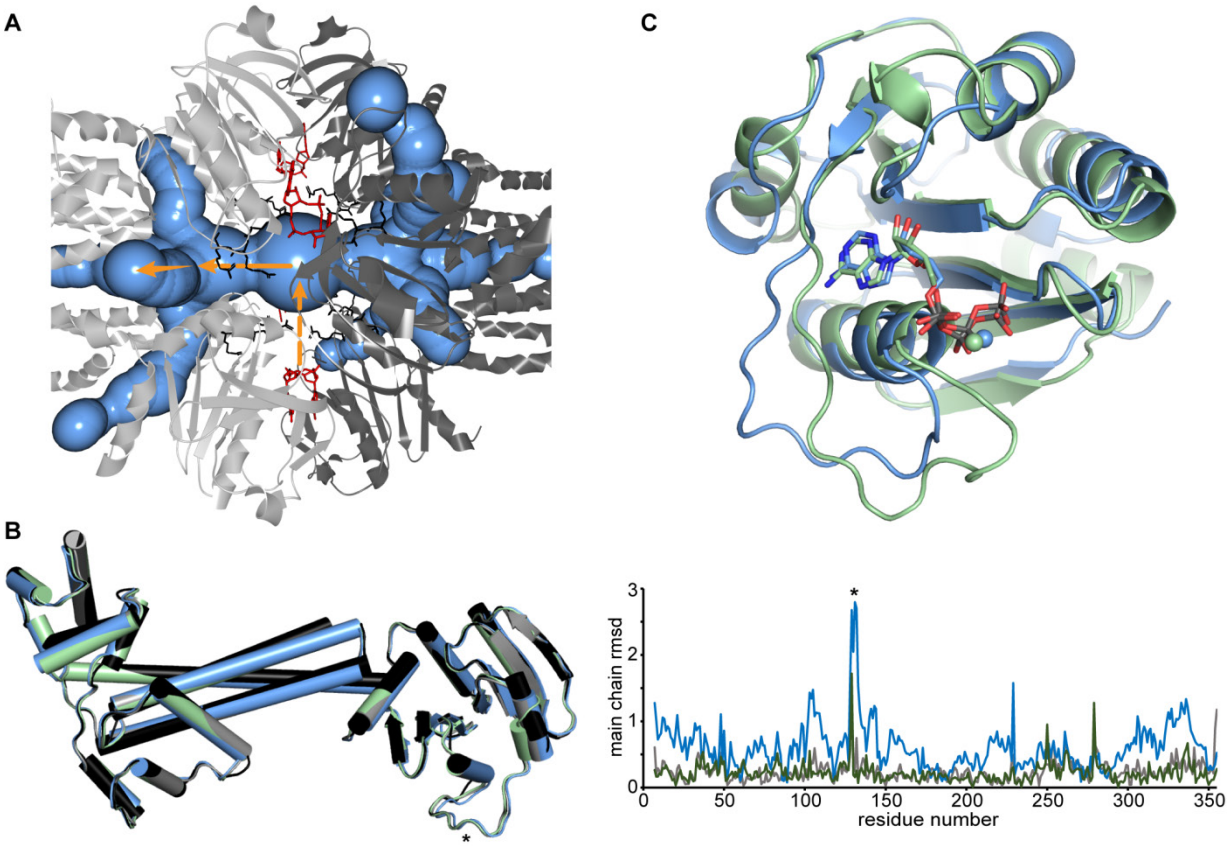

Figure 3: Reaction states of DisA

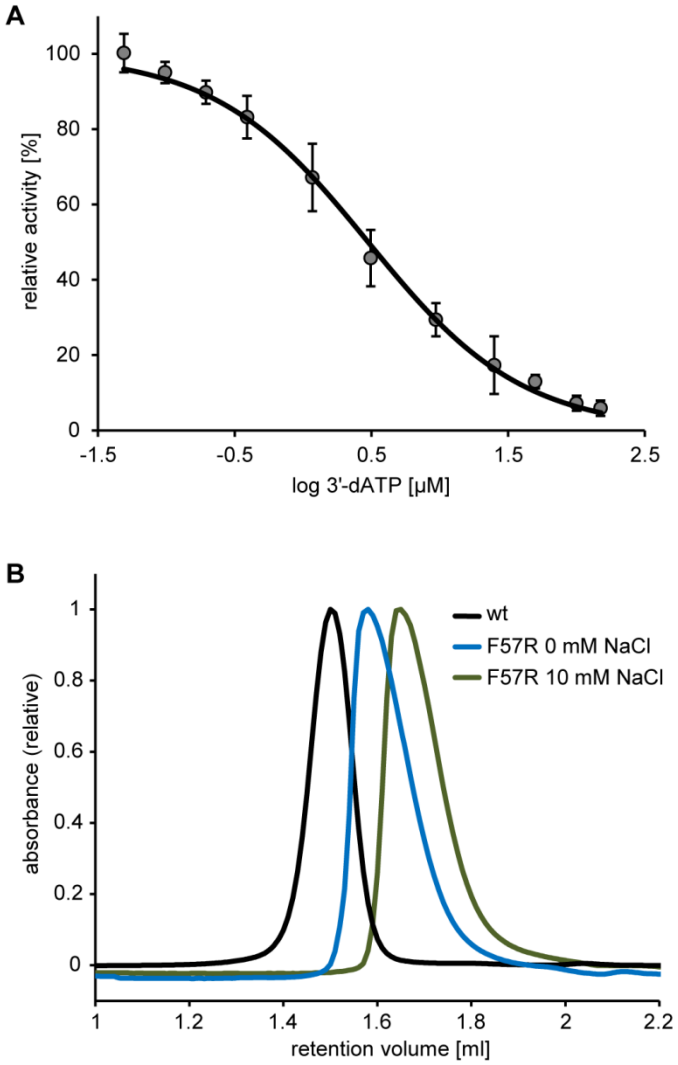

Figure 4: DisA inhibition and regulation

3.2 C-DI-AMP RECOGNITION BY *S. AUREUS* PSTA

Müller, M., Hopfner, K.-P. and Witte, G. (2015) c-di-AMP recognition by Staphylococcus aureus PstA. FEBS letters. 589, 45-51

DOI: 10.1016/j.febslet.2014.11.022

http://www.febsletters.org/article/S0014-5793(14)00827-8/

This publication describes structurally and biochemically how the c-di-AMP receptor PstA from *S. aureus* binds to its ligand c-di-AMP. PstA is the first signal transduction protein specifically recognizing c-di-AMP to be analyzed in detail. Biophysical methods were applied to characterize the oligomeric state of the protein, which proved to be a trimer. Additionally, strong and specific binding of c-di-AMP by PstA was kinetically analyzed by surface plasmon resonance experiments and binding studies with radioactively labeled nucleotides. Finally, the crystal structures of the *apo*, as well as the c-di-AMP bound state of the protein were solved and revealed structural changes upon ligand binding.

Author contribution

I purified PstA, crystallized it with and without c-di-AMP and solved and interpreted the structures. Furthermore, I analyzed the oligomeric state of PstA by size-exclusion chromatography and static light scattering. Additionally, I investigated the binding kinetics and affinity of c-di-AMP and other possible ligands by surface plasmon resonance and thermal shift assays. I wrote the manuscript together with G. Witte. Experimental design and data analysis was supported by G. Witte.

FEBS Letters 589 (2015) 45–51

FEBS Letters

journal homepage: www.FEBSLetters.org

c-di-AMP recognition by *Staphylococcus aureus* PstA

Martina Müller, Karl-Peter Hopfner, Gregor Witte *

Ludwig-Maximilians-Universität München, Gene Center and Dept. of Biochemistry, Feodor-Lynen-Str. 25, 81377 Munich, Germany

ARTICLE INFO

Article history:
Received 16 October 2014
Revised 13 November 2014
Accepted 13 November 2014
Available online 28 November 2014

Edited by Stuart Ferguson

Keywords:
Cyclic-di-AMP
P_{II}-related protein
Ferredoxin-like fold
Crystal structure
Bacterial signal transduction

ABSTRACT

Cyclic-di-AMP (c-di-AMP) is a bacterial secondary messenger involved in various processes, including sensing of DNA-integrity, cell wall metabolism and potassium transport. A number of c-di-AMP receptor proteins have recently been identified in *Staphylococcus aureus*. One of them - PstA - possesses a ferredoxin-like fold and is structurally related to the class of P_{II} signal-transduction proteins. P_{II} proteins are involved in a large number of pathways, most of them associated with nitrogen metabolism. In this study we describe the mode of c-di-AMP binding and subsequent structural changes of *S. aureus* PstA. An altered architecture in PstA compared to canonical P_{II} proteins results in differences in ligand coordination.

1. Introduction

Nucleotide secondary messengers are key components of the signal transduction networks that link sensory input signals to the responses of the cell. The most prominent examples in bacteria are cyclic AMP and (p)ppGpp, both of which control genome wide expression. The cyclic di-nucleotide messenger molecule c-di-GMP acts as a "lifestyle" signal, regulating biofilm formation, cell cycle progression, development and virulence. In the past few years two new members of bacterial nucleotide messengers have been identified, namely c-di-AMP and 3,3-cGAMP. The latter is little characterized but it has been shown to play a role in *Vibrio cholerae* gastrointestinal colonization [1] and is related to the 2,3-cGAMP synthesized by the eukaryotic innate immune DNA sensor cGAS [2,3]. The identification of c-di-AMP in 2008 [4] started a struggle for the identification of c-di-AMP related signaling pathways [5] and we are still at the beginning of understanding how c-di-AMP signaling is initiated, how the signal is transduced and which cellular processes are finally regulated. After the initial discovery of c-di-AMP in the crystal structure of *Thermotoga maritima* DisA [4], more diadenylate cyclase (DAC) domain proteins have been identified in a variety of bacteria [6–10]. Different functions were assigned to c-di-AMP signaling and it has been shown that deletion of all DAC domain proteins is lethal in *Bacillus subtilis* [9]. On the one hand, DNA damage or subsequent post-repair/recombination states of the DNA result in a reduced level of c-di-AMP due to inhibition of DisA, leading to sporulation delay in *B. subtilis* [11]. On the other hand, c-di-AMP has been reported to be involved in cell wall homeostasis [12], fatty acid synthesis [13] and potassium transport [14]. Aside from the DAC domain synthesizing c-di-AMP [4,15], there is little structural information about c-di-AMP degradation by the phosphodiesterase GdpP [16,17] or c-di-AMP-binding receptors. To date, six c-di-AMP receptors have been identified: the transcription factor DarR from *Mycobacterium smegmatis* [13]; ydaO riboswitches [18–20]; the potassium transport associated proteins KtrA and KdpD; the P_{II}-like protein PstA from the pathogen *Staphylococcus aureus* [14]; and the well-characterized protein pyruvate carboxylase, which was unexpectedly shown in a recent structural and biochemical study to be allosterically regulated by c-di-AMP [21].

The fact that c-di-AMP binds to PstA implies that the cyclic dinucleotide might also be involved in regulation of metabolism. PstA shares a ferredoxin-like fold with proteins of the P_{II} signal transduction family, which are omnipresent in bacteria, archaea and plants, and probably belong to the most widespread signal transducing proteins in nature. P_{II} proteins are mainly involved in the regulation of central metabolic processes and in particular cellular nitrogen metabolism (e.g. reviewed in [22]). After sensing of a ligand such as 2-oxoglutarate (2-OG) and/or adenosine nucleotides, P_{II} proteins regulate target proteins via protein–protein interactions with transcription factors, membrane transporters

* Corresponding author. Fax: +49 (0)89 2180 76999.
E-mail address: witte@genzentrum.lmu.de (G. Witte).

http://dx.doi.org/10.1016/j.febslet.2014.11.022

and different enzymes. All P_{II} proteins are trimers and consist of three identical subunits with an approximate molecular weight of 12–13kDa each. P_{II} proteins have a compact core domain with a double βαβ-architecture (ferredoxin-like fold) and inter-subunit clefts for ligand binding. Additional structural features are one large protruding loop (T-loop), a smaller B-loop and a C-terminal loop (C-loop). Whereas the latter are involved in ligand binding, the T-loop is flexible and rarely visible in crystal structures. However, the intrinsic flexibility is probably needed for regulatory protein–protein interactions. In bacteria, the T-loop is often post-translationally modified through uridylation of Tyr51 with effects on the signal transduction. All three ligand binding sites can bind one nucleotide and one 2-OG molecule each. While ATP binding is cooperative with 2-OG, ATP and ADP bind competitively and ADP acts antagonistic to 2-OG. The crystal structure of *Azospirillum brasilense* GlnZ in complex with ATP, 2-OG and a Mg^{2+} ion [23] was the first complex structure to shed light on the mode of ligand binding. Both ATP and 2-OG are bound in the inter-subunit cleft and, together with conserved residues in the binding cleft, coordinate the Mg^{2+} ion.

We solved the crystal structures of *S. aureus* PstA with and without its ligand c-di-AMP and were thus able to analyze the coordination of c-di-AMP and subsequent structural changes in PstA. The overall architecture of PstA differs from P_{II} proteins with respect to the protruding loops that are involved in interactions with both ligands and targets. In agreement with other structures of P_{II} proteins, c-di-AMP is bound in the inter-subunit clefts. In contrast, however, these clefts are closed by the small T-loops bending upwards and not the C-loops as previously observed.

2. Materials and methods

2.1. Cloning, expression and protein purification

S. aureus PstA (SACOL0525) was cloned into the pET28a expression vector via NdeI and NotI restriction sites. His_6-tagged PstA was expressed in *E. coli Rosetta* BL21(DE3) cells grown in LB. After reaching an OD_{600} of 0.6, expression was induced by addition of 0.2 mM IPTG and the temperature was lowered to 18 °C. Cells were harvested after 18 h and lysed in buffer A (50 mM Tris–HCl, 300 mM NaCl, 10 mM Imidazole, 10% v/v Glycerol, pH 7.5) via sonication. The cell lysate was cleared by centrifugation and loaded onto a Ni–NTA column (Qiagen). After washing with buffer A and buffer B (50 mM Tris–HCl, 300 mM NaCl, 40 mM Imidazole, 10% v/v Glycerol, pH 7.5) the protein was eluted with buffer C (50 mM Tris–HCl, 300 mM NaCl, 250 mM Imidazole, 5% v/v Glycerol, pH 7.5). PstA was dialyzed against buffer D (50 mM Tris–HCl, 100 mM NaCl, 5% v/v Glycerol, pH 7.5) and loaded onto a HiTrap Q HP (GE Healthcare). A linear gradient to 100% buffer E (50 mM Tris–HCl, 1 M NaCl, 5% v/v Glycerol, pH 7.5) was used to elute the protein. PstA-containing fractions were pooled, concentrated and loaded onto a HiLoad Superdex 75 column (GE Healthcare) equilibrated with running buffer F (20 mM Tris–HCl, 150 mM NaCl, 5% v/v Glycerol, pH 7.5). The PstA peak fractions were concentrated to 6 mg/ml and flash-frozen in liquid nitrogen for later use.

2.2. Crystallization, data collection and structure refinement

S. aureus PstA crystals were grown by hanging drop vapor-diffusion at 20 °C. Crystals were obtained by mixing 2 μL of protein (6 mg/ml) and 1 μL reservoir solution (55% v/v MPD, 0.1 M sodium acetate pH 4.3, 10 mM calcium chloride) with a total reservoir volume of 300 μL in the well. For co-crystallization of PstA with c-di-AMP, 1 μL of protein (6 mg/ml) supplemented with 0.75 mM c-di-AMP was mixed with 1 μL of reservoir solution (6% w/v PEG 8000, 0.1 M HEPES/NaOH pH 7.0, 0.2 M calcium acetate) with a reservoir volume of 300 μL. Crystals were flash-cooled in liquid nitrogen either directly from their mother liquor or after transfer into mother liquor supplemented with 25% v/v PEG 400 as a cryo-protectant (for crystals with c-di-AMP). Diffraction data were collected at the Swiss Light Source (Paul-Scherrer institute, Villigen, Switzerland) at the beamline X06SA at 100 K. Diffraction data were indexed and scaled using XDS/XSCALE [24]. The structure was determined by molecular replacement using PHASER [25] within the CCP4 package [26] using *Pediococcus pentosaceus* P_{II}-like protein (PDB code 3m05) as search model. Structure refinement comprised cycles of manual model building/refinement steps with Coot [27] and automatic refinement using PHENIX [28]. The data collection and refinement statistics are shown in Table 1. Coordinates and structure factors have been deposited in the Protein Data Bank as 4wk1 and 4wk3. All figures were prepared using PyMOL [29].

2.3. Size-exclusion coupled right-angle laser light scattering (SEC-RALS)

SEC-RALS data were collected using a Malvern/Viscotek system (TD270 RALS- and VE3580 RI-detector) connected to an ÄKTAmicro system equipped with a Superdex 200 Increase (10/300) column (GE Healthcare). To calibrate the system BSA (66kDa) was used. Data were evaluated with the OmniSEC software supplied with the instrument.

2.4. Surface plasmon resonance experiments

Surface plasmon resonance experiments to analyze binding of c-di-AMP to *S. aureus* PstA were performed using a Biacore X100+ system (GE Healthcare). *S. aureus* PstA was coupled to a CM-5 chip via amine coupling chemistry and free activated groups were inactivated using ethanolamine. To increase the sensitivity of the nucleotide binding we saturated the chip surface with PstA (5800 RU). Kinetic data were recorded for injections of c-di-AMP (and other nucleotides) in HBS-EP buffer (150 mM NaCl, 10 mM HEPES/NaOH pH 7.4, 3 mM EDTA, 0.05% P-20). Data from an empty flow cell (FC1) were subtracted as reference to correct for unspecific binding of the analytes to the chip surface. Data were analyzed using the Biacore X100 Evaluation software.

2.5. Thermal shift assays

Thermal stability of PstA in presence of ligands was probed using fluorescence thermal shift assays [30]. 19 μM PstA (+1 mM ligand) in 50 mM Tris–HCl pH 7.5, 150 mM NaCl, 5% v/v glycerol, 5 mM $MgCl_2$ with SYPRO orange (final concentration 4x, Invitrogen) was analyzed in a real-time PCR machine. After equilibration at 5 °C for 30 s the melting curve was measured using a gradient with 0.5 K/30 s from 5 °C to 100 °C and one scan/0.5 K.

2.6. Differential radial capillary action of ligand assay

DRaCALA assays were performed as e.g. described in [14]. 20 μM *S. aureus* PstA or the control ATP-binding protein (human nucleotidyl transferase) in assay buffer (50 mM Tris–HCl pH 7.5, 150 mM NaCl, 5 mM $MgCl_2$) were incubated for 5 min with different concentrations of ATP-α^{32}P (1–10 nM). 3.5 μL of the reaction mixture were spotted on a nitrocellulose membrane, dried and radioactivity was detected using a phosphor-imaging system (GE Healthcare).

Table 1
Crystal parameters, data collection and refinement statistics for *S. aureus* PstA.

Crystal data	PstA	PstA + c-di-AMP
Space group	$P4_332$	H32
Molecules per ASU	1	1
Unit cell parameters		
a, *b*, *c* (Å)	99.32, 99.32, 99.32	68.1, 68.1, 135.74
α, β, γ (°)	90, 90, 90	90, 90, 120
Data collection statistics		
Diffraction source	SLS beamline X06SA	SLS beamline X06SA
Wavelength (Å)	0.99998	0.99998
Data processing statistics		
Resolution range (Å)	70.23–2.60 (2.67–2.60)	50–1.98 (2.03–1.98)
No. of observed reflections	701 580 (14 290)	141 089 (2745)
No. of unique reflections	5565 (392)	8523 (512)
Completeness (%)	99.9 (99.2)	97.7 (81.4)
Multiplicity	36.2 (36.1)	16.6 (5.4)
$I/\sigma I$	33.1 (2.5)	23.6 (2.0)
R_{meas} (%)	7.0 (198)	7.4 (105.3)
Refinement		
Resolution (Å)	44.42–2.60	44.52–1.98
No. of used reflections	5563	8522
R_{work} (%)/R_{free}[a] (%)	25.2/29.2	18.8/22.9
No. of atoms (total)	598	779
Protein	593 (77 residues)	703 (92 residues)
Ligand	1	1 (Ca^{2+}); 43 (c-di-AMP)
Water	4	23
Average B factors (Å^2)		
Wilson B factor	85.36	42.75
Overall	98.12	54.3
Protein	98.11	54.3
Ligands/water	Cl^- 129.5/89.6	c-di-AMP 49.1; Ca^{2+} 70.7/54.2
R.M.S. deviations		
Bond lengths (Å)/angles (°)	0.009/1.18	0.008/1.20
Ramachandran plot analysis		
Favoured (%)	98.6	98.9
Allowed (%)	1.4	1.1
Disallowed (%)	0	0
PDB identifier	4wk3	4wk1

Values in parentheses are for the highest resolution shell.
[a] 10% of the total number of reflections were used for the R_{free} calculations.

3. Results and discussion

The *S. aureus* protein PstA has a ferredoxin-like fold and its core domain shares the highly conserved architecture of the GlnB/K P_{II} proteins to which it is structurally closely related. A comparison of the secondary structure of PstA with canonical P_{II} proteins (e.g. *E. coli* GlnK), however, clearly shows that the lengths of the loops are exchanged (Fig. 1A). The loop connecting the double βαβ-motif comprises only 8 amino acids and is thus substantially shorter than the approximately 20 residue long T-loop typically present in this domain. Vice versa, the 33 residue long B-loop in the vicinity of the ligand binding cleft is significantly larger in *S. aureus* PstA than the eight residue loop in GlnK. The carboxy-terminal C-loop that usually covers the ligand binding cleft is absent in *S. aureus* PstA. As the overall properties of PstA deviate from previously described P_{II} proteins, we first analyzed the biochemical properties of PstA in solution to exclude the possibility that the protein forms different oligomers to the canonical trimeric P_{II} proteins. We thus performed size-exclusion chromatography coupled right-angle light scattering (SEC-RALS) experiments to determine the molecular weight in solution (Fig. 1B and C). Both the SEC-RALS data and the molecular weight determined from the hydrodynamic radius in size-exclusion chromatography show that PstA is a monodisperse trimeric species in solution ($Mw^{theoretical\ (trimer)}$ = 42kDa, $Mw^{SEC\text{-}RALS}$ = 43kDa, Mw^{SEC} = 47kDa). The fact that the apparent molecular weight from size-exclusion chromatography is higher than the molecular weight determined by light scattering is probably due to the protruding loops in PstA. Flexible regions lead to an increase in hydrodynamic radius and thus to a larger retention volume than a globular protein of the same size.

3.1. Binding of c-di-AMP

To probe binding of small molecules we measured the thermal stability of PstA in absence and presence of putative regulatory ligands using fluorescence-based thermal shift assays (TSA). In good agreement with P_{II} proteins [31], PstA shows a remarkably high thermal stability with an approximate melting temperature of 74.5 °C under the conditions used. Since ligand binding usually increases the melting temperature of a protein, we analyzed the melting behavior of PstA in the presence of nucleotides and/or 2-oxoglutarate (2-OG, α-ketoglutaric acid). While guanosine and non-cyclic adenosine nucleotides do not alter the melting temperature, c-di-AMP shifts the melting temperature of PstA by approximately 19 °C to 93.5 °C, indicating a remarkable gain in stability caused by a higher number of interactions within the complex. These observations are in good agreement with experiments by Corrigan et al. [14] that showed binding of c-di-AMP, but not other nucleotides, in differential radial capillary action of ligand assays (DRaCALA). The addition of 1 mM 2-OG had no detectable effect on the melting behavior of PstA.

In order to quantify the affinity and kinetic properties of c-di-AMP binding to PstA, we performed surface plasmon resonance (SPR) experiments. Amino-reactive coupling chemistry was used

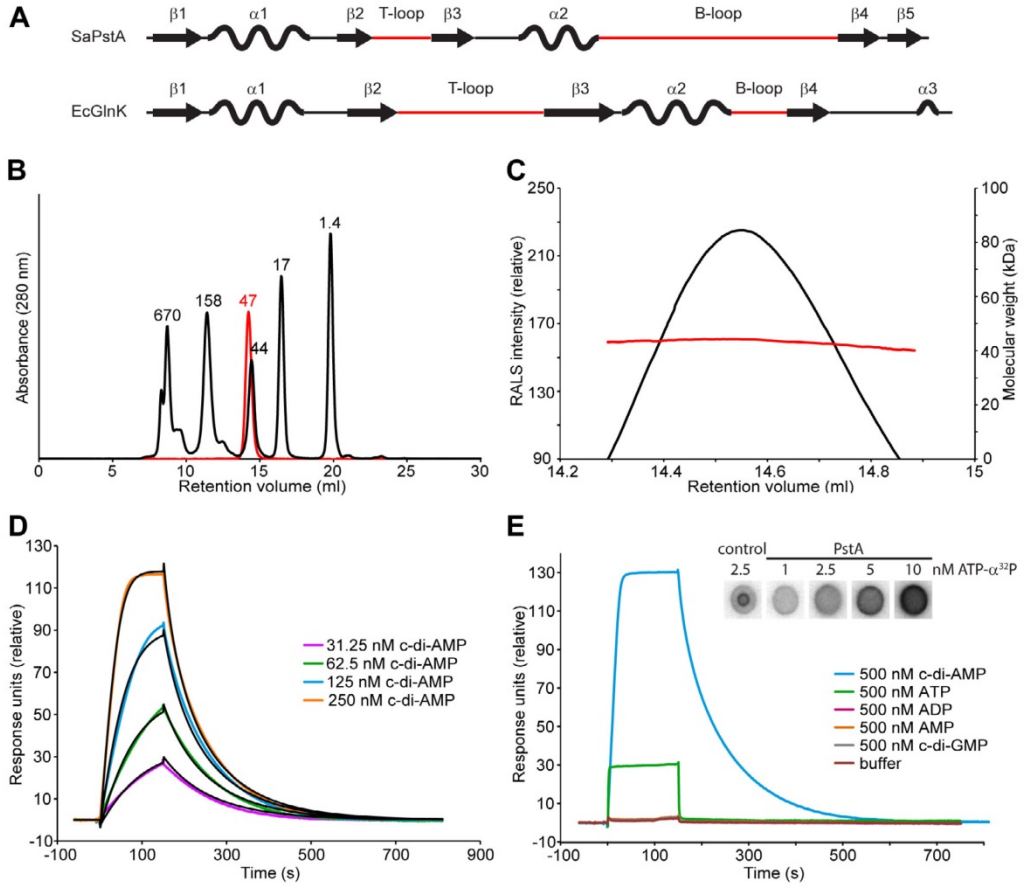

Fig. 1. Biochemical analysis of *S. aureus* PstA. (A) Comparison of the secondary structure of *S. aureus* PstA with a member of the canonical P_{II} protein family (*E. coli* GlnK). The lengths of the T- and B-loops are swapped in PstA compared to GlnK. (B) Size-exclusion chromatogram of a PstA sample (red curve) loaded onto a Superdex 200 Increase column and a molecular weight standard shown in black (peaks labeled with the respective masses of the proteins in kDa). Mw^{SEC}(PstA) = 47kDa was calculated using a calibration curve generated from the Mw-standard. (C) SEC-RALS curve of a PstA peak on the same column as in B. The molecular weight determined by RALS is constant for the entire PstA peak, indicating a monodisperse sample with a molecular weight of $Mw^{SEC\text{-}RALS}$ = 43kDa ($Mw^{theoretical\ (trimer)}$ = 42kDa). (D) Surface plasmon resonance (SPR) experiments. Injections of different concentrations of c-di-AMP (colored curves) over the immobilized *S. aureus* PstA chip-surface (FC2-1). The black curves show the fit of kinetic analysis with $k_a = 6.4 \times 10^5\ M^{-1}\ s^{-1}$, $k_d = 0.007\ s^{-1}$, $RU_{max} = 173$ for the binding of one c-di-AMP molecule to each PstA monomer. (E) Injections of different nucleotides show that ADP, AMP and c-di-GMP do not bind to PstA. ATP only binds to a small extent and this could not be confirmed in a DRaCALA assay. ATP binding is only observed in the positive control.

to covalently immobilize PstA to the chip surface and increasing concentrations of c-di-AMP (31.25–250 nM) in HBS-EP buffer were injected as the analyte (Fig. 1D). PstA displays robust binding of the cyclic di-nucleotide with K_D = 109 nM, an association rate of $k_a = 6.4 \times 10^5\ M^{-1}\ s^{-1}$ and a slow dissociation rate of $k_d = 0.07\ s^{-1}$. We also performed injections with ATP/Mg^{2+}, ADP, AMP, c-di-GMP and 2-OG (Fig. 1E). Only the ATP sample showed binding to PstA, albeit with much lower affinity, and no binding of AMP, ADP, c-di-GMP and 2-OG was detected under the conditions used. A combination of c-di-AMP and 2-OG resulted in comparable binding kinetics and K_D to c-di-AMP alone. The high affinity for c-di-AMP is mainly determined by the relatively fast on-rate and the slow dissociation kinetics. In comparison, the steep RU increase in ATP-binding sensorgrams indicates that both ATP binding and dissociation are much faster (beyond the sampling rate of the SPR instrument and thus $k_a \geqslant 10^7\ M^{-1}\ s^{-1}$), indicating that ATP-binding is energetically less favorable. A DRaCALA assay, however, did not show any binding of radioactively labeled ATP to PstA. Both the very fast on- and off-rates and weak binding observed in the SPR experiment indicate a transient interaction, which we deem unlikely to be of biological significance.

3.2. Crystal structures of PstA in absence and presence of c-di-AMP

To analyze the molecular details of c-di-AMP binding, we crystallized *S. aureus* PstA in the presence and absence of the cyclic dinucleotide. Apo PstA and c-di-AMP-PstA crystallized in the space groups $P4_332$ and H32, respectively, with one molecule per asymmetric unit. Both structures were solved by molecular replacement using the structure of *P. pentosaceus* PEPE_1480 (PDB code 3m05) as a search model, which we identified through homology searches using HHpred [32]. Traceable electron density covered 8 residues from the N-terminal purification tag and PstA residues 1–66 and 92–109 (numbers given for the complex structure). These residues mainly comprise the double βαβ-motif while the loop regions lacked traceable electron density and are thus likely to be flexible in the crystals (Fig. 2A). Statistics of data collection and model refinement are shown in Table 1. As suggested by the secondary structure comparison (Fig. 1A), the structure of PstA shows no obvious changes to the double βαβ-motif of the ferredoxin-like fold but the T- and B-loops are swapped in length with respect to canonical P_{II} proteins. Beta strands β1–β4 form the core of the PstA trimer while α-helices α1 and α2 are on the outside (Fig. 2A and B).

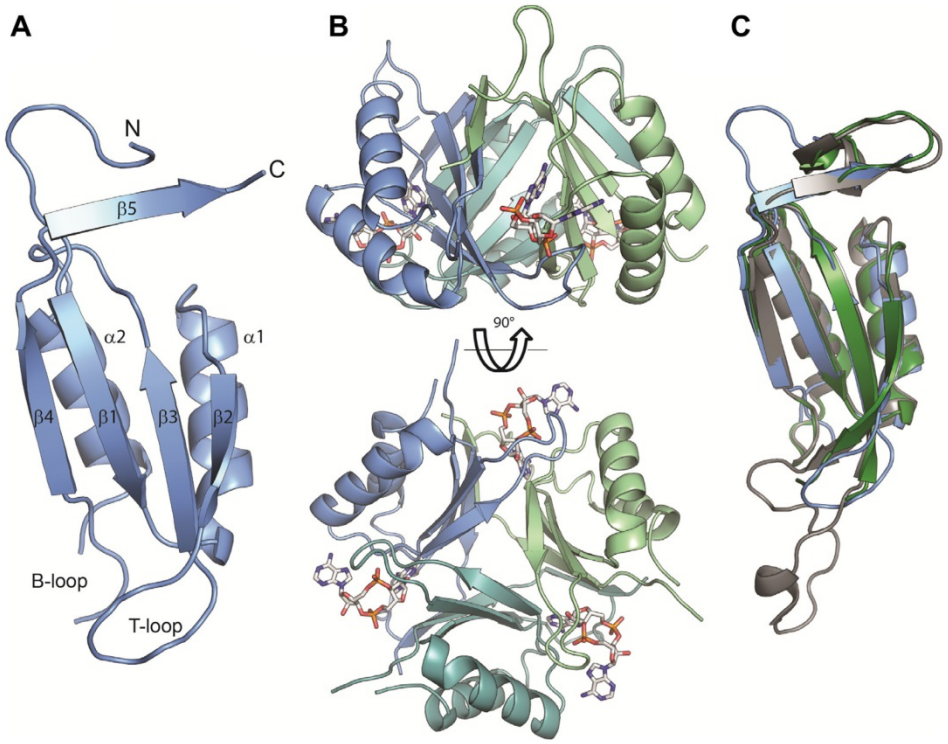

Fig. 2. Crystal structure of *S. aureus* PstA. (A) PstA monomer as present in the asymmetric unit. Residues in the B-loop region could not be traced in the electron density. The strand β5 extends the β-core domain of the neighboring PstA molecule by interacting with β4. (B) PstA trimer (approximate height 25 Å and diameter 40 Å) with bound c-di-AMP in side (upper part) and bottom views (lower part). The c-di-AMP moieties are deeply buried in the inter-subunit clefts. (C) Superposition of PstA and P_{II} proteins. The figure illustrates the structural similarity between *S. aureus* PstA (blue), *A. brasilense* GlnZ (PDB code 3mhy, grey, RMSD 1.18 Å) and *E. coli* GlnK (PDB code 2gnk, green, RMSD 0.854 Å).

The C-terminal β-strand β5 extends towards the neighboring subunit, where it interacts with β4 and thus stabilizes the trimer. The superposition of *S. aureus* PstA, *E. coli* GlnK and also *A. brasilense* GlnZ (Fig. 2C) reveals the high overall structural conservation of the ferredoxin-like core domains.

In the complex structure of PstA with c-di-AMP all three inter-subunit binding clefts are occupied by the cyclic dinucleotide. The c-di-AMP moiety is almost completely buried in the binding cleft and is stabilized by a set of hydrophobic and ionic interactions. The binding cleft is clearly positively charged and almost perfectly matches the shape of the adenosine dinucleotide (Fig. 3A – electrostatic surface). Fig. 3B shows the c-di-AMP molecule with its respective electron density. The buried "inner" half of c-di-AMP is almost completely protected from the solvent area and coordinated by Asn-41, which forms a hydrogen bond with the 2′-hydroxyl group of the ribose, and additionally stabilized via a backbone interaction with Gly-47, which interacts with N^6 of adenine and thereby distinguishes between adenine and guanine cyclic dinucleotides. In comparison to the nucleotide free state, the small T-loop (residues 34–38), which is disordered in the apo state, becomes stabilized in the complex state and bends up towards the second "outer" adenine moiety. The base stacks with residues Phe-36 and Arg-26 and contributes to the extremely good coordination. This shielding and excessive ligand stabilization is in good agreement with the high binding affinity observed by surface plasmon resonance and the melting temperature shift in TSA. Interestingly, c-di-AMP shows a slower association rate than ATP, most probably due to the slower migration into the binding cleft that is just large enough to accommodate this molecule. To date, only one other protein complex with bound c-di-AMP has been reported, which is structurally very different [21] and we have not identified a common recognition motif for c-di-AMP.

3.3. Structural changes upon c-di-AMP binding and signal transduction

The overall structural changes between apo and complex states visible in the crystal structures are mainly short range movements in the core domain and the stabilization of the short T-loop (Fig. 3C and D). These structural changes upon ligand binding are supported by the fact that soaking of apo PstA crystals did not produce any diffracting crystals, possibly due to conformational changes disturbing the crystal lattice during binding of c-di-AMP. The high similarity of the apo and complex structures is reflected in a very low $RMSD_{overall}$ = 0.451 Å and also in the low per-residue RMSDs of the core domains (Fig. 3D). Because of the large amount of flexibility in the loop regions it is not possible to judge if any additional conformational changes in the B-loop occur in vivo. The loop regions have been shown to be crucial for signal transduction in all P_{II} proteins [22] but it is possible that PstA may function differently. Since we have no information on the structural changes of the B-loop due to lack of electron density, we can only speculate how PstA transduces signals, one option being that the longer B-loop instead of the T-loop mediates downstream signaling.

Fig. 3E shows a superposition of the structures of the P_{II} protein GlnZ from *A. brasilense* in complex with ATP/2-OG (PDB code 3mhy) and PstA in complex with c-di-AMP. The overall shape and surface properties are highly similar and the ATP and c-di-AMP binding clefts superpose closely. The "inner" base of c-di-AMP is almost in the same position as the ATP molecule in GlnZ. Interestingly, a second positively charged cavity in the direct

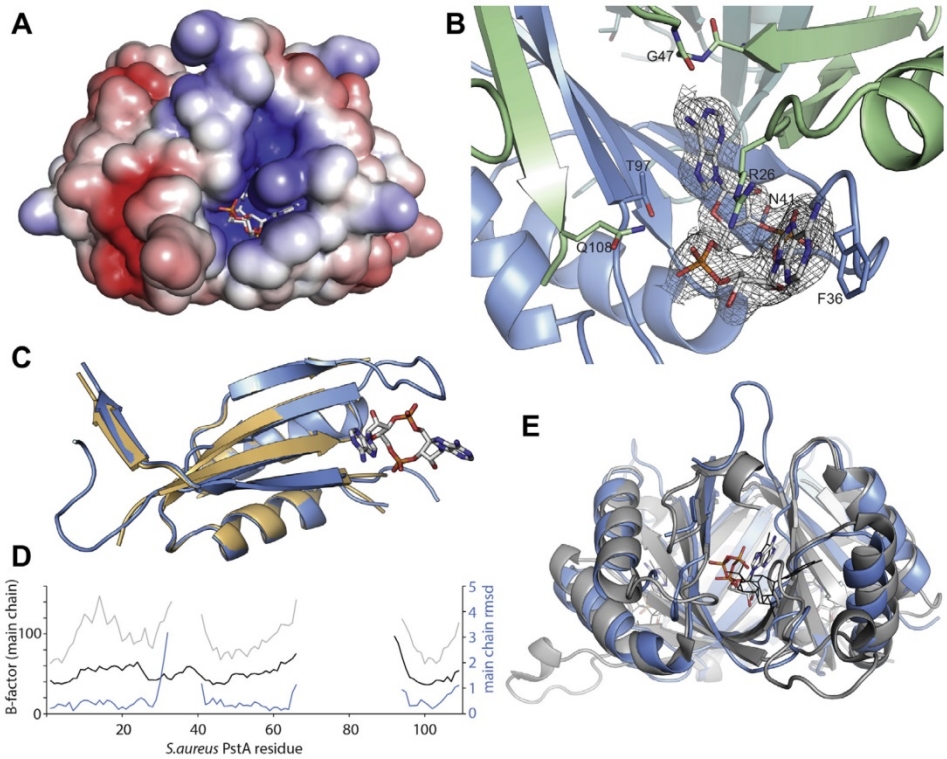

Fig. 3. Ligand binding. (A) PstA in solvent accessible electrostatic surface representation with c-di-AMP bound (blue = 5kT/e to red = −5kT/e). (B) Coordinated c-di-AMP molecule in the inter-subunit cleft with the corresponding electron density at 1σ (simulated annealing composite omit map). The "outer" adenine moiety is stacked by R26 and F36 while the "inner" adenine is specifically recognized at N^6 through a backbone interaction with G47. (C) Superposition of apo state PstA (shown in beige) and its c-di-AMP complex (shown in blue, RMSD 0.451 Å). Although no major structural changes in the overall architecture can be observed upon ligand binding, the T-loop becomes ordered and stabilizes the c-di-AMP moiety. (D) The plot shows the B-factors for the main chains of apo PstA (grey) and PstA-c-di-AMP complex (black) as well as the RMSD values for the Cα-atoms (blue curve, right axis) in the superposition of both structures (c.f. C). The T-Loop (residues 30–40) is clearly stabilized in the c-di-AMP complex. Additionally, the adjacent helix (residues 10–20) binds to the T-loop and thus has lower B-factors in the complex structure than in the apo structure. (E) Superposition of the PstA-c-di-AMP complex (blue) with GlnZ in complex with ATP/Mg^{2+}/2-OG (PDB code 3mhy, shown in grey, RMSD 1.18 Å). The "inner" adenine of c-di-AMP and ATP bound by GlnZ superimpose almost perfectly.

vicinity of the c-di-AMP binding pocket is visible in the electrostatic surface representation (Fig. 3A), which is sufficiently large to accommodate an additional small molecule ligand. As several structures of P_{II} proteins contain 2-OG close to ATP [23] bridged by a Mg^{2+} ion, this cavity might also be a binding site for a negatively-charged ligand. Even though our thermal shift assays and SPR experiments do not indicate binding of 2-OG by PstA under the conditions used, we cannot exclude the possibility that this ligand (or another small molecule) might bind in addition to c-di-AMP. From the structural point of view the second cavity would certainly allow accommodation of a ligand but its function remains to be analyzed in further studies.

We were able to structurally analyze c-di-AMP sensing by a signal transducing protein for the first time. Even though PstA shares its overall structural elements with canonical P_{II} proteins, significant differences, such as the swapped lengths of the B- and T-loops and the missing C-loop, result in altered ligand binding properties. Future research will show which target proteins are affected by PstA and the mechanism through which this occurs. This study substantially broadens our understanding of how c-di-AMP is recognized by target proteins.

Acknowledgements

We thank the staff of SLS X06SA for excellent onsite support and beamtime allocation, K. Lammens and D. Kostrewa for support with X-ray data, R. Byrne for comments on the manuscript and the Hopfner group for discussions. This work was funded by grants from the Deutsche Forschungsgemeinschaft (DFG) WI3717/2-1 to G.W. and GRK1721 to G.W. and K.-P.H., M.M. is supported by GRK1721.

Appendix A. Supplementary data

Supplementary data associated with this article can be found, in the online version, at http://dx.doi.org/10.1016/j.febslet.2014.11.022.

References

[1] Davies, Bryan W., Bogard, Ryan W., Young, Travis S. and Mekalanos, John J. (2012) Coordinated regulation of accessory genetic elements produces cyclic di-nucleotides for *V. cholerae* virulence. Cell 149, 358–370.
[2] Ablasser, A., Goldeck, M., Cavlar, T., Deimling, T., Witte, G., Rohl, I., Hopfner, K.P., Ludwig, J. and Hornung, V. (2013) CGAS produces a 2′-5′-linked cyclic dinucleotide second messenger that activates STING. Nature 498, 380–384.
[3] Gao, P., Ascano, M., Wu, Y., Barchet, W., Gaffney, B.L., Zillinger, T., Serganov, A.A., Liu, Y., Jones, R.A., Hartmann, G., Tuschl, T. and Patel, D.J. (2013) Cyclic [G(2′,5′)pA(3′,5′)p] is the metazoan second messenger produced by DNA-activated cyclic GMP-AMP synthase. Cell 153, 1094–1107.
[4] Witte, G., Hartung, S., Büttner, K. and Hopfner, K.P. (2008) Structural biochemistry of a bacterial checkpoint protein reveals diadenylate cyclase activity regulated by DNA recombination intermediates. Mol. cell 30, 167–178.
[5] Römling, U. (2008) Great times for small molecules: c-di-AMP, a second messenger candidate in Bacteria and Archaea. Sci. Signaling 1, pe39.
[6] Bai, Y., Yang, J., Zhou, X., Ding, X., Eisele, L.E. and Bai, G. (2012) Mycobacterium tuberculosis Rv3586 (DacA) is a diadenylate cyclase that converts ATP or ADP into c-di-AMP. PLoS ONE 7, e35206.

[7] Corrigan, R.M., Abbott, J.C., Burhenne, H., Kaever, V. and Gründling, A. (2011) C-di-AMP is a new second messenger in *Staphylococcus aureus* with a role in controlling cell size and envelope stress. PLoS Pathog. 7, e1002217.
[8] Kamegaya, T., Kuroda, K. and Hayakawa, Y. (2011) Identification of a *Streptococcus pyogenes* SF370 gene involved in production of c-di-AMP. Nagoya J. Med. Sci. 73, 49–57.
[9] Mehne, F.M., Gunka, K., Eilers, H., Herzberg, C., Kaever, V. and Stulke, J. (2013) Cyclic di-AMP homeostasis in bacillus subtilis: both lack and high level accumulation of the nucleotide are detrimental for cell growth. J. Biol. Chem. 288, 2004–2017.
[10] Woodward, J.J., Iavarone, A.T. and Portnoy, D.A. (2010) C-di-AMP secreted by intracellular Listeria monocytogenes activates a host type I interferon response. Science 328, 1703–1705.
[11] Oppenheimer-Shaanan, Y., Wexselblatt, E., Katzhendler, J., Yavin, E. and Ben-Yehuda, S. (2011) C-di-AMP reports DNA integrity during sporulation in *Bacillus subtilis*. EMBO Rep. 12, 594–601.
[12] Luo, Y. and Helmann, J.D. (2012) Analysis of the role of *Bacillus subtilis* sigma(M) in beta-lactam resistance reveals an essential role for c-di-AMP in peptidoglycan homeostasis. Mol. Microbiol. 83, 623–639.
[13] Zhang, L., Li, W. and He, Z.G. (2013) DarR, a TetR-like transcriptional factor, is a cyclic di-AMP-responsive repressor in *Mycobacterium smegmatis*. J. Biol. Chem. 288, 3085–3096.
[14] Corrigan, R.M., Campeotto, I., Jeganathan, T., Roelofs, K.G., Lee, V.T. and Gründling, A. (2013) Systematic identification of conserved bacterial c-di-AMP receptor proteins. Proc. Natl. Acad. Sci. U.S.A. 110, 9084–9089.
[15] Mehne, F.M., Schroder-Tittmann, K., Eijlander, R.T., Herzberg, C., Hewitt, L., Kaever, V., Lewis, R.J., Kuipers, O.P., Tittmann, K. and Stulke, J. (2014) Control of the diadenylate cyclase CdaS in *Bacillus subtilis*: an autoinhibitory domain limits cyclic Di-Amp production. J. Biol. Chem. 289, 21098–21107.
[16] Cho, K.H. and Kang, S.O. (2013) *Streptococcus pyogenes* c-di-AMP phosphodiesterase, GdpP, influences SpeB processing and virulence. PLoS ONE 8, e69425.
[17] Du, B., Ji, W., An, H., Shi, Y., Huang, Q., Cheng, Y., Fu, Q., Wang, H., Yan, Y. and Sun, J. (2014) Functional analysis of c-di-AMP phosphodiesterase, GdpP, in *Streptococcus suis* serotype 2. Microbiol. Res. 169, 749–758.
[18] Gao, A. and Serganov, A. (2014) Structural insights into recognition of c-di-AMP by the ydaO riboswitch. Nat. Chem. Biol. 10, 787–792.
[19] Nelson, J.W., Sudarsan, N., Furukawa, K., Weinberg, Z., Wang, J.X. and Breaker, R.R. (2013) Riboswitches in eubacteria sense the second messenger c-di-AMP. Nat. Chem. Biol. 9, 834–839.
[20] Ren, A. and Patel, D.J. (2014) C-di-AMP binds the ydaO riboswitch in two pseudo-symmetry-related pockets. Nat. Chem. Biol. 10, 780–786.
[21] Sureka, K., Choi, P.H., Precit, M., Delince, M., Pensinger, D.A., Huynh, T.N., Jurado, A.R., Goo, Y.A., Sadilek, M., Iavarone, A.T., Sauer, J.D., Tong, L. and Woodward, J.J. (2014) The cyclic dinucleotide c-di-AMP is an allosteric regulator of metabolic enzyme function. Cell 158, 1389–1401.
[22] Huergo, L.F., Chandra, G. and Merrick, M. (2013) P(II) signal transduction proteins: nitrogen regulation and beyond. FEMS Microbiol. Rev. 37, 251–283.
[23] Truan, D., Huergo, L.F., Chubatsu, L.S., Merrick, M., Li, X.D. and Winkler, F.K. (2010) A new P(II) protein structure identifies the 2-oxoglutarate binding site. J. Mol. Biol. 400, 531–539.
[24] Kabsch, W. (2010) Xds. Acta Cystallogr. Sect. D, Biol. Crystallogr. 66, 125–132.
[25] McCoy, A.J., Grosse-Kunstleve, R.W., Adams, P.D., Winn, M.D., Storoni, L.C. and Read, R.J. (2007) Phaser crystallographic software. J. Appl. Crystallogr. 40, 658–674.
[26] Winn, M.D., Ballard, C.C., Cowtan, K.D., Dodson, E.J., Emsley, P., Evans, P.R., Keegan, R.M., Krissinel, E.B., Leslie, A.G., McCoy, A., McNicholas, S.J., Murshudov, G.N., Pannu, N.S., Potterton, E.A., Powell, H.R., Read, R.J., Vagin, A. and Wilson, K.S. (2011) Overview of the CCP4 suite and current developments. Acta Cystallogr. Sect. D, Biol. Crystallogr. 67, 235–242.
[27] Emsley, P. and Cowtan, K. (2004) Coot: model-building tools for molecular graphics. Acta Cystallogr. Sect. D, Biol. Crystallogr. 60, 2126–2132.
[28] Afonine, P.V., Grosse-Kunstleve, R.W., Echols, N., Headd, J.J., Moriarty, N.W., Mustyakimov, M., Terwilliger, T.C., Urzhumtsev, A., Zwart, P.H. and Adams, P.D. (2012) Towards automated crystallographic structure refinement with phenix.refine. Acta Cystallogr. Sect. D, Biol. Crystallogr. 68, 352–367.
[29] L.L.C. Schrödinger, The PyMOL Molecular Graphics System, Version 1.3r1, 2010.
[30] Boivin, S., Kozak, S. and Meijers, R. (2013) Optimization of protein purification and characterization using Thermofluor screens. Protein Expression Purif. 91, 192–206.
[31] Moure, V.R., Razzera, G., Araujo, L.M., Oliveira, M.A., Gerhardt, E.C., Muller-Santos, M., Almeida, F., Pedrosa, F.O., Valente, A.P., Souza, E.M. and Huergo, L.F. (2012) Heat stability of Proteobacterial PII protein facilitate purification using a single chromatography step. Protein Expression Purif. 81, 83–88.
[32] Söding, J. (2005) Protein homology detection by HMM-HMM comparison. Bioinformatics 21, 951–960.

4 DISCUSSION

C-di-AMP was discovered only very recently and there are still more open questions than answers on how synthesis, signaling and degradation of this second messenger work. In the following chapters some of these poorly understood aspects and possible explanations will be described.

4.1 HOW IS C-DI-AMP SYNTHESIS REGULATED?

So far, DisA is the only DAC domain protein which's c-di-AMP synthesis mechanism was analyzed in detail. However, the catalytically active residues of DAC domains are highly conserved between different proteins and species and a similar reaction mechanism can be assumed for all of them. Still, the regulation of the enzymatic activity differs between the three classes of DAC proteins – DisA, DacA and DacB – and is far from being understood.

The rate limiting step of the cyclase reaction seems to be product release rather than the reaction itself for DisA. This is due to the narrow tunnels connecting the active sites of the protein to the surface, which are just large enough for c-di-AMP to pass through [40]. However, this is only the case for octameric DisA and not for DacA or DacB, which possess a different domain organization. In order to form a functional active site, two DAC domains need to come into close proximity in a head-to-head orientation. This is true for DisA, which forms a very stable and rigid octamer with four active sites in its center. It was shown that DacA lacking its transmembrane helices forms an active dimer in solution, even though it does not in the protein crystal, indicating a rather unstable dimerization [34]; the oligomeric state of the full-length protein was not studied so far. However, maximal activity of DacA is only obtained after interaction with its activator CdaR, and even then DacA is less active than DisA [31]. The activation of DacA by CdaR might be due to stabilization of the active dimer conformation or through structural changes in the active site. Still, the conditions for c-di-AMP synthesis are less ideal than in DisA, as DisA is more active than DacA. Furthermore, the function of the transmembrane helices and whether they have an influence on the enzymatic activity is still unknown. Structural analysis of full-length DacA and the DacA-CdaR complex will answer these open questions on c-di-AMP synthesis by DacA.

The activity of DacB is negatively regulated by its N-terminal α-helical YojJ domain, as point mutations and deletion of this domain result in strongly increased activity [31,36]. The uncharacterized DacB homolog BC_4920 from *B. cereus* crystallizes in a way that the YojJ domains interact with each other and the DAC domains do not form functional dimers (Figure 22). Based on this, it was suggested that DacB oligomerizes in a similar inactive hexameric conformation in solution. However, the structure of the oligomer is not compact but widely expanded and it

seems very unlikely that a DacB oligomer is present in this or a similar conformation in solution. It remains to be shown whether the interactions observed in the crystal structure are only due to crystal packing or indeed represent the inactive state of DacB as present in solution. Furthermore, the mechanism of DacB activation is unknown. In order to form a functional active site the DacB oligomer needs to undergo drastic rearrangements upon a yet unknown stimulus. To answer these open questions, first of all the oligomeric state of DacB in solution needs to be studied in more detail and by suitable techniques, as the protein is rather unstable and tends to aggregate. Moreover, the mode of DacB activation by interaction partners, small molecule ligands or different mechanisms needs to be studied to fully understand the function of this c-di-AMP synthase.

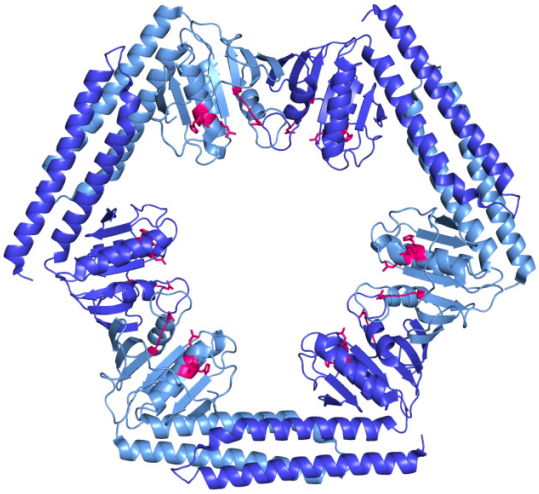

Figure 22: Hexamer formation in the crystal of the *B. cereus* DacB homolog; the catalytically essential DGA and RHR motifs are highlighted (PDB 2fb5 [37])

DisA is constitutively active and is inactivated by interaction with branched DNA or RadA [21,29]. Branched DNA structures occur for example at stalled replication forks or during homologous recombination and inhibition of DisA serves as a signal for the cell to stop sporulation until the DNA damage is repaired [20]. DisA comprises a C-terminal HhH domain responsible for DNA binding. Since DisA forms a symmetrical octamer, four DNA binding domains are on each side of the oligomer (Figure 23 A). The four-fold symmetry of the HhH domains is ideal for binding to holliday junctions. However, comparison with *E. coli* RuvA [101], a protein involved in holliday junction processing, shows that the HhH domains of DisA need to rearrange in order to allow DNA binding. One of the loops interacting with DNA is partially buried; moreover the DNA would clash with DisA in the conformation present in the crystal structure (Figure 23 B). Therefore it is likely that the HhH domains of DisA rotate in order to bind to DNA and this rearrangement leads to further structural changes resulting in inactivation of DisA.

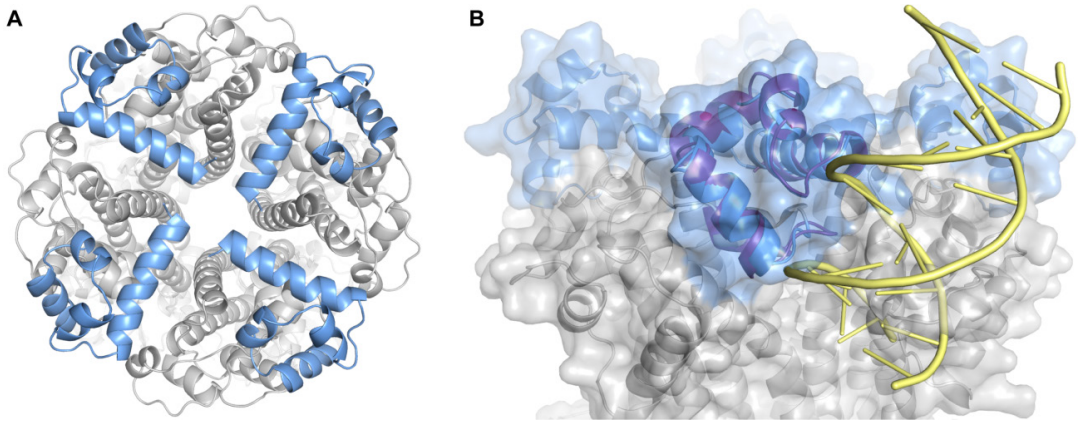

Figure 23: (**A**) HhH domains of octameric *T. maritima* DisA (PDB 4yvz [40]). (**B**) *T. maritima* DisA (HhH domains blue) in superposition with the HhH domain of *E. coli* RuvB (purple) in complex with DNA (yellow); PDB 1c7y [101].

So far it is not understood how DisA is inactivated upon binding to DNA. The rotation of the HhH domains might be transduced by the helical spine domain and finally lead to structural changes in the active site. However, when only one DisA octamer binds to a branched DNA structure and is inhibited, the remaining DisA molecules are still active and produce c-di-AMP. Therefore the drop in the intracellular c-di-AMP concentration would be very small and probably not sufficient for the cell to sense it. This is why DNA binding probably triggers other processes affecting more than one DisA octamer (Figure 24). One possibility is that DisA disassembles. The DisA octamer is very stable in solution and does not show any dissociation in size exclusion chromatography or small angle X-ray scattering experiments. However, rotation of the HhH domains upon binding to DNA might induce further conformational changes disturbing the interactions between the monomers. After dissociation of one DisA octamer, another could bind to the branched DNA structure and more and more DisA complexes would be successively inactivated. Another reason for efficient inactivation of DisA *in vivo* might be the interaction with RadA. DisA and RadA were shown to interact *in vivo* and overexpression phenotypes of DisA can be rescued by overexpression of RadA [29]. However, our own unpublished data shows that the interaction is very weak *in vitro*, when no DNA is present. Therefore RadA might be recruited to the DisA-DNA complex rather than to DisA alone. Still, the mechanism of DisA inactivation by RadA is not known. RadA comprises a LonC protease domain and might therefore degrade DisA. Clearly, the function of RadA needs to be studied in more detail to fully understand its interaction with DisA. The third possibility of DisA inactivation is the recruitment or activation of effector proteins by the DisA-DNA complex. These proteins might e.g. be phosphodiesterases, which degrade c-di-AMP in addition to DisA being less active. However, there is no experimental evidence for this theory so far.

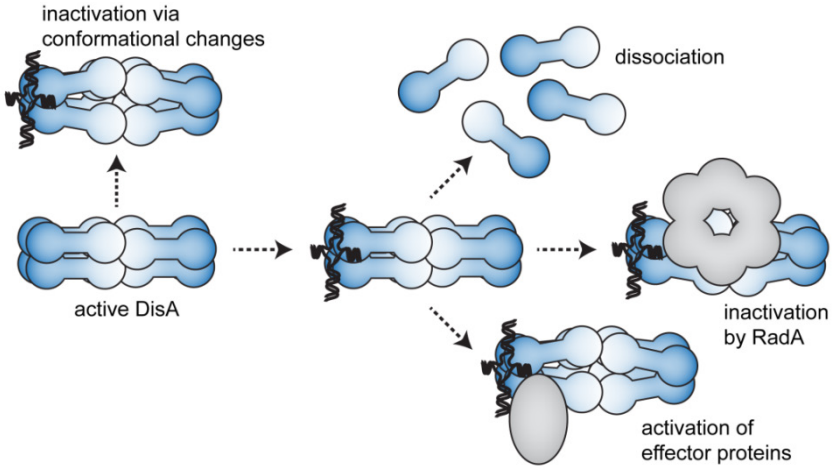

Figure 24: Theories on DisA inactivation after binding to DNA

Finally, it is unknown how the drop in the c-di-AMP concentration upon DisA inactivation is sensed and by which mechanisms it delays sporulation. The c-di-AMP receptors identified so far seem not to be involved in sporulation; therefore the key protein is probably a receptor that has not been found yet. Moreover, it remains unclear how the cell distinguishes between c-di-AMP from different DAC domain proteins to initiate the corresponding response. One way might be compartmentation, as DacA is associated to the cell membrane and DisA co-localizes with DNA [20]. Therefore, DacA might signal cell wall and membrane related issues, while DisA signals DNA damage. Nevertheless, diffusion of a small molecule such as c-di-AMP is fast and its radius of action therefore covers the whole bacterial cell. Today the regulation of c-di-AMP synthesis and its sensing is still poorly understood and future studies will hopefully answer these questions.

4.2 C-DI-AMP RECEPTOR PSTA

PstA was found to specifically bind c-di-AMP with high affinity in *S. aureus*, *B. subtilis* and *L. monocytogenes*. Crystallization studies revealed that PstA adopts a trimeric ferredoxin like fold typical for P_{II} proteins. However, poor sequence homology, altered ligand binding loops and a different function show that PstA is only distantly related to canonical P_{II} proteins [60–63]. The B- and T-loops are swapped in length and presumably fulfill complementary functions. The T-loop, which is the longer of the two loops in canonical P_{II} proteins and is usually involved in interaction with target proteins, comprises only few amino acids in PstA and interacts with c-di-AMP. On the other hand, the B-loop, which is the longer loop in PstA, might bind to downstream targets or signaling proteins. It was suggested that the B-loop becomes more ordered in the c-di-AMP bound state; however, the electron density of this flexible loop in the corresponding crystal structures is very diffuse and hardly

interpretable. Moreover, the structure in solution is difficult to analyze and therefore unknown. Possibly, the interaction of PstA with its downstream targets does not take place *via* the B-loop, but *via* the compact head domain of the protein. In this case the rearrangement of the T-loop upon c-di-AMP binding might facilitate interaction with target proteins. P_{II}(-like) proteins were shown to transduce signals by different mechanisms upon binding to small molecule ligands such as ATP or ADP. For example, ADP bound *E. coli* GlnK interacts with the ammonia channel AmtB by insertion of its long T-loops into the channel's pores and thereby blocks it (Figure 25 A) [102]. On the other hand, *Synechococcus elongatus* P_{II} binds to one of its targets, the transcription factor activator PipX, mainly *via* its core, but still the T-loops play an important role by forming a 'cage' around the three PipX monomers bound simultaneously (Figure 25 B) [103]. Finally, *Azospirillum brasilense* GlnZ in complex with ADP binds to three monomers of the nitrogenase regulatory enzyme DraG exclusively *via* its core domain and not by interaction with the B- or T-loops (Figure 25 C) [104].

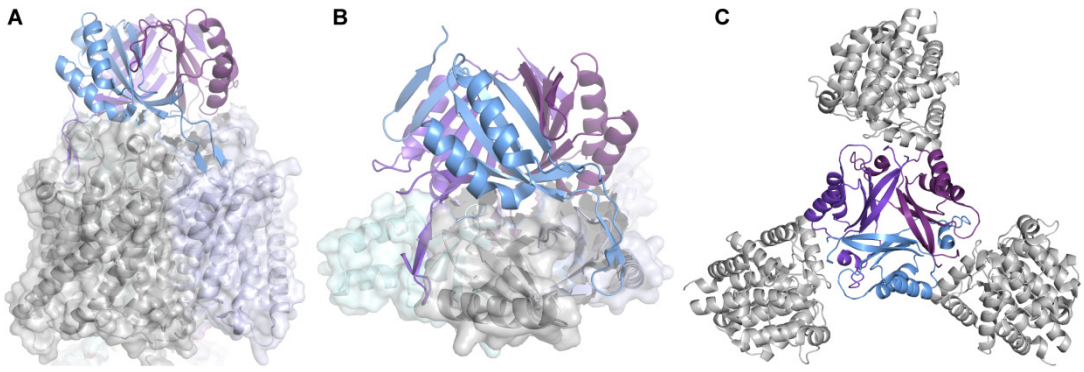

Figure 25: (**A**) *E. coli* GlnK in complex with the ammonia channel AmtB (PDB 2nuu [102]). (**B**) *S. elongates* P_{II} in complex with the transcription factor regulator PipX (PDB 2xg8 [103]). (**C**) *A. brasilense* GlnZ in complex with the nitrogenase regulatory enzyme DraG (PDB 3o5t [104]).

The identification of PstA's target proteins is most important for correct interpretation of the PstA crystal structures; however, no interaction partner of PstA was found so far. Even though PstA is neither essential nor universal, all species comprising a PstA protein harbor also a DAC, therefore interaction with c-di-AMP is likely conserved and important [61–63]. A genetic link between PstA and the thymidylate kinase tmk is observed in different organisms, but no experimental evidence confirming this possible interaction partner was given so far. Pull-down experiments might allow identification of proteins interacting with PstA and reveal the signaling pathway this protein is involved in.

Only two c-di-AMP binding proteins have been crystallized so far – PstA and the *L. monocytogenes* pyruvate carboxylase. However, the c-di-AMP binding sites of both proteins are not conserved. The only common feature is that c-di-AMP is bound

in a surface accessible pocket between two subunits. Still, this observation is not sufficient to deduce a general c-di-AMP binding motif or fold.

It is still not known why c-di-AMP is essential in most bacterial species studied so far. The function of c-di-AMP seems to be mainly associated to K^+ and cell wall metabolism and homeostasis. However, all widely spread c-di-AMP receptors identified were shown to be not essential. Therefore the essential receptor is either still missing or the sum of all individual parts makes c-di-AMP important. It was suggested that c-di-AMP does not activate an essential process but indirectly inhibit a toxic mechanism [71]. However, evidence for such a mode of action was only shown for *L. monocytogenes* so far and, what is more, it is still unknown what this toxic mechanism might be. Further search for c-di-AMP receptors and more detailed investigation of the pathways already identified will reveal the essential mechanism.

4.3 C-DI-AMP PATHWAYS AS DRUG TARGETS

The intracellular concentration of c-di-AMP needs to be tightly regulated, as increased as well as decreased levels of this second messenger lead to severe phenotypes. Moreover, c-di-AMP was found to be essential in all but one species studied so far. Furthermore, bacteria with decreased levels of c-di-AMP possess a less stable cell wall and are therefore more susceptible towards cell wall targeting antibiotics [74,81,83,84]. This is why DAC inhibitors, or similarly PDE activators, might prove to have beneficial effects in antimicrobial therapy. DAC inhibitors might not be sufficient to kill bacteria efficiently, as strains with conditionally depleted DACs are still able to grow slowly. However, those substances might be powerful in combination with cell wall targeting antibiotics such as β-lactams.

3′-dATP is a potent competitive inhibitor of DisA. The substance is derived from cordycepin (3′-deoxy adenosine), an adenosine analog produced by the fungus Cordyceps. Cordyceps is not only applied in traditional Chinese medicine, but was also shown to exhibit various medically beneficial properties in treatment of e.g. cancer and inflammatory diseases. Many of the effects observed could be assigned to cordycepin. When cordycepin is taken into the cell, it is first phosphorylated to 3′-dAMP, 3′-dADP or 3′-dATP and subsequently inhibits various enzymes, finally inducing apoptosis. Even though the effects of cordycepin, being an ATP analog, are rather unspecific, the substance is tested against leukemia in phase 2 clinical trials (reviewed e.g. in [105,106]). In addition to the therapeutic potential against e.g. cancer, cordycepin was shown to inhibit growth of Clostridium species with similar efficiency as tetracycline or chloramphenicol [88]. Cordycepin definitely inhibits several different enzymes in bacteria; however, DAC domain proteins are certainly among them. 3′-dATP is probably not suitable to be administered as an antimicrobial drug, since severe side-effects can be expected due to it interfering with many different enzymes. Still, 3′-dATP is commercially available and might therefore be

interesting for research purposes. The second DisA inhibitor described is Bromophenol-TH [87]. This substance was identified in a kinase inhibitor library and acts as an allosteric inhibitor of DisA. Binding of Bromophenol-TH changes fluorescence of a tryptophan residue. Unfortunately, the authors failed to mention the species their DisA originates from, as for example *B. subtilis* DisA does not possess any tryptophan. Therefore it is not possible to speculate on the mode of inhibition by bromophenol-TH by comparison with the *T. maritima* DisA crystal structure. However, the allosteric binding of bromophenol-TH is likely to be specific for DisA, or even only for the DisA used by the authors, and does probably not affect other DAC domain proteins.

DAC inhibition is certainly beneficial in many bacterial species, but not all. Intracellular bacteria such as *L. monocytogenes* and *M. tuberculosis* secrete c-di-AMP into the cytosol of their host cells. C-di-AMP is then recognized as a PAMP by STING or DDX41 and the immune response is initiated. It was shown that the more c-di-AMP is produced and secreted, the stronger is the immune response, measured *via* the IFN-β concentration. This strong immune response leads to efficient killing of the bacteria and therefore bacterial strains with high c-di-AMP levels exhibit a less virulent phenotype [23,74,76,78,85,89]. Consistently, reduced c-di-AMP levels lead to less IFN-β production and a more virulent phenotype in *M. tuberculosis* [76,85]. In contrast, a low c-di-AMP concentration results in a destabilized cell wall in *L. monocytogenes*, therefore to more cell lysis and in consequence a strong immune response [74]. Therefore increased, as well as decreased levels of c-di-AMP in *L. monocytogenes* are beneficial for the host, while only an increase in the c-di-AMP concentration triggers a strong immune response during *M. tuberculosis* infections. This is why inhibition of the PDE instead of the DAC might be promising in therapy against *M. tuberculosis*. In general, bacteria with high intracellular c-di-AMP concentrations are less susceptible towards cell wall antibiotics, as the cell wall is more stable; however, they exhibit a less virulent phenotype [24,27,30,74–76,78,81,84–86]. The reason for this is not entirely understood. In *S. pyogenes* knockout of the PDE negatively affects the virulence factor SpeB and this bacterial strain is therefore less pathogenic in a mouse model [75]. In *S. pneumoniae* knockout of one or both its PDEs leads to almost 100% survival of mice, the reason is however unknown [27].

Depending on the bacterial species, the effects of high or low c-di-AMP concentrations obviously differ. C-di-AMP is essential in most bacteria. Moreover, due to the cell wall being more stable in high c-di-AMP conditions the bacteria are more resistant to cell wall antibiotics and undergo less lysis. Therefore less bacterial DNA and other PAMPs are released to trigger an immune response. On the other hand, PDEs seems to have a function in virulence factor processing and c-di-AMP itself acts as a PAMP. The species specific differences need to be studied in more detail to understand where they originate from and how they might be used for specific and efficient antimicrobial therapy.

5 REFERENCES

1 Alberts, B. (2002) Molecular biology of the cell 4th ed., Garland Science, New York.

2 Sutherland, E. W. and Rall, T. W. (1958) Fractionation and characterization of a cyclic adenine ribonucleotide formed by tissue particles. J. Biol. Chem. **232**, 1077–1092.

3 Gancedo, J. M. (2013) Biological roles of cAMP: variations on a theme in the different kingdoms of life. Biol. Rev. **88**, 645–668.

4 Görke, B. and Stülke, J. (2008) Carbon catabolite repression in bacteria: many ways to make the most out of nutrients. Nat. Rev. Microbiol. **6**, 613–624.

5 Ahuja, N., Kumar, P. and Bhatnagar, R. (2004) The adenylate cyclase toxins. Crit. Rev. Microbiol. **30**, 187–196.

6 McDonough, K. A. and Rodriguez, A. (2012) The myriad roles of cyclic AMP in microbial pathogens: from signal to sword. Nat. Rev. Microbiol., Nature Publishing Group **10**, 27–38.

7 Cashel, M. and Gallant, J. (1969) Two compounds implicated in the function of the RC gene of Escherichia coli. Nature **221**, 838–841.

8 Liu, K., Bittner, A. N. and Wang, J. D. (2015) Diversity in (p)ppGpp metabolism and effectors. Curr. Opin. Microbiol., Elsevier Ltd **24**, 72–79.

9 Gaca, A. O., Colomer-Winter, C. and Lemos, J. A. (2015) Many means to a common end: the intricacies of (p)ppGpp metabolism and its control of bacterial homeostasis. J. Bacteriol. **197**, 1146–1156.

10 Ross, P., Weinhouse, H., Aloni, Y., Michaeli, D., Weinberger-Ohana, P., Mayer, R., Braun, S., de Vroom, E., van der Marel, G. A., van Boom, J. H., et al. (1987) Regulation of cellulose synthesis in Acetobacter xylinum by cyclic diguanylic acid. Nature **325**, 279–281.

11 Kalia, D., Merey, G., Nakayama, S., Zheng, Y., Zhou, J., Luo, Y., Guo, M., Roembke, B. T. and Sintim, H. O. (2013) Nucleotide, c-di-GMP, c-di-AMP, cGMP, cAMP, (p)ppGpp signaling in bacteria and implications in pathogenesis. Chem. Soc. Rev. **42**, 305–341.

12 Römling, U., Galperin, M. Y. and Gomelsky, M. (2013) Cyclic di-GMP: the first 25 years of a universal bacterial second messenger. Microbiol. Mol. Biol. Rev. **77**, 1–52.

13 Ochoa de Alda, J. A. G., Ajlani, G. and Houmard, J. (2000) Synechocystis Strain PCC 6803 cya2, a Prokaryotic Gene That Encodes a Guanylyl Cyclase. J. Bacteriol. **182**, 3839–3842.

14 Cadoret, J.-C., Rousseau, B., Perewoska, I., Sicora, C., Cheregi, O., Vass, I. and Houmard, J. (2005) Cyclic nucleotides, the photosynthetic apparatus and response to a UV-B stress in the Cyanobacterium Synechocystis sp. PCC 6803. J. Biol. Chem. **280**, 33935–33944.

15 Marden, J. N., Dong, Q., Roychowdhury, S., Berleman, J. E. and Bauer, C. E. (2011) Cyclic GMP controls Rhodospirillum centenum cyst development. Mol. Microbiol. **79**, 600–615.

16 An, S.-Q., Chin, K.-H., Febrer, M., McCarthy, Y., Yang, J.-G., Liu, C.-L., Swarbreck, D., Rogers, J., Dow, J. M., Chou, S.-H., et al. (2013) A cyclic GMP-dependent signalling pathway regulates bacterial phytopathogenesis. EMBO J., Nature Publishing Group **32**, 2430–2438.

17 Davies, B. W., Bogard, R. W., Young, T. S. and Mekalanos, J. J. (2012) Coordinated regulation of accessory genetic elements produces cyclic di-nucleotides for V. cholerae virulence. Cell, Elsevier Inc. **149**, 358–370.

18 Zhu, D., Wang, L., Shang, G., Liu, X., Zhu, J., Lu, D., Wang, L., Kan, B., Zhang, J.-R. and Xiang, Y. (2014) Structural Biochemistry of a Vibrio cholerae Dinucleotide Cyclase Reveals Cyclase Activity Regulation by Folates. Mol. Cell, Elsevier Inc. **55**, 931–937.

19 Gao, J., Tao, J., Liang, W., Zhao, M., Du, X., Cui, S., Duan, H., Kan, B., Su, X. and Jiang, Z. (2015) Identification and characterization of phosphodiesterases that specifically degrade 3′3′-cyclic GMP-AMP. Cell Res., Nature Publishing Group **25**, 539–550.

20 Bejerano-Sagie, M., Oppenheimer-Shaanan, Y., Berlatzky, I., Rouvinski, A., Meyerovich, M. and Ben-Yehuda, S. (2006) A Checkpoint Protein That Scans the Chromosome for Damage at the Start of Sporulation in Bacillus subtilis. Cell **125**, 679–690.

21 Witte, G., Hartung, S., Büttner, K. and Hopfner, K.-P. (2008) Structural Biochemistry of a Bacterial Checkpoint Protein Reveals Diadenylate Cyclase Activity Regulated by DNA Recombination Intermediates. Mol. Cell **30**, 167–178.

22 Corrigan, R. M. and Gründling, A. (2013) Cyclic di-AMP: another second messenger enters the fray. Nat. Rev. Microbiol., Nature Publishing Group **11**, 513–524.

23 Woodward, J. J., Iavarone, A. T. and Portnoy, D. A. (2010) c-di-AMP secreted by intracellular Listeria monocytogenes activates a host type I interferone response. Science (80-.). **328**, 1703–1705.

24 Corrigan, R. M., Abbott, J. C., Burhenne, H., Kaever, V. and Gründling, A. (2011) c-di-AMP Is a New Second Messenger in Staphylococcus aureus with a Role in Controlling Cell Size and Envelope Stress. PLoS Pathog. **7**.

25 Kamegaya, T., Kuroda, K. and Hayakawa, Y. (2011) Identification of a Streptococcus Pyogenes SF370 Gene Involved in Production of c-di-AMP. Nagoya J. Med. Sci. **73**, 49–58.

26 Bai, Y., Yang, J., Zhou, X., Ding, X., Eisele, L. E. and Bai, G. (2012) Mycobacterium tuberculosis Rv3586 (DacA) Is a Diadenylate Cyclase That Converts ATP or ADP into c-di-AMP. PLoS One **7**.

27 Bai, Y., Yang, J., Eisele, L. E., Underwood, A. J., Koestler, B. J., Waters, C. M., Metzger, D. W. and Bai, G. (2013) Two DHH subfamily 1 proteins in Streptococcus pneumoniae possess cyclic di-AMP phosphodiesterase activity and affect bacterial growth and virulence. J. Bacteriol. **195**, 5123–5132.

28 Zheng, C., Wang, J., Luo, Y., Fu, Y., Su, J. and He, J. (2013) Highly efficient enzymatic preparation of c-di-AMP using the diadenylate cyclase DisA from Bacillus thuringiensis. Enzyme Microb. Technol., Elsevier Inc. **52**, 319–324.

29 Zhang, L. and He, Z.-G. (2013) Radiation-sensitive gene A (RadA) targets DisA, DNA integrity scanning protein A, to negatively affect its cyclic-di-AMP synthesis activity in Mycobacterium smegmatis. J. Biol. Chem. **288**, 22426–22436.

30 Ye, M., Zhang, J. J., Fang, X., Lawlis, G. B., Troxell, B., Zhou, Y., Gomelsky, M., Lou, Y. and Yang, X. F. (2014) DhhP, a cyclic di-AMP phosphodiesterase of Borrelia burgdorferi, is essential for cell growth and virulence. Infect. Immun. **82**, 1840–1849.

31 Mehne, F. M. P., Gunka, K., Eilers, H., Herzberg, C., Kaever, V. and Stülke, J. (2013) Cyclic di-AMP homeostasis in Bacillus subtilis: both lack and high-level accumulation of the nucleotide are detrimental for cell growth. J. Biol. Chem. **288**, 2004–2017.

32 Commichau, F. M., Dickmanns, A., Gundlach, J., Ficner, R. and Stülke, J. (2015) A jack of all trades: the multiple roles of the unique essential second messenger cyclic di-AMP. Mol. Microbiol. **97**, 189–204.

33 Corrigan, R. M., Bowman, L., Willis, A. R., Kaever, V. and Gründling, A. (2015) Crosstalk between two Nucleotide-Signaling Pathways in Staphylococcus aureus. J. Biol. Chem. **290**, 5826–5839.

34 Rosenberg, J., Dickmanns, A., Neumann, P., Gunka, K., Arens, J., Kaever, V., Stülke, J., Ficner, R. and Commichau, F. M. (2015) Structural and biochemical analysis of the essential diadenylate cyclase CdaA from Listeria monocytogenes. J. Biol. Chem. **290**, 6596–6606.

35 Nicolas, P., Mäder, U., Dervyn, E., Rochat, T., Leduc, A., Pigeonneau, N., Bidnenko, E., Marchadier, E., Hoebeke, M., Aymerich, S., et al. (2012) Condition-Dependent Transcriptome Reveals High-Level Regulatory Architecture in Bacillus subtilis. Science (80-.). **335**, 1103–1106.

36 Mehne, F. M. P., Schröder-Tittmann, K., Eijlander, R. T., Herzberg, C., Hewitt, L., Kaever, V., Lewis, R. J., Kuipers, O. P., Tittmann, K. and Stülke, J. (2014) Control of the Diadenylate Cyclase CdaS in Bacillus subtilis: An Autoinhibitory Domain Limits c-di-AMP Production. J. Biol. Chem. **289**, 21098–21107.

37 Zhang, R. . Z. M. . G. S. . A. J. . C. F. . J. A. The crystal structure of the hypothetical membrane spanning protein from Bacillus cereus. To be Publ.

38 Flórez, L. A., Roppel, S. F., Schmeisky, A. G., Lammers, C. R. and Stülke, J. (2009) A community-curated consensual annotation that is continuously updated: the Bacillus subtilis centred wiki SubtiWiki. Database **2009**.

39 Campos, S. S., Ibarra-Rodriguez, J. R., Barajas-Ornelas, R. C., Ramírez-Guadiana, F. H., Obregón-Herrera, A., Setlow, P. and Pedraza-Reyes, M. (2014) Interaction of apurinic/apyrimidinic endonucleases Nfo and ExoA with the DNA integrity scanning protein DisA in the processing of oxidative DNA damage during Bacillus subtilis spore outgrowth. J. Bacteriol. **196**, 568–578.

40 Müller, M., Deimling, T., Hopfner, K.-P. and Witte, G. (2015) Structural analysis of the di-adenylate cyclase reaction of DNA-integrity scanning protein A (DisA) and its inhibition by 3′-dATP. Biochem. J. **489**, 367–374.

41 Oppenheimer-Shaanan, Y., Wexselblatt, E., Katzhendler, J., Yavin, E. and Ben-Yehuda, S. (2011) c-di-AMP reports DNA integrity during sporulation in Bacillus subtilis. EMBO Rep., Nature Publishing Group **12**, 594–601.

42 Manikandan, K., Sabareesh, V., Singh, N., Saigal, K., Mechold, U. and Sinha, K. M. (2014) Two-Step Synthesis and Hydrolysis of Cyclic di-AMP in Mycobacterium tuberculosis. PLoS One **9**.

43 Kranzusch, P. J., Lee, A. S. Y., Wilson, S. C., Solovykh, M. S., Vance, R. E., Berger, J. M. and Doudna, J. A. (2014) Structure-Guided Reprogramming of Human cGAS Dinucleotide Linkage Specificity. Cell, Elsevier Inc. **158**, 1011–1021.

44 Ablasser, A., Goldeck, M., Cavlar, T., Deimling, T., Witte, G., Röhl, I., Hopfner, K.-P., Ludwig, J. and Hornung, V. (2013) cGAS produces a 2′-5′-linked cyclic dinucleotide second messenger that activates STING. Nature **498**, 380–384.

45 Gao, P., Ascano, M., Wu, Y., Barchet, W., Gaffney, B. L., Zillinger, T., Serganov, A. A., Liu, Y., Jones, R. A., Hartmann, G., et al. (2013) Cyclic [G(2',5')pA(3',5')p] is the metazoan second messenger produced by DNA-activated cyclic GMP-AMP synthase. Cell **153**, 1094–1107.

46 Hornung, V., Hartmann, R., Ablasser, A. and Hopfner, K.-P. (2014) OAS proteins and cGAS: unifying concepts in sensing and responding to cytosolic nucleic acids. Nat. Rev. Immunol., Nature Publishing Group **14**, 521–528.

47 Zhang, L., Li, W. and He, Z.-G. (2013) DarR, a TetR-like transcriptional factor, is a cyclic di-AMP-responsive repressor in Mycobacterium smegmatis. J. Biol. Chem. **288**, 3085–3096.

48 Hänelt, I., Tholema, N., Kröning, N., Vor der Brüggen, M., Wunnicke, D. and Bakker, E. P. (2011) KtrB, a member of the superfamily of K+ transporters. Eur. J. Cell Biol. **90**, 696–704.

49 Corrigan, R. M., Campeotto, I., Jeganathan, T., Roelofs, K. G., Lee, V. T. and Gründling, A. (2013) Systematic identification of conserved bacterial c-di-AMP receptor proteins. Proc. Natl. Acad. Sci. **110**, 9084–9089.

50 Levin, E. J. and Zhou, M. (2014) Recent progress on the structure and function of the TrkH/KtrB ion channel. Curr. Opin. Struct. Biol., Elsevier Ltd **27**, 95–101.

51 Vieira-Pires, R. S., Szollosi, A. and Morais-Cabral, J. H. (2013) The structure of the KtrAB potassium transporter. Nature **496**, 323–328.

52 Bai, Y., Yang, J., Zarrella, T. M., Zhang, Y., Metzger, D. W. and Bai, G. (2014) Cyclic di-AMP impairs potassium uptake mediated by a c-di-AMP binding protein in Streptococcus pneumoniae. J. Bacteriol. **196**, 614–623.

53 Kim, H., Youn, S.-J., Kim, S. O., Ko, J., Lee, J.-O. and Choi, B.-S. (2015) Structural Studies of Potassium Transport Protein KtrA Regulator of Conductance of K+ (RCK) C domain in Complex with Cyclic Diadenosine Monophosphate (c-di-AMP). J. Biol. Chem. **290**, 16393–16402.

54 Gries, C. M., Bose, J. L., Nuxoll, A. S., Fey, P. D. and Bayles, K. W. (2013) The Ktr potassium transport system in Staphylococcus aureus and its role in cell physiology, antimicrobial resistance and pathogenesis. Mol. Microbiol. **89**, 760–773.

55 Chin, K.-H., Liang, J.-M., Yang, J.-G., Shih, M.-S., Tu, Z.-L., Wang, Y.-C., Sun, X.-H., Hu, N.-J., Liang, Z.-X., Dow, J. M., et al. (2015) Structural Insights into the Distinct Binding Mode of Cyclic di-AMP with SaCpaA-RCK. Biochemistry.

56 Heermann, R. and Jung, K. (2010) The complexity of the "simple" two-component system KdpD/KdpE in Escherichia coli. FEMS Microbiol. Lett. **304**, 97–106.

57 Xue, T., You, Y., Hong, D., Sun, H. and Sun, B. (2011) The Staphylococcus aureus KdpDE two-component system couples extracellular K+ sensing and Agr signaling to infection programming. Infect. Immun. **79**, 2154–2167.

58 Moscoso, J. A., Schramke, H., Zhang, Y., Tosi, T., Dehbi, A., Jung, K. and Gründling, A. (2015) Binding of c-di-AMP to the Staphylococcus aureus sensor kinase KdpD occurs via the USP domain and down-regulates the expression of the Kdp potassium transporter. J. Bacteriol.

59 Huergo, L. F., Chandra, G. and Merrick, M. (2013) PII signal transduction proteins: nitrogen regulation and beyond. FEMS Microbiol. Rev. **37**, 251–283.

60 Müller, M., Hopfner, K.-P. and Witte, G. (2015) c-di-AMP recognition by Staphylococcus aureus PstA. FEBS Lett. **589**, 45–51.

61 Campeotto, I., Zhang, Y., Mladenov, M. G., Freemont, P. S. and Gründling, A. (2015) Complex Structure and Biochemical Characterization of the Staphylococcus aureus cyclic di-AMP binding Protein PstA, the Founding Member of a New Signal Transduction Protein Family. J. Biol. Chem. **290**, 2888–2901.

62 Gundlach, J., Dickmanns, A., Schröder-Tittmann, K., Neumann, P., Kaesler, J., Kampf, J., Herzberg, C., Hammer, E., Schwede, F., Kaever, V., et al. (2015) Identification, characterization and structure analysis of the c-di-AMP binding PII-like signal transduction protein DarA. J. Biol. Chem. **290**, 3069–3080.

63 Choi, P. H., Sureka, K., Woodward, J. J. and Tong, L. (2015) Molecular basis for the recognition of cyclic-di-AMP by PstA, a PII-like signal transduction protein. Microbiologyopen **4**, 361–374.

64 Nelson, J. W., Sudarsan, N., Furukawa, K., Weinberg, Z., Wang, J. X. and Breaker, R. R. (2013) Riboswitches in eubacteria sense the second messenger c-di-AMP. Nat. Chem. Biol., Nature Publishing Group **9**, 834–839.

65 Ren, A. and Patel, D. J. (2014) c-di-AMP binds the ydaO riboswitch in two pseudo-symmetry–related pockets. Nat. Chem. Biol., Nature Publishing Group **10**, 780–786.

66 Gao, A. and Serganov, A. (2014) Structural insights into recognition of c-di-AMP by the ydaO riboswitch. Nat. Chem. Biol., Nature Publishing Group **10**, 787–792.

67 Sureka, K., Choi, P. H., Precit, M., Delince, M., Pensinger, D. A., Huynh, T. N., Jurado, A. R., Goo, Y. A., Sadilek, M., Iavarone, A. T., et al. (2014) The Cyclic Dinucleotide c-di-AMP Is an Allosteric Regulator of Metabolic Enzyme Function. Cell, Elsevier Inc. **158**, 1389–1401.

68 Schär, J., Stoll, R., Schauer, K., Loeffler, D. I. M., Eylert, E., Joseph, B., Eisenreich, W., Fuchs, T. M. and Goebel, W. (2010) Pyruvate carboxylase plays a crucial role in carbon metabolism of extra- and intracellularly replicating Listeria monocytogenes. J. Bacteriol. **192**, 1774–1784.

69 St Maurice, M., Reinhardt, L., Surinya, K. H., Attwood, P. V, Wallace, J. C., Cleland, W. W. and Rayment, I. (2007) Domain architecture of pyruvate carboxylase, a biotin-dependent multifunctional enzyme. Science (80-.). **317**, 1076–1079.

70 Rao, F., See, R. Y., Zhang, D., Toh, D. C., Ji, Q. and Liang, Z.-X. (2010) YybT is a signaling protein that contains a cyclic dinucleotide phosphodiesterase domain and a GGDEF domain with ATPase activity. J. Biol. Chem. **285**, 473–482.

71 Whiteley, A. T., Pollock, A. J. and Portnoy, D. A. (2015) The PAMP c-di-AMP Is Essential for Listeria monocytogenes Growth in Rich but Not Minimal Media due to a Toxic Increase in (p)ppGpp. Cell Host Microbe, Elsevier Inc. **17**, 788–798.

72 Geiger, T. and Wolz, C. (2014) Intersection of the stringent response and the CodY regulon in low GC Gram-positive bacteria. Int. J. Med. Microbiol., Elsevier GmbH. **304**, 150–155.

73 Liu, S., Bayles, D. O., Mason, T. M. and Wilkinson, B. J. (2006) A cold-sensitive Listeria monocytogenes mutant has a transposon insertion in a gene encoding a putative membrane protein and shows altered (p)ppGpp levels. Appl. Environ. Microbiol. **72**, 3955–3959.

74 Witte, C. E., Whiteley, A. T. and Burke, T. P. (2013) Cyclic di-AMP Is Critical for Listeria monocytogenes Growth, Cell Wall Homeostasis, and Establishment of Infection. MBio **4**.

75 Cho, K. H. and Kang, S. O. (2013) Streptococcus pyogenes c-di-AMP Phosphodiesterase, GdpP, Influences SpeB Processing and Virulence. PLoS One **8**, e69425.

76 Yang, J., Bai, Y., Zhang, Y., Gabrielle, V. D., Jin, L. and Bai, G. (2014) Deletion of the cyclic di-AMP phosphodiesterase gene (cnpB) in Mycobacterium tuberculosis leads to reduced virulence in a mouse model of infection. Mol. Microbiol. **93**, 65–79.

77 Tang, Q., Luo, Y., Zheng, C., Yin, K., Ali, M. K., Li, X. and He, J. (2015) Functional Analysis of a c-di-AMP-specific Phosphodiesterase MsPDE from Mycobacterium smegmatis. Int. J. Biol. Sci. **11**, 813–824.

78 Huynh, T. N., Luo, S., Pensinger, D., Sauer, J.-D., Tong, L. and Woodward, J. J. (2015) An HD-domain phosphodiesterase mediates cooperative hydrolysis of c-di-AMP to affect bacterial growth and virulence. PNAS **112**, 747–756.

79 Rao, F., Ji, Q., Soehano, I. and Liang, Z.-X. (2011) Unusual heme-binding PAS domain from YybT family proteins. J. Bacteriol. **193**, 1543–1551.

80 Tan, E., Rao, F., Pasunooti, S., Pham, T. H., Soehano, I., Turner, M. S., Liew, C. W., Lescar, J., Pervushin, K. and Liang, Z.-X. (2013) Solution structure of the PAS domain of a thermophilic YybT protein homolog reveals a potential ligand-binding site. J. Biol. Chem. **288**, 11949–11959.

81 Luo, Y. and Helmann, J. D. (2012) Analysis of the role of Bacillus subtilis sigmaM in beta-lactam resistance reveals an essential role for c-di-AMP in peptidoglycan homeostasis. Mol. Microbiol. **83**, 623–639.

82 Gándara, C. and Alonso, J. C. (2015) DisA and c-di-AMP act at the intersection between DNA-damage response and stress homeostasis in exponentially growing Bacillus subtilis cells. DNA Repair (Amst)., Elsevier B.V. **27**, 1–8.

83 Dengler, V., McCallum, N., Kiefer, P., Christen, P., Patrignani, A., Vorholt, J. A., Berger-Bächi, B. and Senn, M. M. (2013) Mutation in the C-Di-AMP Cyclase dacA Affects Fitness and Resistance of Methicillin Resistant Staphylococcus aureus. PLoS One **8**.

84 Zeevi, M. K., Shafir, N. S., Shaham, S., Friedman, S., Sigal, N., Nir-Paz, R., Boneca, I. G. and Herskovits, A. A. (2013) Listeria monocytogenes MDR transporters and c-di-AMP that contribute to Type I interferons induction, play a role in cell wall stress. J. Bacteriol. **195**, 5250–5261.

85 Dey, B., Dey, R. J., Cheung, L. S., Pokkali, S., Guo, H., Lee, J.-H. and Bishai, W. R. (2015) A bacterial cyclic dinucleotide activates the cytosolic surveillance pathway and mediates innate resistance to tuberculosis. Nat. Med., Nature Publishing Group **21**, 401–406.

86 Griffiths, J. M. and O'Neill, A. J. (2012) Loss of function of the GdpP protein leads to joint β-lactam/ glycopeptide tolerance in Staphylococcus aureus. Antimicrob. Agents Chemother. **56**, 579–581.

87 Zheng, Y., Zhou, J., Sayre, D. and Sintim, H. O. (2014) Identification of bromophenol thiohydantoin as an inhibitor of DisA, a c-di-AMP synthase, from a 1000 compound library, using the coralyne assay. Chem. Commun., Royal Society of Chemistry **50**, 11234–11237.

88 Ahn, Y. J., Park, S. J., Lee, S. G., Shin, S. C. and Choi, D. H. (2000) Cordycepin: Selective growth inhibitor derived from liquid culture of Cordyceps militaris against Clostridium spp. J. Agric. Food Chem. **48**, 2744–2748.

89 Schwartz, K. T., Carleton, J. D., Quillin, S. J., Rollins, S. D., Portnoy, D. A. and Leber, J. H. (2012) Hyperinduction of Host Beta Interferon by a Listeria monocytogenes Strain Naturally Overexpressing the Multidrug Efflux Pump MdrT. Infect. Immun. **80**, 1537–1545.

90 Burdette, D. L. and Vance, R. E. (2012) STING and the innate immune response to nucleic acids in the cytosol. Nat. Immunol. **14**, 19–26.

91 Cai, X., Chiu, Y. H. and Chen, Z. J. (2014) The cGAS-cGAMP-STING pathway of cytosolic DNA sensing and signaling. Mol. Cell, Elsevier Inc. **54**, 289–296.

92 Sauer, J.-D., Sotelo-Troha, K., Moltke, J. Von, Monroe, K. M., Rae, C. S., Brubaker, S. W., Hyodo, M., Hayakawa, Y., Woodward, J. J., Portnoy, D. A., et al. (2011) The N-Ethyl-N-Nitrosourea-Induced Goldenticket Mouse Mutant Reveals an Essential Function of Sting in the In Vivo Interferon Response to Listeria monocytogenes and Cyclic Dinucleotides. Infect. Immun. **79**, 688–694.

93 Barker, J. R., Koestler, B. J., Victoria, K., Barker, J. R., Koestler, B. J., Carpenter, V. K., Burdette, D. L., Waters, C. M. and Vance, R. E. (2013) Interferon Responses during STING-Dependent Recognition of Cyclic di-AMP Mediates Type I Interferon Responses during Chlamydia trachomatis Infection. MBio **4**.

94 Burdette, D. L., Monroe, K. M., Sotelo-Troha, K., Iwig, J. S., Eckert, B., Hyodo, M., Hayakawa, Y. and Vance, R. E. (2011) STING is a direct innate immune sensor of cyclic di-GMP. Nature, Nature Publishing Group **478**, 515–518.

95 Wu, J., Sun, L., Chen, X., Du, F., Shi, H., Chen, C. and Chen, Z. J. (2013) Cyclic GMP-AMP is an endogenous second messenger in innate immune signaling by cytosolic DNA. Science **339**, 826–30.

96 Huang, Y.-H., Liu, X.-Y., Du, X.-X., Jiang, Z.-F. and Su, X.-D. (2012) The structural basis for the sensing and binding of cyclic di-GMP by STING. Nat. Struct. Mol. Biol., Nature Publishing Group **19**, 728–730.

97 Sun, L., Wu, J., Du, F., Chen, X. and Chen, Z. J. (2013) Cyclic GMP-AMP synthase is a cytosolic DNA sensor that activates the type I interferon pathway. Science **339**, 786–91.

98 Zhang, Z., Yuan, B., Bao, M., Lu, N., Kim, T. and Liu, Y.-J. (2011) The helicase DDX41 senses intracellular DNA mediated by the adaptor STING in dendritic cells. Nat. Immunol. **12**, 959–965.

99 Parvatiyar, K., Zhang, Z., Teles, R. M., Ouyang, S., Jiang, Y., Iyer, S. S., Zaver, S. A., Schenk, M., Zeng, S., Zhong, W., et al. (2012) The helicase DDX41 recognizes the bacterial secondary messengers cyclic di-GMP and cyclic di-AMP to activate a type I interferon immune response. Nat. Immunol. **13**, 1155–1161.

100 Ebensen, T., Libanova, R., Schulze, K., Yevsa, T., Morr, M. and Guzmán, C. A. (2011) Bis-(3',5')-cyclic dimeric adenosine monophosphate: Strong Th1/Th2/Th17 promoting mucosal adjuvant. Vaccine, Elsevier Ltd **29**, 5210–5220.

101 Ariyoshi, M., Nishino, T., Iwasaki, H., Shinagawa, H. and Morikawa, K. (2000) Crystal structure of the holliday junction DNA in complex with a single RuvA tetramer. Proc. Natl. Acad. Sci. U. S. A. **97**, 8257–62.

102 Conroy, M. J., Durand, A., Lupo, D., Li, X.-D., Bullough, P. A., Winkler, F. K. and Merrick, M. (2007) The crystal structure of the Escherichia coli AmtB-GlnK complex reveals how GlnK regulates the ammonia channel. Proc. Natl. Acad. Sci. U. S. A. **104**, 1213–1218.

103 Llácer, J. L., Espinosa, J., Castells, M. A., Contreras, A., Forchhammer, K. and Rubio, V. (2010) Structural basis for the regulation of NtcA-dependent transcription by proteins PipX and PII. Proc. Natl. Acad. Sci. U. S. A. **107**, 15397–15402.

104 Rajendran, C., Gerhardt, E. C. M., Bjelic, S., Gasperina, A., Scarduelli, M., Pedrosa, F. O., Chubatsu, L. S., Merrick, M., Souza, E. M., Winkler, F. K., et al. (2011) Crystal structure of the GlnZ-DraG complex reveals a different form of P II - target interaction. PNAS **108**, 18972–18976.

105 Tuli, H. S., Sharma, A. K., Sandhu, S. S. and Kashyap, D. (2013) Cordycepin: a bioactive metabolite with therapeutic potential. Life Sci., Elsevier Inc. **93**, 863–869.

106 Yue, K., Ye, M., Zhou, Z., Sun, W. and Lin, X. (2013) The genus Cordyceps: a chemical and pharmacological review. J. Pharm. Pharmacol. **65**, 474–493.

6 ACKNOWLEDGEMENTS

First of all: Thank you Gregor! For being a great supervisor, always supporting me with theoretical and practical advice, chocolate and good ideas during cookie meetings, coffee breaks and anyway all the time. I enjoyed doing my PhD with you and learned a lot!

Furthermore, I would like to thank the whole AG Hopfner for the great working atmosphere, where you always find someone to help you with scientific or technical problems. Special thanks goes to the 'last lab' – where everyone is always willing to listen, whether you are happy or grumpy or need advice.

I also thank Olga for a lot of help in the lab, as well as my students Kim and Carlos who both did a great job.

Finally, I thank Patrik for constant support outside of the lab and always being there.